Doctoral theses at NTNU, 2021:345

Henki Ødegaard

Rock Stress Estimation for Unlined Pressure Tunnel Design

Doctoral thesis

NTNU
Norwegian University of Science and Technology
Thesis for the Degree of
Philosophiae Doctor
Faculty of Engineering
Department of Geoscience and Petroleum

NTNU
Norwegian University of
Science and Technology

Henki Ødegaard

Rock Stress Estimation for Unlined Pressure Tunnel Design

Thesis for the Degree of Philosophiae Doctor

Trondheim, November 2021

Norwegian University of Science and Technology
Faculty of Engineering
Department of Geoscience and Petroleum

NTNU
Norwegian University of
Science and Technology

NTNU
Norwegian University of Science and Technology

Thesis for the Degree of Philosophiae Doctor

Faculty of Engineering
Department of Geoscience and Petroleum

ISBN 978-82-326-6292-0 (printed ver.)
ISBN 978-82-326-6139-8 (electronic ver.)
ISSN 1503-8181 (printed ver.)
ISSN 2703-8084 (online ver.)

Doctoral theses at NTNU, 2021:345

Printed by NTNU Grafisk senter

Abstract

In underground hydropower projects rock tunnels are used extensively to convey water for the purpose of generating power. As these tunnels represent a major cost element in typical hydropower developments, efforts are made to ensure that the tunnel design is cost-efficient. Under Norwegian tradition the principal cost reducing measure is to keep most of the tunnel length unlined and steel line only a relatively short section of the tunnel. This approach requires that the rock stress in the unlined tunnel sections exceeds the internal water pressure. To avoid hydraulic failure of the tunnel, information on the underground state of stress thus is crucial.

Before the emergence of reliable methods for the measurement of rock stress, the final design of pressure tunnels was based solely on rock stress estimates made from crude assessments of the overlying weight of rock, the so-called overburden criteria. For many years, these criteria have been popular tools and their use has continued to date—even for final liner considerations. While the overburden criteria were important tools in the early days of unlined pressure tunnel design, and to some extent still are, experience has demonstrated their inability of providing reliable rock stress estimates.

Today, it is generally recognized that *in-situ* measurement is the only reliable way to estimate rock stresses for the purpose of finding the safe location of the transition between unlined- and steel lined pressure tunnel. The current approach to rock stress estimation typically involves performing stress measurements at relatively few test locations, and to use interpolative techniques to assess stresses between and beyond locations. As the distance between test locations increases, so does the risk of leaving tunnel sections with insufficient stress undetected.

In this thesis, a new methodology for rock stress estimation is suggested to mitigate this undesirable situation, involving a reduction of the distance between test locations by performing measurements more regularly along the entire length of unlined pressure tunnel. For this approach to be financially and practically feasible, measurements must be made more rapid and more efficiently than they are done with the currently available test methods.

A new hydraulic jacking test protocol, the rapid step-rate test (RSRT), is proposed as an alternative to the available methods. This test protocol has been developed through a series of laboratory controlled experiments conducted in a custom-built true-triaxial test rig. The experiments involved hydraulic jacking tests conducted on cubical specimens of rock, each containing a pre-existing planar fracture. As the normal stress on the stimulated fracture was

known through control of the confining pressures and the fracture geometry, the capability of hydraulic jacking test protocols could be tested efficiently—resulting in the RSRT. The experimental results suggested that the RSRT enabled reliable estimates on fracture normal stresses.

During the laboratory experiments the specimens were also monitored with AE-sensors, allowing for detailed observations of the fracture geometry from mapping of the AE hypocentres. A clear correlation between fracture closure and bursts of AE events could be observed, serving as a potential aid in detecting fracture closure.

The RSRT protocol was tested in full-scale field conditions at the Løkjelsvatn HPP. The field experiments confirmed the laboratory findings that fracture closure could be detected through analysis of the fracture closure stages of the RSRT, and further that the normal stress estimates were representative for the *in-situ* state of stress. Unfavourable testing conditions, affecting some of the tests, were identified—indicating that special efforts should be made to avoid air-entrapment inside the hydraulic system and to avoid locating boreholes too close to each other. The importance of establishing test sections sufficiently far away from the tunnel near-field was also realized.

Through field- as well as laboratory testing the RSRT protocol has demonstrated a promising ability in estimating fracture normal stress, and it is therefore believed that the new test protocol may serve as a rapid alternative to current rock stress estimation methods that is well suited for adoption in the proposed new rock stress testing methodology.

Preface and acknowledgements

The research presented in this thesis has been conducted at the Norwegian University of Science and Technology (NTNU), Department of Geoscience and Petroleum, with Professor Bjørn Nilsen as the main supervisor. My co-supervisor has been Dr. Roger Olsson, adjunct professor at the same department.

The research was funded through the Research Council of Norway and is conducted as part of the Norwegian Research Centre for Hydropower Technology, HydroCen. The work has been conducted through a 4-year PhD position where 75% of the time was allocated to research and the remaining 25% to teaching and other relevant scientific duties. The teaching has included co-supervision of five master students and lecturing and organizing assignments for the course TGB4185 Engineering Geology, Basic Course. Other relevant scientific duties have included work related to my post as board member of the Norwegian national group to the ISRM, including sitting four years as the General Chair for EUROCK 2020.

First, I would like express sincere gratitude to my main supervisor, Professor Bjørn Nilsen for his endless support, his kind guidance, and for his thorough and critical assessment of my scientific work throughout these four years as a PhD Candidate. Bjørn, you are also an excellent traveling companion, making our various field trips and visits in Norway and abroad both fun and interesting.

I also want to thank my many colleagues at the Department of Geoscience and Petroleum for their company and support throughout these four years—you know who you are! To Bibek, with whom I have shared offices the last four years, I just want to say that it has been an absolute pleasure, and I really look forward to working with you again in a not too distant future.

I am grateful for the support received from Multiconsult during my four-year leave of absence, and for the kind interest in my research shown by many of my Multiconsult colleagues. The Norwegian Tunnelling Society, NFF, is thanked for providing financial support through the NFF scholarship.

To you my dear sons, Mattis and Mikkel, I express my deepest appreciation for your daily unspoken reminder that there are more important things in this world than the design of unlined pressure tunnels. To the rest of my super family, living in Trondheim, Lofoten, Røros, Sør-Odal, Oslo, Mo i Rana, Valldal, Ålesund and Hamar, I just want to thank you for your love,

support, and for the many excellent ways you all are able to maintain a straight face as I drone on about some pressure tunnel related fun-fact.

Finally, my deepest appreciation goes to the love of my life, my fantastic wife. Karina, you are the best, and I love you and your calm, patient, fun, and loving nature. EDDDDM!

DET ER DEN DRAUMEN

Det er den draumen me ber på
at noko vedunderleg skal skje,
at det må skje –
at tidi skal opna seg
at hjarta skal opna seg
at dører skal opna seg
at berget skal opna seg
at kjeldor skal springa –
at draumen skal opna seg,
at me ei morgonstund skal glida inn
på ein våg me ikkje har visst um.

Olav H. Hauge (1966)

Contents

Paper III **Rock Stress Measurements for Unlined Pressure Tunnels: A True Triaxial Laboratory Experiment to Investigate the Ability of a Simplified Hydraulic Jacking Test to Assess Fracture Normal Stress**

Paper IV **Simplified hydraulic jacking test to assess fracture normal stress for unlined pressure tunnels—a field experiment using the Rapid Step-Rate Test**

Paper V **Improved design of unlined air cushion surge chambers**

1 Introduction

1.1 Background

Hydroelectric power generation is the world's primary source of renewable electricity, providing almost half of all the renewable energy worldwide—making it the foundation of low-carbon electricity generation. The International Energy Agency, IEA, predicts a 17 % increase in the world's hydropower capacity by 2030, a 230 GW increase from the present 1 330 GW (IEA 2021). A trend of increasing activity has also been seen in Norway in recent years, following a period of lower activity after the boom of new hydroelectric plants lasting from the end of World War II until the early 1980s (Lia et al. 2015). This renewed activity includes new developments and upgrades of existing plants, resulting in 324 MW of new hydropower capacity in Norway in 2020, increasing the total installed capacity to 33 GW (IHA 2021). As the Norwegian hydropower market is fairly mature, in the sense that the economically attractive projects are either non-permittable or already developed, new schemes are typically smaller and less profitable. Cost-effective design solutions are therefore required to realize these projects, and it is hoped that the work presented in this thesis might serve as a contribution towards cost-effective and safe hydropower design.

The long-standing Norwegian tradition for research on innovative and cost-effective hydropower solutions is continued through the Norwegian Research Centre for Hydropower Technology, HydroCen, which was established in 2016. The main objective of this research centre is to: "*enable the Norwegian hydropower sector to meet complex challenges and exploit new opportunities through innovative technological solutions*." Within this framework the following four work packages were defined:

1. Hydropower structures
2. Turbine and generators
3. Market and services
4. Environmental design

This PhD project is organised as part of Work Package 1—Hydropower structures, which covers all construction elements in a power plant, from dams, intakes, tunnel system, and power stations. The research presented in this thesis is related to the design of unlined pressure tunnels, and more specifically to the process of estimating rock stress, the magnitude of which is of great importance for the safe and economic design of unlined pressure tunnels. Two other PhD projects, related to tunnels and rock engineering, have also been part of Work Package 1.

These projects included a project dealing with issues related to swelling rocks in hydropower tunnels (PhD Lena Selen), and another project investigating the long term impact of tunnels from frequent start-/stop power production (PhD Bibek Neupane). Even though all three projects were related to rock engineering and hydropower tunnels, they had different scopes, and thus did not overlap to any significant extent. Fruitful discussion was, however, possible due to a common interest in optimal design of unlined pressure tunnels.

The design of pressurised waterways, used for hydropower purposes, is in Norway is regulated through §5-16 of the national dam safety regulations (Damsikkerhetsforskriften). Regarding rock stress estimation for pressure tunnel design these regulations are rather general, basically stating that pressurised waterways must be designed and placed in such a way that no harmful leakages or deformations occur in the surrounding rock mass. Whilst the regulation also state that assessments of overburden, leakage and stability should be emphasized—there is no precise requirement for measuring stress. This is unsatisfactory considering that the key design requirement for unlined pressure tunnels is that the rock stress magnitude must exceed the internal water pressure—along the entire unlined length of tunnel (Broch 1982). Should this requirement not be met, hydraulic failure of the tunnel may occur, with potential for very large leakages.

While the importance of sufficient stress is well-acknowledged is the line of action chosen for achieving information on the underground state of stress variable and, in the authors opinion, not always optimal. Empirical overburden criteria for assessing rock stresses, such as the renowned Norwegian Criterion for Confinement, have historically been important tools for the design of unlined pressure tunnels, and still might serve as useful tools during preliminary planning (Rancourt 2010). Their continued use for final design purposes is, however, worrying since it is today generally recognized that overburden criteria cannot provide reliable estimates of rock stress (Merritt 1999).

A recent Norwegian example demonstrating the inadequacy of using overburden criteria for final liner considerations, is the hydraulic failure of the Bjørnstokk HPP pressure tunnel in 2016. At this plant was the final liner design was based solely on stress estimates obtained from overburden criteria, with no stress measurements. Later investigations found that the failure was caused by insufficient stress levels near the downstream end of the unlined pressure tunnel, and that the failure could have been avoided had the final liner design been based on rock stress measurements (Nordal et al. 2018).

Though omitting stress measurements altogether might represent an extreme case, there are also other unresolved issues related to reliable rock stress estimation. More research is needed to address these issues, and the present work seeks to serve as a contribution in this direction.

1.2 Thesis scope and objective

The objective of this PhD-project was to contribute to an improved basis for the final design of unlined pressure tunnels, with emphasis on rock stress estimation. To obtain this objective the research was aimed at the following subtasks:

1. Contributing to an increased awareness of the uncertainties associated with the use of traditional overburden criteria for rock stress estimation
2. Proposing an improved methodology for the estimation of rock stress in connection with final design of unlined pressure tunnels
3. Developing a hydraulic jacking test protocol that can enable rapid rock stress estimates based on simplified test procedures that are adapted to the typical underground field-conditions
4. Investigating the field correlation between the new hydraulic jacking test protocol and the hydraulic fracturing (HF) tests
5. Investigating a potential correlation between acoustic emission (AE) activity and fracture normal stress by linking AE-events with fracture closure

Initially, it was planned to assess and compare the two most commonly employed rock stress measurement techniques used for final liner design in Norway, the hydraulic fracturing (HF) test and hydraulic jacking (HJ) test. This approach was, however, soon left since it turned out that the basis for assessing HJ tests results and comparing these to the HF test was hard to establish due to the lack of coherent procedures for the execution and interpretation of HJ tests. Additionally, few relevant cases where the simplified HJ tests and HF tests had been performed at the same location could be found.

1.3 Organisation of thesis and note on contributions

This thesis consists of five papers and a synthesis aimed at establishing the interrelation between the individual papers, and to provide additional background information and perspective on the overall research topic. The five papers together make the main part of this thesis, and the details of these papers are listed below together with a brief note on contributions for each paper.

Paper I

Engineering Geological Investigation and Design of Transition Zones in Unlined Pressure Tunnels

Authors: Ødegaard H, Nilsen B

Paper presented at the ISRM International Symposium - 10th Asian Rock Mechanics Symposium, Singapore, 29.10-2.11 2018

The paper was written by Henki Ødegaard and reviewed by Bjørn Nilsen.

Paper II

Design of Unlined Pressure Tunnels in Norway – Limitations of Empirical Overburden Criteria and Significance of In-Situ Rock Stress Measurements

Authors: Ødegaard H, Nilsen B, Barkved H

Paper published in conference proceedings from the ISRM International Symposium - EUROCK 2020 (the physical event was not held)

The paper was written by Henki Ødegaard. Håvard Barkved gathered and analysed the data used in the comparison of rock stress estimates made from *in-situ* measurements and overburden criteria, as part of his Master's thesis. Bjørn Nilsen reviewed the manuscript.

Paper III

Rock Stress Measurements for Unlined Pressure Tunnels: A True Triaxial Laboratory Experiment to Investigate the Ability of a Simplified Hydraulic Jacking Test to Assess Fracture Normal Stress

Authors: Ødegaard H, Nilsen B.

Paper published in Rock Mechanics and Rock Engineering, https://doi.org/10.1007/s00603-021-02452-9

The paper was written by Henki Ødegaard, who also conducted all experiments, data gathering and analysis. Ødegaard was also responsible for designing the experimental setup, including the development of the true trixaial test rig used during the experiments. Bjørn Nilsen performed review of the manuscript.

Paper IV

Simplified hydraulic jacking test to assess fracture normal stress for unlined pressure tunnels—a field experiment using the Rapid Step-Rate Test

Authors: Ødegaard H, Nilsen B.

The paper is submitted to Rock Mechanics and Rock Engineering

The paper was written by Henki Ødegaard. The field experiments were conducted as a cooperation between Ødegaard, Master Student Erlend Andreassen and test specialists from the company Injeksjonsteknikk AS. Henki Ødegaard was responsible for test design, experimental setup, and data analysis. Bjørn Nilsen reviewed the manuscript.

Paper V

Improved design of unlined air cushion surge chambers

Authors: Ødegaard H, Vereide K, Nilsen B.

Paper published in the International journal on hydropower and dams

The paper was written by Henki Ødegaard with co-author Kaspar Vereide responsible for hydraulic design and cost-estimates. The paper was reviewed by Kaspar Vereide and Bjørn Nilsen.

2 Theoretical framework

A general overview of the key considerations for rock stress estimation, as used in the context of unlined pressure tunnel design, is given in the following—together with a brief introduction to the historical development of unlined pressure tunnel design in Norway.

The design of unlined pressure tunnels requires consideration of various rock engineering aspects which, in addition to the aforementioned rock stress magnitude, include rock mass quality, topography, groundwater, permeability, excavation method and rock support. As an exhaustive review of all aspects of rock engineering design for unlined pressure tunnels is considered beyond the scope of this thesis, focus will be on the main topic—rock stress estimation for unlined pressure tunnels. For a broader overview of the rock engineering aspects of unlined pressure tunnel design reference is made to the well-established international guidelines on the topic such as Brekke and Ripley (1987), Benson (1989) and Merritt (1999).

A distinction will be made between *unlined* pressure tunnels, having no impermeable liner separating the rock mass and the pressurised water, and *lined* pressure tunnels where an impermeable liner is installed in the tunnel, either as concrete embedded liner or as a free-standing pipe. In the case of unlined tunnels the water will be in direct contact with the surrounding rock, thus exerting a pressure upon it, while in the case of lined tunnels the water pressure will be sustained entirely by the liner. A pressure tunnel supported by sprayed concrete liners or cast in place concrete structures, reinforced or not, will not be considered a lined tunnel in the context of this thesis, since such concrete structures generally must be considered pervious (Brekke and Ripley 1987).

Distinguishing unlined tunnels from lined tunnels is important since the cost of constructing steel lined tunnels is much higher than unlined tunnels, making the required length of lined tunnel a matter of economic feasibility for the often financially marginal hydropower schemes. In some Norwegian projects the linear length of a lined tunnel can cost as much as 3-5 times more than the cost of an unlined tunnel (NVE 2016).

2.1 Historical development

The history of Norwegian unlined pressure tunnel design, used for hydropower purposes, started with the Herlandsfoss HPP in 1919. This plant had originally been designed with penstocks, high-pressure steel pipes installed on the surface, to convey the pressurised water down to the powerhouse, see Fig. 1 and Fig. 2 where this type of design is shown. High price and general steel shortage following World War I did, however, require the designers of the plant to minimize the length of steel-liner, motivating the then rather radical solution of replacing the steel penstocks with an unlined pressure tunnel.

Fig. 1: Vemork HPP, with a above ground powerhouse and steel penstocks installed on the mountainside (Lanting 2021).

The new design required that the unlined tunnel section at Herlandsfoss HPP could sustain a static water pressure, or head, of 137 m. At the time, only a limited number of comparable projects existed, such as the world's very first pressure tunnel, the New Croton Aqueduct in the U.S., constructed in 1890 (White 1913) and the Rondout pressure tunnel, a water supply tunnel in the U.S. (Berkey and Sanborn 1922). The 1910 failure of the Kandergrund pressure tunnel in Switzerland (Jaeger 1979) was also known at the time—causing some concern to the designers (Schjerven 1921).

Upon filling of the Herlandsfoss HPP pressure tunnel in April 1919 only minor leaks could first be detected, but these soon became more prominent—and about 5 hours after reaching 127 m head the water pressure could no longer be maintained in the tunnel, and the tunnel was drained and inspected. During the inspection a newly developed flat-lying fracture could be observed, from where water was rushing back. At the time of inspection the fracture was still dilated by 5 mm, but as the water leakage receded the fracture could be observed to close

entirely (Schjerven 1921). The root cause of this failure was insufficient rock stress—causing the pressurised water to hydraulically jack fractures intersected by the tunnel (Selmer-Olsen 1970). Following the failure significant rehabilitation works had to be done, including the extension of the steel liner a further 150 m into the hillside, such that the previously unlined section of pressure tunnel ended up steel lined all the way to the shaft bottom. The plant was later successfully commissioned, but the failure of another unlined pressure tunnel only two years later, the Skar HPP in 1921, discouraged engineers in pursuing the unlined concept for several decades.

As a side note it can be mentioned that two earthquakes were registered at the same time as the failure of the Herlandsfoss HPP, and it was discussed at the time whether these earthquakes could have been the triggering factor (Schjerven, 1921; Vogt and Vogt, 1922). With present days knowledge on triggering of earthquakes, including so-called induced seismicity, the opposite seems to represent a more likely scenario—i.e. that the hydraulic failure caused the seismicity. This would in that case represent a very early case of induced seismicity, a phenomenon discussed in more detail in Chapter 2.4.3.

Following World War II most new hydroelectric plants in Norway were located underground for security reasons. When power stations were located underground, so were the penstocks—and inclined, steel-lined, pressure shafts, connected to a flat-lying headrace tunnel became a common design in 1950-1960, see Fig. 2.

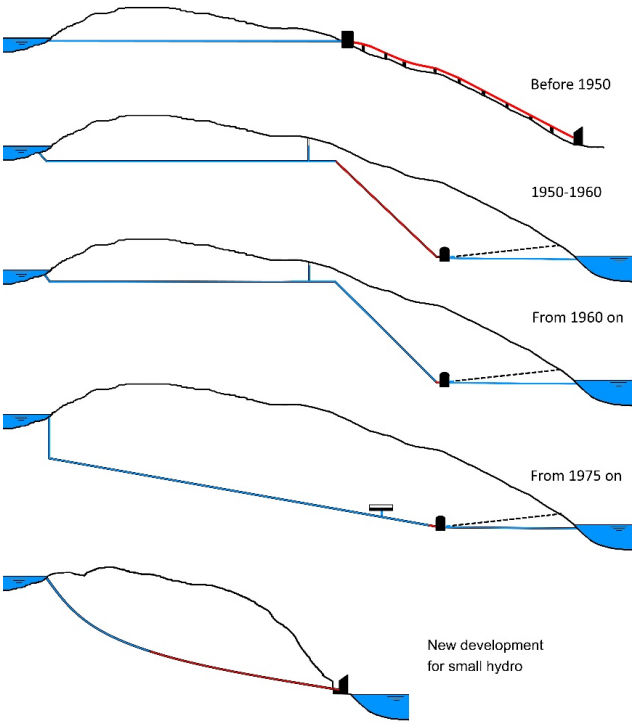

Fig. 2: Historical development of pressure tunnel design, modified from Broch (1982). Red colour is used to illustrate the steel-lined section of the waterway

Motivated by the potential large cost savings when reducing the length of steel liner, engineers again went for the unlined concept in the late 1950s, but this time locating the unlined pressure shaft deeper into the hillsides, where it was believed that the risk of hydraulic failure would be reduced from the higher weight of overlying rock mass. Following the successful commissioning of the Tafjord K3 plant, with a record breaking 286 m head, the unlined concept became the new norm from the 1960s.

Other notable updates of the typical unlined pressure tunnel design include the introduction of unlined air cushion surge chambers (Svee 1972) - discussed in Paper V, deep vertical shaft drilling and the introduction of inclined pressure tunnels as alternative to pressure shafts. In Norway, there has been a gradual increase in the magnitude of water pressure sustained by unlined pressure tunnels and shafts, with the 1030 m of head at the Nye Tyin HPP holding the current world record, see Fig. 3.

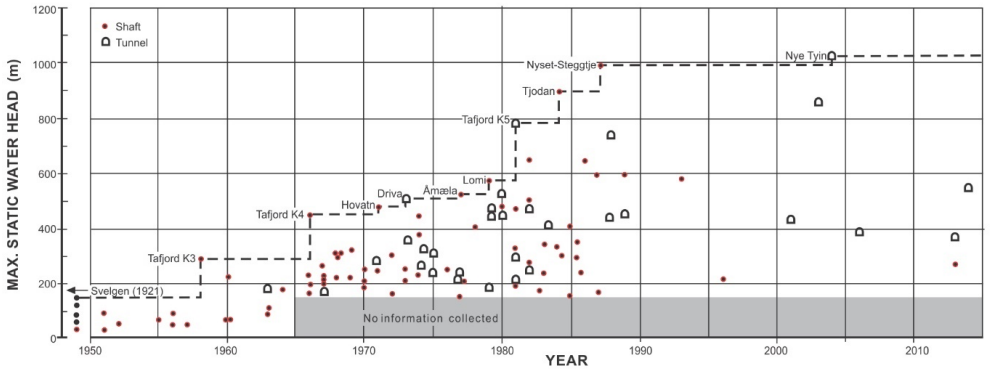

Fig. 3: Overview of the pressure development of Norwegian unlined pressure tunnels and shafts. Figure from Palmstrom and Broch (2017)

In recent years new drilling technologies have enabled efficient directional drilling of large-diameter boreholes or micro-tunnels, with the desirable ability of performing all drilling operations from the downstream end, thus minimizing activities in the upstream end, see bottom part of Fig. 2. Tunnel diameters vary but are typically within a 0.5–1.5 m range in the common hard-rock hydropower applications in Norway. Hydropower projects using such technologies to construct pressure tunnels are typically based on a small (<10 MW) run-of-river developments, but can in principle also be used for larger developments. Like ordinary pressure tunnels these micro-tunnels can be fully- or only partly steel lined.

2.2 Pressure tunnel design

An idealized longitudinal section of the waterway of a typical underground hydropower plant is shown in Fig. 4, including the following main elements: (1) reservoir and intake structure; (2) unlined waterway; (3) surge shaft; (4) sand trap; (5) steel lined waterway; (6) access tunnel; (7) power station complex, housing turbines, generators and the transformer; (8) downstream surging arrangement; (9) tailrace tunnel. Characteristic for typical Norwegian design is that most of the waterway is kept unlined, limiting the steel lined section to a relatively short section upstream of the powerhouse. The required total length of steel liner is mainly governed by the rock stress magnitude, but a certain length is in any case required to ensure a sufficiently low hydraulic gradient between the pressure tunnel and the “dry” power station (Bergh-Christensen et al. 2013).

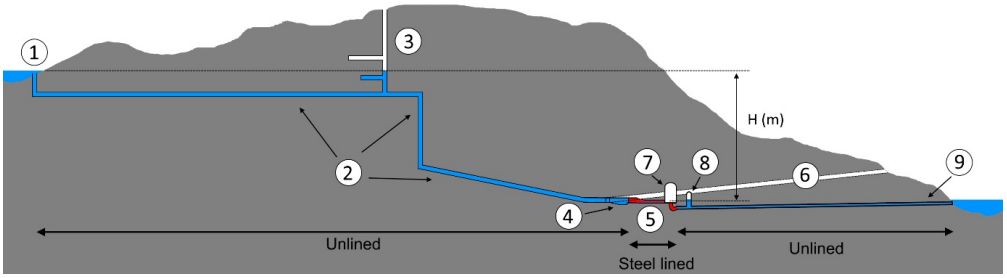

Fig. 4: Idealised long section of a typical Norwegian underground hydroelectric development

The upper dotted line in Fig. 4 represents the hydraulic grade line, i.e. the level of the upstream water reservoir. The vertical distance from the turbine to the hydraulic grade line defines the gross hydraulic head, H, and is a measure of the maximal water pressure inside the pressurised waterway. The potential hydraulic power, P, of the plant is governed by the volumetric flow rate available for energy production, Q (m^3/s), together with the gross hydraulic head, H, according to Equation 1 (Novák et al. 2007):

$$P = \frac{\eta \rho g Q H}{1000} (kW) \qquad 1.$$

where η is the given turbine efficiency, ρ the density of water and g the gravitational constant. Thus, it is desirable to increase the hydraulic head in terms of the plant's potential power—but at the same time the water pressure that the waterway has to sustain will also increase.

As mentioned in Chapter 1.1 the key design requirement for the location of the unlined pressure tunnels is to ensure that everywhere along the unlined section of the tunnel is the magnitude of rock mass stress exceeds the internal water pressure. The design of unlined pressure tunnel therefore requires knowledge of the underground state of stress. Today is such information is typically obtained through *in-situ* rock stress measurements. In the early days of pressure tunnel design, reliable rock stress measurement methods did not exist–leading engineers to base their tender design on various empirical criteria where rock stresses were estimated through crude calculation of overburden weight. While this approach can still be useful for preliminary assessments of the underground state of stress, see Rancourt (2010), is it now generally accepted that such criteria are highly uncertain and that they should not be used for the final

design of unlined pressure tunnels (Marulanda et al.,1986; USACE, 1997; Hartmaier et al., 1998; Merritt, 1999), and also discussions in Papers I and II of this thesis.

Although it is also possible to perform stress measurements during early stages of the project, e.g. from deep holes drilled from the surface down to tunnel grade, such measurements are typically cost-intensive and often technically difficult to perform. The common approach to rock stress estimation for unlined pressure tunnel design is therefore to base the tender design on rough rock stress estimates based on empirical criteria and postponing the rock stress measurement to the constructional stage, when measurements can be made from within the pressure tunnel. This approach requires contractual flexibility to be incorporated in the tender documents, allowing for construction stage changes to the tender design if so deemed necessary from the investigation results, as discussed by e.g. Benson (1989), Merritt (1999), Halvorsen and Roti (2013), and as also in Paper I of this thesis.

While some interpolation of stress data between measuring locations invariably is necessary when estimating stresses for such extensive engineering structures as pressure tunnels, it must be remembered that topographical, geological, and lithological changes can all affect the state of stress over relatively short distances (Hudson et al. 2003). This is the key argument for performing distributed rock stress measurements, rather than point measurement as discussed in Paper I.

To account for the inherent uncertainties of rock stress estimation a factor of safety (FoS) against hydraulic failure is commonly included when assessing the minimum requirement of rock stress (Benson 1989). While the maximal static water pressure is equal to the hydraulic head, higher pressures can occur from dynamic pressure surges occurring during normal operation of the plant. In Norway different values of FoS are therefore traditionally used for the two situations, typically between 1.2–1.3 when considering the dynamic (surge) pressure and 1.3–1.5 when it is the static pressure that is considered (Aasen et al. 2013).

The effect of the water-hammer, the potentially harmful dynamic pressure transient occurring whenever the turbine discharge changes, traditionally has not been required to satisfy any safety factor against hydraulic failure, since it has been believed that it is of too short duration to cause any harmful effect on the rock mass (Benson 1989; Helwig 1987). Recent research has, however, indicated that the water hammer can be a contributing factor for block falls in the tunnel caused by cyclic fatigue processes close to the tunnel periphery (Neupane et al. 2020).

2.3 Rock stress

Stresses exist naturally in Earth's crust and originate from various processes taking place over geological time, including gravitational forces, tectonic activity, and residual stresses from geological processes, such as the cooling of a magma .

Rock stress can refer to the state of stress at a point, referred to as the stress tensor, or as stress on a plane, called the stress vector (Gudmundsson 2011). In the following the concept of stress as a vector quantity will be used, as it is more intuitively understood, and more in line with how it is used in most rock engineering applications.

A simple explanation of stress is given in Price and Cosgrove (1990), and the following section is inspired by the practical explanation provided there. Imagine that an intact cube of granite with 0.3 m edge length is subject to evenly distributed force, F, of 100 kN, the equivalent of a mass of approximately 10 000 kg, see Fig. 5.

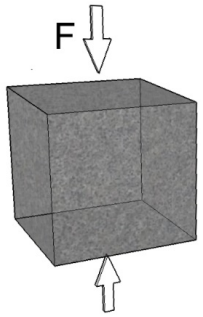

Fig. 5: A simplified model showing a 300 mm cube of granite subjected to a uniaxial force, F

While this force will cause only infinitesimal deformation of the cube, the same 100 kN of force will easily crush a granite cube the size of a sugar lump. The reason for the difference in behaviour is the difference in stress felt by the two specimens. Stress is given the SI unit Pascal (N/m^2) and is defined as the force F (N) per unit area A (m^2), such that

$$\sigma = \frac{F}{A} \qquad 2.$$

The symbol σ is commonly used to signify a normal stress, i.e. that the force generating the stress acted normal to the reference plane (in the above example: the cube's surface), and the

symbol τ is used to signify a shear stress, i.e. where the force generating the stress acts parallel to the plane in question.

In the above example the stress felt by the larger cube would be about 1 MPa, only a fraction of typical granite strength. The normal stress on the smaller specimen, however, assuming a 1 cm cube, would be 1000 MPa, far more than can be sustained by any granite.

In earth's crust true tensional stresses are rare (Cosgrove 1995). The sign convention in rock mechanics is therefore that compressional stresses are positive and tensile stresses negative, contrary to many other engineering disciplines. In most rock engineering applications stress magnitude is referred to in megapascal (MPa), which is 10^6 Pa.

At any point in a rock mass three mutually perpendicular planes, devoid of shear stress, can be defined. The normal stresses acting on the three planes, indicated with arrows in Fig. 6 are termed principal stresses, and are commonly denoted σ_1, σ_2 and σ_3—the maximum, intermediate and minimum principal stresses, respectively. The most common stress state in the upper parts of Earth's crust is one where the principal stresses are unequal, such that $\sigma_1 > \sigma_2 > \sigma_3$. This stress state is termed polyaxial stress or true-triaxial stress.

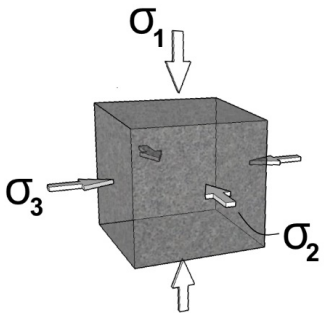

Fig. 6: Principal stresses acting on an imaginary cubical volume of rock

In the proximity of an engineering structure, such as a tunnel, the state of stress will differ from that away from the tunnel. This perturbed stress field close to the structure is called the *near-field*, as opposed to the stress field beyond the influence of the tunnel, which is called the *far-field*, see Fig. 7.

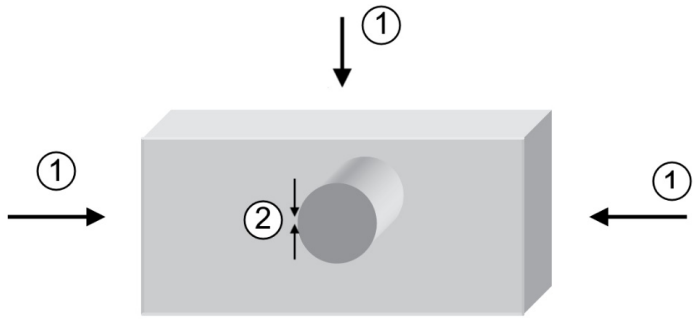

Fig. 7: The difference between the far field stresses (1) and near-field stress (2). Figure modified from (Hudson et al. 2003)

While the stress concentrations in the near-field are highly important when considering the rock support design of a tunnel, the far-field stress is of prime concern when assessing the risk for hydraulic failure of unlined pressure tunnels. The simple reason is that, while the stress state in the near-field could promote hydraulic failure close to the tunnel, any further fracture propagation is governed by the far-field stress state. This is why efforts usually are made to perform rock stress measurements at sufficient distance from the engineering structure in question to ensure that the results are representative for the *far-field*.

2.4 Hydraulic failure of pressure tunnels

Hydraulic failure of pressure tunnels can cause excessive water leakage from the pressure tunnel into the surrounding rock mass, potentially causing serious damage to nearby infrastructure, and often requiring costly rehabilitation works in the failed tunnel. Numerous cases of such hydraulic failures have been reported, see Brekke and Ripley (1987), highlighting the importance of having sufficient knowledge on the underground state of stress.

The broad term *hydraulic failure* is commonly used when describing failure of rock masses caused by excessive water pressure, and it includes the mobilization of pre-existing fractures through hydraulic jacking (extension fracture), shearing (shear fracture), or a combination of the two (Lu, 1987; Rancourt, 2010; Gudmundsson, 2011). It is known that hydraulic failure of unlined pressure tunnels will occur when the tunnel is subjected to an internal water pressure that is sufficiently high to reduce the effective principal stress to a point where the system reaches failure, resulting in a large increase in the rock mass permeability (Rancourt 2010).

2.4.1 Mode of failure

The normal- and shear stress on a plane of arbitrary orientation, such as a planar fracture in a rock mass, will vary as functions of the principal stresses. The relationship can be expressed in the following useful form, assuming a situation of plane stress, where the effect of the intermediate principal stress is ignored (Gudmundsson 2011):

$$\sigma_n = \frac{\sigma_1 + \sigma_3}{2} + \frac{\sigma_1 - \sigma_3}{2} cos2\alpha \quad 3.$$

and for shear stress

$$\tau = \frac{\sigma_1 - \sigma_3}{2} sin2\alpha \quad 4.$$

where σ_n is the normal stress, τ the shear stress and α the angle between the fracture in question and the direction of σ_1.

The same shear- and normal stress relationship can be demonstrated graphically by use of Mohr's circles, as shown in Fig. 8. By constructing a line extending from the centre of the Mohr's circle, through its periphery, at an angle 2α to the normal stress axis, the normal- and shear stress on the plane in question can be found at the line's intersection with the circle.

The various failure modes associated with hydraulic failure can be explained by the use of Mohr's circles: Imagine that the filling up of an unlined pressure tunnel increase the water pressure in the rock mass by some amount P_w. With an increase of water pressure follows a reduction of the effective normal stresses in the rock, but the shear stress remains unchanged, shown as a leftward shift of the Mohr's circle while keeping its diameter unchanged, see Fig. 8 (b). This new stress state is not stable, causing shear failure as indicated by the Mohr's circle touching the failure line. After the failure will stress relief occur due to the shear slip, reducing the maximum principal stress—and a new stable stress state is established. This is represented by the grey, slightly smaller Mohr's circle shown in Fig. 8 (b).

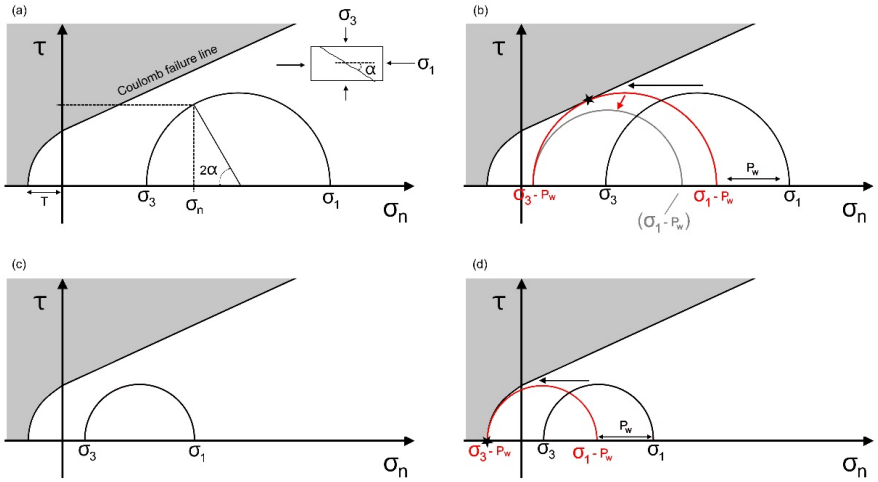

Fig. 8: Hydraulic failure of rock fractures in the rock mass, based on the idealised failure envelope. The star shown in (b) and (d) indicate where the Mohr's circle touches the failure line, indicating failure. The idealised failure line presented in the figures is a combination of the Mohr-Coulomb criteria for shear failure and the Griffith criteria of tensile failure. Figure modified from Cosgrove (1995)

Should, however, the initial stress difference (σ_1-σ_3) be smaller, as illustrated in Fig. 8 (c), the same water pressure increase can cause a different failure mode, as illustrated in Fig. 8 (d). In this case the Mohr's circle touches the failure line in the tensional regime, at an effective stress exceeding the tensile strength of the rock, T, causing extensional failure (hydraulic fracturing) rather than shear failure.

Hybrid failure modes, where fractures fail in both tension and shear can also occur (Gudmundsson, 2011; Vavryčuk, 2014). It has also been described how pre-existing fractures can be activated in shear mode from interactions with nearby extensional failure (hydraulic fracturing), thus causing both extensional and shear failure at the same time but on separate fractures (Dusseault, 2013; Zangeneh et al., 2015).

As discussed in Chapter 2.3 the state of stress near the tunnel will differ from that found away from the tunnel in the far-field. Therefore, a given fluid pressure can cause local hydraulic failure in the near-field, but still be too low to trigger failure further away from the stress concentrations surrounding the tunnel. Should, however, the pressure be sufficiently large to promote failure also in the far-field, the fracture can propagate to significant lengths—potentially causing very serious water leakage.

2.4.2 Fracture propagation

While a propagating fracture to some extent follows pre-existing fractures, will the fracture tend to propagate in a plane that is approximately normal to the direction of σ_3, basically because this is what requires the least amount of energy (Zoback 2007). In the presence of an engineering structure where the stress field is perturbed, a hydraulic fracture can initiate in a direction that is not normal to the far-field σ_3 direction, but once it propagates away from that structure, the fracture will tend to twist and re-align to a plane normal to σ_3 as has been demonstrated from mine-back studies (Warren and Smith 1985), microseismicity studies (Zang et al., 2017b; Guglielmi et al., 2021), in laboratory experiments (Abass et al., 1994; Mao et al. 2017) and also through numerical studies (Zangeneh et al., 2015; Lavrov et al. 2016). A principle drawing of this situation is provided in Fig. 9.

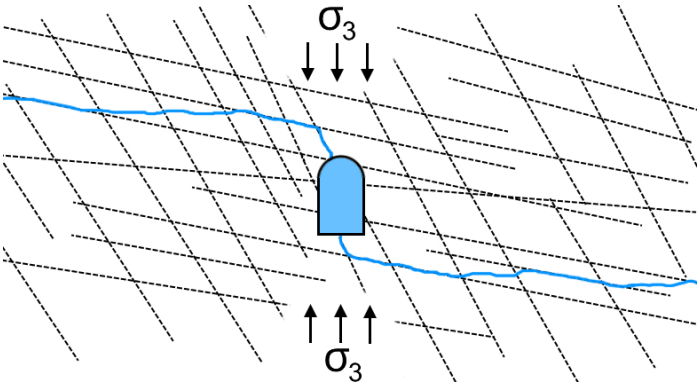

Fig. 9: Simplified representation of hydraulic fracture propagation in a jointed rock mass

As illustrated in Fig. 9 the propagating fracture is not only jacking open pre-existing fractures, but new hydraulic fractures are also created. This is entirely representative of typical field scale conditions, as it is known that the pressure required to propagate a hydraulic fracture, even in intact strong rocks, needs only to be slightly in excess of the minimum principal stress. In other words is the strength of the intact rock essentially unimportant once the hydraulic fracture is initiated and propagated only a very short distance (Hubbert and Willis, 1957; Kehle 1964; Fairhurst, 2003; Zoback 2007).

2.4.3 Seismic response to hydraulic failure

That earthquakes can be triggered by fluid injection was first realised in the 1960s, when a clear correlation between earthquake activity and the injection of wastewater into the rock mass was discovered at the Rocky Mountain Arsenal in the U.S. (Healy et al 1968, in Zoback, 2007). This type of seismic response is created by shear movement, or slip, on faults—and it can be

sufficiently strong to cause damage to surface structures (Rutqvist et al. 2014). In later years such induced seismicity has provably represented a significant challenge for petroleum related injection operations and for deep geothermal projects (Rutqvist and Stephansson, 2003; Häring et al., 2008; Zoback and Kohli, 2019).

That induced seismicity also can be caused by the filling of unlined pressure tunnels seems clear since the basic mechanism is the same, i.e, introduction of pressurised water to a stresses rock mass. A recent case of induced seismicity in such a setting was reported from the hydraulic failure of the Bjørnstokk HPP pressure tunnel in 2016 (Nordal et al. 2018). At this plant a M 2.6 earthquake was believed to have been triggered as a consequence of filling up the unlined tunnel, suggesting that this incident must have been associated with some degree of shear failure. Seismic response has also been reported in association of the hydraulic failure of the pressure tunnel at Fossmark HPP (Garshol 1988). In hindsight it also seems likely that the two earthquakes reported at the same time as the hydraulic failure of the Herlandsfoss HPP in 1919, mentioned in Chapter 2.1, were actually triggered by the pressurised water from the tunnel.

The important insight from the many cases of injection induced earthquakes is that critically stressed faults are quite common in Earth's crust, such that only relatively small changes in effective stresses can cause seismic slip on faults (Engelder 1993).

On a smaller scale the seismic response from hydraulic stimulation of fractures can also be investigated through the analysis of higher frequency seismic response, as done through microseismic (MS) or acoustic emission (AE) studies. Such studies can provide useful information on the fracture propagation and fracture orientation, as well as some insights to the acoustic response from fracture re-opening and closure (Zang et al., 2017a; Gehne, 2018).

Attempts have also been made to link the AE activity registered during fracture closure with fracture normal stress, based on the hypothesis that the moment of fracture closure would provide a unique AE response, see Chitrala et al. (2011) and Bunger et al. (2014). While the link between fracture closure, normal stress and AE response has not been entirely established yet, it is believed to represent a useful supplement to the determination of fracture closure, as discussed in Paper III in this thesis.

2.5 Rock stress estimation for unlined pressure tunnels

The first Norwegian hydroelectric plant using results from rock stress measurements as basis for their final liner design was the Tjodan HPP, where hydraulic fracturing tests were performed in 1981 (Hansen and Hanssen 1988). Since then, stress measurements have become

fairly standard when assessing rock stresses for unlined pressure tunnel design, and hydraulic fracturing (HF) test and variants of hydraulic jacking (HJ) tests are the preferred test methods. Common for both these types of tests is that they seek to find the normal stress acting across a hydraulically stimulated fracture through the injection of water into a sealed-off section of borehole.

The simple reason why the HF test and the various HJ tests are popular in the hydropower industry is that they are fairly reliable, easy to execute, and that they closely resemble the actual situation occurring in a pressure tunnel. Another great benefit is that such tests can be done in fairly deep boreholes, making testing in boreholes sufficiently deep to reach the far-field region away from the tunnel fairly straight-forward.

It can be commented that the two terms *rock stress estimation* and *rock stress measurement* are used somewhat interchangeably in this thesis. The term *estimation* is, however, included to indicate that some judgement is involved, and the term *measurement* usually used to describe a particular test method. This distinction is made to reflect that it is hard to establish precise values for the state of stress *in-situ*—following the notation given by the ISRM (Hudson and Cornet 2003).

2.5.1 Hydraulic fracturing

The hydraulic fracturing test method is based on rapid pressurisation of an intact section of borehole until failure occurs, and then to perform several rounds of re-pressurisation to assess the pressure at which the fracture closes back.

When the borehole is pressurised will a tangential tension, σ_Θ, develop in the borehole wall. Once this tension exceeds the tangential compression induced around the borehole by the *in-situ* rock stress, and also overcomes the tensile strength of the rock, T, a fracture will develop in the sealed off section (Fairhurst 2003). When the borehole is drilled in the direction of one of the principal stresses the orientation of the induced fracture plane will be normal to the minimum principal stress, as shown in Fig. 10.

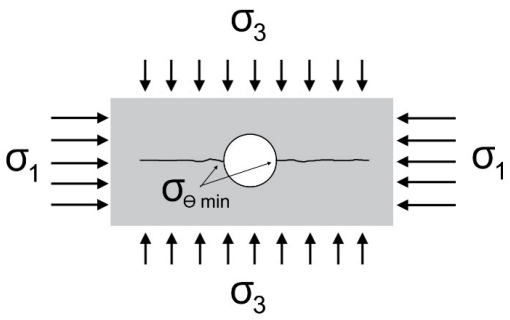

Fig. 10: Cross section of a borehole drilled in the direction of σ_2 showing how the fracture propagates perpendicularly to the direction of σ_3. Figure modified from Haimson (1993).

The pressure in the sealed of section when failure occurs is termed the breakdown pressure, P_b, which can be found from the hydraulic fracturing criterion introduced by Hubbert and Willis (1957):

$$P_b = T + 3\sigma_3 - \sigma_1 - P_0 \tag{5}$$

where σ_1 and σ_3 are the maximum and minimum principal stresses, respectively, and P_0 is the pore pressure in the rock. Through consecutive rounds of pressurisation the fracture will first re-open, at a pressure P_r that is lower than the P_b since the tensional strength of the rock no longer needs to be overcome (Bredehoeft et al. 1976):

$$P_r = 3\sigma_3 - \sigma_1 - P_0 \tag{6}$$

Once opened, is the fracture allowed to close back by shutting off the pump but without venting, such that the test section is shut-in. When doing so the pressure will first drop at a fast rate and then at a slower rate as the fracture closes. The pressure at the end of the initial fast pressure drop is called the instantaneous shut-in pressure, P_S, and it is taken as a measure of the normal stress acting across the stimulated fracture σ_n. Since the fracture is assumed to have opened normal to σ_3 it follows that

$$P_s = \sigma_3 \tag{7}$$

Picking the appropriate P_s value is, however, not always straight-forward—introducing some uncertainty to the σ_3 estimates. Some authors have even questioned the general validity of using shut-in pressure as a reliable measure of σ_3. It is argued that the pressure decline and fracture

closure behaviour is affected by many uncertain processes rendering fracture closure determination too uncertain, and further that the interpretation relies too heavily on the assumption of the ideal fracture geometry (Rutqvist and Stephansson, 1996; Raaen, 2006; Gederaas and Raaen, 2009; Savitski and Dudley, 2011). Other authors argue that the use of shut-in pressures from HF tests can provide highly reliable estimates of σ_3 if tests are conducted under favourable testing conditions, which would include using water as the hydraulic fluid, performing tests in open-hole sections, and ensuring that the boreholes are aligned with the principal stress directions (Zoback, 2007; Zoback and Kohli, 2019).

The orientation of the induced fracture, and thus the σ_3 direction, is usually found by using impression packers, where deformable rubber is inflated to provide the trace of the induced fracture, or by the use of geophysical imaging techniques (Haimson and Cornet 2003). None of these techniques do, however, indicate the fracture orientation away from the borehole wall.

2.5.2 Hydraulic jacking tests

The term hydraulic jacking test is commonly used to describe simple borehole tests where water is injected to find the pressure required to hydraulically jack open pre-existing fractures intersected by the borehole, and from analysis of the pressure development during opening and later closure of the fracture to infer the normal stress acting across the fracture. While the process of hydraulically opening a fracture, oriented randomly to the principal stress directions, locally will alter the stress state, will the normal stress acting across the stimulated fracture remain unchanged, making such test highly attractive for estimating fracture normal stress (Cornet et al. 2003).

Several hydraulic jacking test variants exists, including the step-rate test (Felsenthal 1974), the flowback test (Nolte 1982) the cyclic hydraulic jacking test (Rutqvist and Stephansson 1996), the modified Lugeon test (Philippe et al. 2019), and some more simplified test variants, see Doe and Korbin (1987) and Hartmaier et al. (1998).

For rock stress estimation in connection with unlined pressure tunnel design, the simplified versions of the hydraulic jacking tests are often preferred due to their easy execution and relatively low cost. The typical test approach is to perform several measurements in boreholes of various orientations to increase the likelihood of intersecting the critical joint sets, i.e. those oriented normal to σ_3. When a sufficient number of tests are conducted, is it generally assumed that the assembly of the lowest normal stress estimates will tend to be representative of σ_3

(Hartmaier et al. 1998). This leaves some uncertainty to the stress estimates as it relies on having tested the critical joint sets.

The common Norwegian approach to the HJ test protocol, which is quite similar to that presented in Doe and Korbin (1987), is to pressurise the borehole in a series of pre-set pressure increments, or steps, each step typically maintained for a few minutes, until a sudden increase of flow can be observed, indicating that a fracture has been hydraulically jacked open. The pressure is thereafter lowered in similar steps down to ambient pressure. Throughout the entire test cycle is the flowrate and pressure monitored. The pressure and flow data for each test are then plotted in a flow versus pressure (qP) diagram, and the jacking pressure is found from an assessment of where the qP-plot becomes non-linear (Doe and Korbin, 1987; Hartmaier et al., 1998), see Fig. 11.

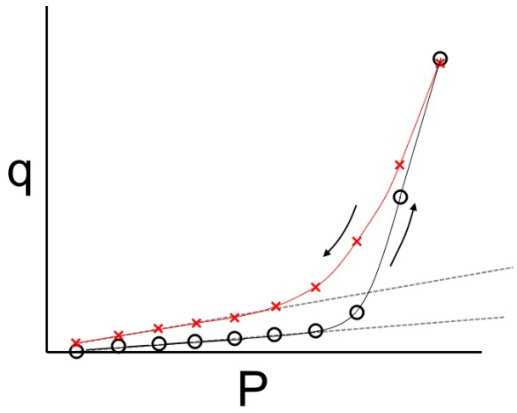

Fig. 11: Idealised qP-plot from a hydraulic jacking test. The dotted lines are included to highlight the deviation from the linear trend. The circles indicate the qP-points during the ascending pressure stage, and the crosses indicate the points on the descending part of the test

As illustrated in Fig. 11 the pressure at which the qP-graph becomes non-linear can differ between the ascending and descending stages of the test, introducing some uncertainty as to which pressure best represents the actual normal stress. According to Rutqvist and Stephansson (1996) the pressure observed during the descending stage, i.e. during fracture closure, should be used, as the fracture opening stage can be affected by gradual opening of the fracture due to effects from non-linear fracture stiffness. The same conclusion was made during the laboratory experiments presented in Paper III in this thesis.

There is also a rather specialized HJ test variant termed the HTPF tests, see Haimson and Cornet (2003), where the complete stress field can be estimated. This is done by performing several hydraulic jacking tests on individual fractures to find the normal stress acting across

them. Provided that normal stress estimates are made from at least eight fractures, each with known and different orientations, the complete stress field can be determined by establishing a best fit function to the normal stress estimates and the orientation of the tested fractures (Cornet 1993). Due to the rather complex procedures this type of HJ test is less commonly used for rock stress estimates of unlined pressure tunnel design, and is thus not any further commented on here.

3 Methodology

3.1 Laboratory testing

The laboratory work conducted as part of this PhD-research includes hydraulic jacking tests conducted on 300 mm cubical granite specimens, with each specimen containing a single planer fracture of known orientation. The normal stress on these fractures could be controlled through confining the specimens in a true-triaxial test frame custom built for the purpose. The experimental setup thus allowed for hydraulic jacking in conditions representative for the field conditions whilst having "ground-truth" in the form of a pre-set and known rock stress acting across the stimulated fracture. An overview of the test frame is shown in Fig. 12, and the full details of the entire test rig and the experimental setup are described in Paper III.

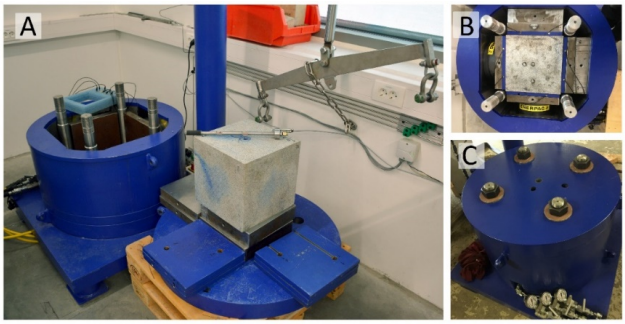

Fig. 12: Overview of the test frame. (A) The specimen resting on the spacer platens prior to specimen assembly (B) a specimen mounted inside the test frame, with AE system connected (black cables sticking out) and (C) the test frame with the top lid on, ready to install packer and start the test

Prior to testing, considerable efforts had been made in the planning and construction of the test rig. The idea behind the experiments was inspired by the work of other researchers who had presented highly relevant research using large scale true-triaxial test rigs to perform laboratory scale hydraulic stimulation of boreholes, and in particularity the work of Frash et al. (2013), Stanchits et al. (2014) and Mao et al. (2017).

After securing funding for the envisaged test rig, the design concept of the main test frame, the key component of the test rig, were settled with the vital support by the mechanical engineers at Sollie Solutions AS, the company selected for manufacturing the test frame.

Several important design updates were also made following a visit to the rock mechanical laboratory at the Colorado School of Mines, where a similar test rig had been developed under the lead of Professor Marte Gutierrez. Once the final design was landed, the test frame was made to order by Sollie Solutions AS, who were also responsible for all aspects of the detailed design.

Once the test frame had been delivered a long commissioning period followed to assemble the entire test rig, including hydraulics, pumps, monitoring- and control systems. Several persons were heavily involved in the rather comprehensive commissioning phase:

1. Assembling the modular test frame (done by the Author)
2. Fixing hydraulic connections and pressure monitoring for the injection pump and for the hand pumps (done by Noralf Vedvik from the NTNU engineering workshop, and in part by the Author)
3. Designing the monitoring system according to the Authors specification, and connecting it (done by Steffen Wærnes Moen from the NTNU engineering workshop, and in part by the Author)
4. Programming the LabView control system required for monitoring and control of the test rig (done by Torkjell Breivik from the NTNU engineering workshop)
5. Machining holes and grooves for the AE sensors in the sensor platens (done by Terje Bjerkan from the NTNU engineering workshop)
6. Initial trials of the test frame (done by the Author with support from Gunnar Vistnes and Jon Drotninghaug, both at the NTNU Rock Mechanical lab)
7. Initial trials of the AE system (done by the Author with valuable contributions made by Lars Nordø as part of his MSc-project)

To test the capabilities of the test rig, and to explore various test protocols, a large number of trials were performed before conducting the experiments described in Paper III (Ødegaard and Nilsen 2021).

3.2 Field work

Extensive field work in the form of full-scale hydraulic jacking tests has also been conducted as part of this thesis. The testing was performed at two hydroelectric plants, the Leikanger HPP and the Løkjelsvatn HPP, both of which are located in Western Norway. At the time of testing the plants were in the constructional stages of development.

The main field campaign was aimed at trying out the RSRT protocol in full field-scale conditions, the experimental campaign and test results from which are presented in full in Paper IV of this thesis.

The author was responsible for the test design and participated in all testing. For the practical execution of the tests the company Injeksjonsteknikk AS was responsible. The company, specialising in rock grouting operations, provided experienced personnel in addition to all testing equipment.

In addition to the field-work related to the full-scale jacking tests described above, several site visits to other HPPs were also made during the PhD period. Although these site visits did not directly result in scientific outcome in the form of publications, they provided valuable insights into various challenges faced when constructing unlined pressure tunnels as briefly described below:

- Bjørnstokk HPP (8.2 MW, run-of-river). The plant was visited during two days in November 2017 when the plant was in full operation. In 2016 a hydraulic failure had occurred in the downstream end of the pressure tunnel, and the author together with a group of researchers from NTNU was allowed inside the failed section of the pressure tunnel. The author conducted detailed mapping of the hydraulically induced fracture. The fracture was still clearly visible and could be readily accessed from within the now dry tunnel section (following the rehabilitation works the penstock had been extended further upstream, leaving the old pressure tunnel as a dry penstock tunnel). Unfortunately, it has not yet been possible to gain permission for the publication of the field observations. Still, the site visit was important for the general understanding of the hydraulic failure of pressure tunnels.
- Hatlestad HPP (4.5 MW, run-of-river). The plant was visited in June of 2018, during the commissioning stage, with the main purpose to enable data collection for a MSc student co-supervised by the author. The site visit was also valuable in providing first-hand experience of potential problems with the installation of steel liners in large

diameter boreholes (Ø610), including issues with sealing the transition between the steel-lined and the unlined section, and the general challenge associated with water sealing works in small-diameter waterways.

- Lidal HPP (7.8 MW, run-of-river). The plant was visited in June 2018 when it was in full operation. The purpose of the visit was to assess the possibility to conduct hydraulic jacking experiments inside the penstock tunnel. It was considered of interest to conduct measurements here since an unusual reduction of the minimum principal stress σ_3 had been reported as the tunnel entered deeper into the massif, opposite to the expected stress increase. Due to practical constraints no additional hydraulic jacking tests could be made here.
- Storåvatn HPP (25 MW, storage plant). The plant was visited January 2020, when it still was under construction. The site visit was made to observe during the execution of hydraulic jacking tests. During testing important observations were made regarding potential issues with flowmeters during pressure controlled HJ tests. The importance of sufficient pump capacity was also demonstrated when no pressure increase could be seen in some of the boreholes.

4 Brief comments on individual papers and their interrelation

4.1 Paper I

This paper provides a general introduction to the topic of rock stress estimation for the final design of unlined pressure tunnels, and addresses the uncertainty of only using overburden criteria to estimate stresses. A suggested new methodology for the estimation of rock stresses is outlined, involving rock stress measurements in a more distributed manner along the entire tunnel, thus replacing the current approach of performing measurements at relatively few locations. The new methodology would reduce the need for extensive and uncertain interpolation of stress data, thus reducing the risk of leaving regions with inferior rock stress magnitude undetected.

To facilitate this new approach, without excessive testing costs, a simplified and more efficient manner of estimating stresses must be adopted. It is believed that simplified hydraulic jacking tests could be well-suited for the purpose. Such tests have been used since the 1980s in Norway, and are typically of relatively low-cost and easy to execute. An example of one such hydraulic jacking test protocol is briefly presented, based on the typical manner of which such tests are conducted in Norway.

The paper also explains how the design process associated with the final design of unlined pressure tunnels is special in the sense that the tender design needs to be verified through investigations that can be made only during the constructional stage of the development. To prepare for tender change adjustment of the tunnel layout, as deemed necessary from rock stress test results, it is proposed to include a specific plan in the tender documents that describes how measurements should be done and how the outcome of these investigations can be accommodated in the design. An example of such a plan, the Investigation Strategy Plan, is outlined in the paper.

This paper thus addresses the overall objective of this thesis, i.e., to contribute to an improved basis for the final design of unlined pressure tunnels by addressing subtasks 1 and 2 of the main objective, see Chapter 1.2.

4.2 Paper II

This paper follows up the argumentation in Paper I on limitations associated with the use of overburden criteria, and the argument is further substantiated through the comparison of σ_3 values found through the use of traditional overburden criteria with σ_3 values found from measurements from the same location. Comparing results from 19 different plants showed how the estimates made through the use of overburden criteria can differ quite significantly from the measured values, demonstrating the inadequacies of the overburden criteria when used for final liner considerations.

The argument from Paper I that a simplified hydraulic jacking test protocol is needed to carry out the proposed new stress estimation methodology is reiterated, and a plan for the development and testing of such a test protocol is presented. The paper also briefly presents the experimental setup for the true-triaxial rig intended to be used in the development of the new test protocol.

Together with Paper I does this paper address Subtasks 1 and 2 of the main Objective.

4.3 Paper III

This paper presents a new simplified hydraulic jacking test protocol which was developed through a series of laboratory experiments conducted in the new true-triaxial test rig, thus following up on the plans outlined in Paper II. The results from the laboratory experiments demonstrates how the new hydraulic jacking test protocol, the Rapid Step-Rate Test (RSRT), can be used to estimate fracture normal stress. The RSRT protocol is presented in detail, and an explanation on how the RSRT can be used to assess fracture normal stress by adopting some of the principles used for step-rate tests and flowback tests is given. The paper provides the first complete description of the experimental setup using a custom-built true triaxial test rig to conduct hydraulic jacking tests. The design choices made to ensure that the laboratory conditions would resemble the actual field scale condition are highlighted.

The link between acoustic emission (AE) and fracture behaviour is also explored, and it is shown how fracture closure can be associated with sudden bursts of AE activity—potentially aiding in the interpretation of fracture normal stress. It is also shown how 3D monitoring of the AE-hypocentres can aid in mapping the orientation of the stimulated fracture.

In the paper it is concluded that the RSRT protocol enables simplified and efficient hydraulic jacking tests that enable estimates of the normal stress magnitude of the stimulated fractures. It is further reported that the pressure observed during the fracture closure stage provided the

most accurate stress estimates, and that the estimates from the re-opening stage were less suitable.

It is suggested that a field verification of the RSRT should be aimed at, and suggestions on how the test protocol can be adapted to field conditions are provided.

This paper answers Subtask 3 of the main Objective.

4.4 Paper IV

This paper presents the field scale experiments conducted underground at two test sites, the Leikanger HPP and the Løkjelsvatn HPP. While successful tests could be achieved only at the Løkjelsvatn site, valuable experience was also achieved during the tests at the Leikanger HPP– and a description of these failed tests are therefore included in the paper.

The experimental campaign at the Løkjelsvatn plant provided the first field-verification of the RSRT protocol, demonstrating how the test protocol developed in Paper III could readily be adapted to field conditions. During the field tests the same characteristic pressure development, as previously had been seen in the laboratory experiments, could be observed—indicating that the field scale RSRT also enables the detection of fracture closure.

The paper presents a simple model explaining the observed fracture behaviour during the closure stage of the RSRT, explaining how the distinct changes in pressure decline observed during the test can be associated with stages of fracture closure. The stress estimates made from the RSRT were compared with the stress estimates made during a foregoing measurement campaign at the same test location. The foregoing campaign had been conducted as part of the plant's final liner design and included both HF tests and overcoring tests. The comparison showed that the minimum principal stress magnitude found from the two different campaigns corresponded quite well.

The paper also describes examples on how unfavourable test conditions can prevent meaningful stress estimates or render the test results not representative for the far field state of stress.

This paper addresses Subtasks 4 and 5 of the main Objective of this thesis.

4.5 Paper V

The paper is a direct result of the interdisciplinary nature of HydroCen, with the original idea behind the paper conceived during a coffee break discussion between the main author (rock engineer) and second author (hydraulic engineer). The main objective has been to discuss hydraulic- and rock engineering design considerations for unlined air cushion surge chambers (ACSCs), and as a starting point for this, a compilation of the layout of all Norwegian ACSCs is made.

In the paper three new design ideas are proposed, and a case study describing the adoption of one of these, the tentative installation of a closing device, is presented for the ACSC at Kvilldal HPP. This case study suggests that large cost savings associated with reduced down-time during necessary de-watering of the waterway could be realised by the installation of the proposed gated plug. The conceptual design of such a plug is presented together with a cost-estimate for the post-construction installation of the plug at Kvilldal HPP.

While not directly addressing rock stress estimation, the paper is considered relevant for the thesis since it aims at improving pressure tunnel design by providing suggestions on how traditional ACSC design can benefit from some simple design modifications. It is also relevant because the final design of ACSCs require sufficient rock stress to avoid hydraulic (or pneumatic) failure, and the same approach to rock stress estimation for unlined pressure tunnels be adopted ACSCs.

5 Discussion

5.1 The approach to rock stress estimation for final liner design

The inherent presumption of overburden criteria, i.e. that the minimum principal stress magnitude varies solely as a function of the weight of overburden, is misleading and render such criteria unsuitable for any reliable rock stress estimation. This is now well established in international literature, and the comparison of stress data presented in Paper II (Ødegaard et al. 2020) provides further examples on how stress estimates made from the use of overburden criteria can deviate significantly from the measured stress magnitude. For this reason, rock stress measurements are now performed routinely as part of the final liner design decision. What is less understood, or at least receiving less attention, is the risk associated with only performing measurements at "key locations" and then to assume that the stress magnitude prevails away from the test location. This approach can lead to cases where stresses are found adequate at the test location, but turn out inferior further into the rock mass, e.g. as observed at some recent Norwegian HPPs[1] and as reported in Haimson (1992).

It is suggested that the best way to reduce the risk of leaving regions of inferior stress undetected is to perform rock stress measurements more regularly along the entire length of pressurised waterway, and not too far behind the advancing excavation front, see Paper I (Ødegaard and Nilsen 2018). In this way local regions of unexpectedly low stress can be detected, and the appropriate design adjustments made in a timely manner. To keep the associated costs of testing within acceptable levels such tests must be both effective, not causing undue hinderance to the normal excavation cycle, and simplified in execution and interpretation. With this as basis a laboratory campaign was designed, aimed at developing a hydraulic jacking test protocol that could satisfy the requirements on simplicity and cost-effectiveness, whilst at the same time providing reliable stress estimates.

5.2 Developing and testing the RSRT protocol

The test rig developed to explore the envisaged hydraulic test protocol was designed in such a way that the normal stress acting across the fracture being tested could be controlled. This was considered a significant benefit as it enabled effective experimentation using various test protocols to see which test approaches worked and which did not work. The experimental setup

[1] Unpublished test data from the Lidal HPP and from a second HPP (the identity of which must be kept undisclosed due to ongoing legal issues).

also provided additional insight to the fracture behaviour during testing through the detailed real-time monitoring of injection pressure, confining pressure and the AE response.

Various hydraulic jacking test protocols were tried out during these initial trials, including the pressure controlled hydraulic jacking tests commonly used in Norway, see Chapter 2.5.2. To avoid the often time-consuming test protocols associated with such tests, alternative approaches were sought. The step-rate test (SRT), a type of hydraulic jacking test popular in the petroleum industry, seemed like a promising alternative since this test protocol did not require steady-state conditions at each step, but still had proved reliable in estimating normal stresses. Inspired by the SRT various step-rate test protocols were tried out, finally ending up with the RSRT protocol. An experimental campaign was thereafter designed where hydraulic jacking tests on four different rock specimens were performed in laboratory using the RSRT protocol, the results from which are reported in Paper III (Ødegaard and Nilsen 2021). Through these laboratory experiments was it found that the true normal stress magnitude could be estimated when analysing the fracture closure stage of the RSRT. Stress estimates made through the analysis of the fracture opening stages of the tests were, however, less representative for the true normal stress—yielding both over- and underestimates.

Following the promising results from the laboratory campaign the RSRT was tried out underground at the Løkjelsvatn HPP, with the aim of obtaining a field verification of the test protocol. Since the laboratory setup from the very start had been designed to allow for easy field adaption, the RSRT protocol could readily be transferred to the field. The test protocol performed satisfactory even from the very first field tests: Not only was the pressure development observed during the tests comparable to the observations made in the lab, suggesting that fracture closure could be detected, but the stress estimates also matched the anticipated stress levels at the test location. Similar to the laboratory findings, the field results indicated that the normal stress estimates should be made during the fracture closure stage of the test, supporting the findings of Rutqvist and Stephansson (1996).

5.3 Interpreting the RSRT data

The interpretative techniques used to analyse the RSRT data are fairly straight forward, adhering to the aspirations of test simplicity and effectiveness. Traditional qP-plots (flow versus pressure) are arguably the most common method to present hydraulic jacking tests data, and they can also be used when analysing the RSRT results. Such plots do, however, miss the aspect of time, which can be disadvantageous since the intuitive understanding of what happens

during the tests can be lost. It was therefore demonstrated how the RSRT protocol allowed for interpretation of fracture closure from simple pressure-time (Pt) plots. This could be done through the identification of characteristic breakpoints on the bilinear pressure decline curve developing during the fracture closure stages of the RSRT. The basis for this interpretative technique is derived from the interpretation the flowback tests, following the "stiffness approach" proposed by Raaen et al. (2001).

The essence of this approach is linked to the observation that when a hydraulically opened fracture is allowed to gradually close back, in a controlled manner, the pressure will decline linearly—the slope of which represents the stiffness of the open fracture. Once the fracture starts to close the slope of the pressure decline curve will gradually steepen until it reaches a new linear stage, and this new slope is believed to be representative for the "stiffness" of the closed fracture, see Fig. 13.

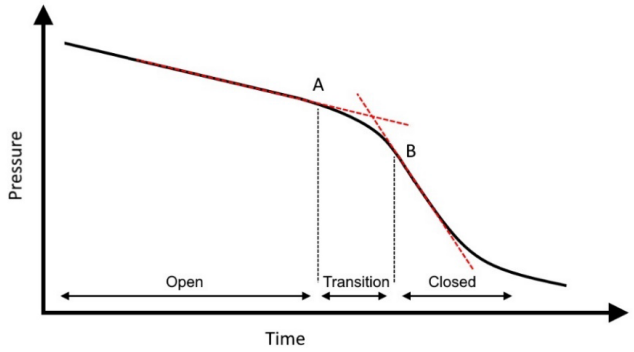

Fig. 13: Idealised stages of fracture closure during the second half of a RSRT. Figure modified from (Savitski and Dudley 2011)

The distinct inflection points (A and B in Fig. 13) thus represents the pressure in the fracture at different stages of fracture closure, which can be used to assess the normal stress acting across the stimulated fracture. Exactly which of these two points that best represents the actual normal stress is subject to some debate in the literature. During the laboratory tests the initial linear stage could be observed only partially, but a clear breakpoint could be detected before the pressure decline followed the anticipated second linear stage of pressure decline, suggesting that this was the same as Point B in Fig. 13. The stress estimate based on this provided good normal stress estimates. The field tests did, however, clearly show both linear stages, and it was found that onset of fracture closure (Point A in Fig. 13) provided the best normal stress estimates.

During the field campaign some practical challenges were encountered that affected some of the tests in a negative way. These issues were mainly related to cases of poorly oriented boreholes, where neighbouring boreholes ended up too close each other, causing cross-hole leakage that invalidated some tests. Two boreholes were also drilled such that they ended up too close to the tunnel periphery, making stress estimates in these boreholes less representative for the *in-situ* stress magnitude. Such unfavourable circumstances could have been avoided if closer follow-up of the drilling process had been made.

Another limitation of the field scale RSRT experiments was that no information on the geometry of the stimulated fractures was obtained. While the fracture orientation could have been obtained through microseismic monitoring, or from the use of a downhole AE-probe, such efforts were considered impracticable and too complicated for the allocated time-frame for testing. The length of the test section also prevented the use of impression packers, which in any case are considered of limited value since they do not provide any information on the fracture orientation away from the borehole.

While the fractures stimulated during the field scale RSRT experiments could have initated in a direction that was not normal to the minimum principal stress, e.g. promoted by pre-existing fractures of stress concentrations near the borehole, does it seems likely that further fracture propagation away from the borehole must have aligned in a plane approxiamtely normal to σ_3. The reason for this assumption is twofold: firstly, fracture propagation in any other direction would be prevented by the fact that σ_3 reportedly is much smaller than the other two principal stresses, and; secondly, the normal stress estimates made from the successful RSRT test cycles were surprisingly close to the σ_3 magnitude found from the preceding HF and OC tests.

It is known from the analysis of flowback tests that normal stress estimates could be prevented when the fracture twists away from the borehole in a manner that prevents hydraulic communication between the borehole and the fracture during testing (Jung et al. 2016). The fairly similar normal stress estimates between boreholes of different orientation supports the notion that such effects have not been significant during the succesful RSRT experiments conducted at the Løkjelsvatn HPP.

The AE-monitoring conducted in the laboratory experiments enabled accurate delineation of the fracture plane through a point-cloud plot of the AE hypocentres. This 3D visualisation was not only valuable to verify the fracture orientation, it could also be used to control that only one single fracture was stimulated during testing. The AE-data also provided valuable

information of the fracture behaviour during testing, demonstrating how AE-signals originate from the dynamic contact of fracture surfaces, not only from fracture propagation.

While the gradual nature of the RSRT protocol prevented any clear detection of fracture closure from AE data, a distinct burst of AE events could be linked to fracture closure when the fracture was allowed to close rapidly. The timing of this AE response was, however, found to be somewhat delayed relative to the actual fracture closure, preventing a clear link between AE event rate bursts and fracture normal stress. It is still considered that AE-monitoring represents a very useful supplement to experimental hydraulic jacking tests in the laboratory, and also for research-type field investigations.

A recurring theme during the development and testing of the RSRT protocol has been to maintain simplicity in execution, materials, and interpretative techniques. While the overall idea behind the development of this rapid test protocol has been to enable a larger number of measurements in the context of unlined pressure tunnel design, is it believed that the unique qualities of the RSRT also could make it an attractive alternative to other stress estimation techniques.

5.4 Suggestions and recommendations for further research

While the field campaign conducted at the Løkjelsvatn HPP provided a first field verification of the RSRT, the number of tests was relatively low, and limited to a single test location. It is therefore suggested that the RSRT protocol is tested at more locations to see if the same promising test behaviour can be observed there.

It is also suggested that the link between fracture closure and AE response is further studied as this potentially could aid in assessing fracture normal stress during hydraulic jacking- or fracturing tests.

While being recognized as a major challenge in both the petroleum- and geothermal industries, induced seismicity caused by the filling-up of unlined pressure tunnels has received little attention. Since the basic mechanisms behind induced seismicity are the same across industries, is it believed that the hydropower industry could benefit from more research on the cause-, extent- and consequence of induced seismicity triggered by the filling of unlined pressure tunnels. This could also be expanded to investigating ways to conduct AE monitoring of pressure tunnels during filling to get an early warning in case of incipient hydraulic failure or other undesirable rock mass responses to water filling. It is believed that such monitoring could

be done through the installation of field-scale AE-sensors or by installing fibreoptic cables enabling distributed acoustic sensing (DAS).

As a potential expansion of the use of the RSRT beyond stress estimation for unlined pressure design, is it suggested that the test is evaluated and tried out as a way to assess the allowable, or safe, pressure during rock mass grouting. As the RSRT protocol in principle also can be done with more viscous fluids than water, it would also be interesting to conduct tests by using ordinary rock grout instead of water, so that the RSRT could be done as an integral part of grouting operations.

6 Conclusions

The main findings of the PhD research can be summarised as follows:

1. The magnitude of minimum principal stress σ_3 can vary irrespectively of the topography above the point of interest, effectively making empirical overburden criteria, such as the Norwegian Criterion for Confinement, unsuitable for reliable estimate of σ_3. Therefore, *in-situ* stress measurements, not overburden criteria, must form the basis for rock stress estimation in connection with the final liner design of unlined pressure tunnels.
2. To reduce the risk of leaving unlined tunnel sections with insufficient rock stress, stress measurements should be performed in a distributed manner, replacing the current tradition of performing measurements at relatively few test locations, requiring uncertain interpolation of stress data.
3. A new hydraulic jacking test protocol, the RSRT, has been developed in an effort to facilitate the large number of measurement locations required when conducting distributed measurements.
4. Through laboratory- and field-scale experiments it has been demonstrated that the RSRT protocol can provide efficient and representative estimates of fracture normal stress. It has also been shown that the test protocol can be adopted to field-scale conditions, making the RSRT directly usable for field-scale estimates of fracture normal stress.
5. Being a flow-controlled hydraulic jacking tests, the RSRT is considered more robust than pressure-controlled hydraulic jacking tests since it requires no flowmeter or PID-control, effectively reducing the number of components that can fail during testing. Test execution is also fairly simple, minimizing the required operator intervention by the semi-automated test protocol
6. The normal stress estimates made through the field scale RSRT experiments were comparable to the σ_3 magnitude found from the preceding rock stress measurement campaign. This suggested that the fractures stimulated during the RSRT had aligned in a plane approximately normal to the σ_3 direction, thus effectively making the normal stress estimate a direct estimate of σ_3.

7. From the laboratory scale RSRT experiments a clear link between fracture closure and a sudden increase in the AE event rate could be seen, suggesting that fracture closure can be detected from AE data—potentially serving as an aid to the interpretation of fracture normal stress.

The overall objective of this thesis was to contribute to an improved basis for the final design of unlined pressure tunnels, with emphasis on rock stress estimation. It is believed that this objective has been achieved through: (A) demonstrating how stress measurements are required for reliable stress estimates; (B) proposing a new methodology for rock stress estimation for unlined pressure tunnels; (C) developing a new hydraulic jacking test method, the RSRT, that can be integrated in the new methodology, and; (D) through lab- and field experiments showing how the RSRT protocol can be used for efficient estimates of fracture normal stress.

7 References

Abass HH, Brumley JL, Venditto JJ (1994) Oriented Perforations - A Rock Mechanics View. Paper presented at the SPE Annual Technical Conference and Exhibition, New Orleans, Louisiana, 1994/1/1/

Benson RP (1989) Design of unlined and lined pressure tunnels Tunnelling and Underground Space Technology incorporating Trenchless Technology Research 4:155-170 doi:https://doi.org/10.1016/0886-7798(89)90049-7

Bergh-Christensen J, Broch E, Ravlo A (2013) Norwegian High Pressure Concrete Plugs. In: Broch E, Grasbakken E, Stefanussen W (eds) Norwegian Hydropower Tunnelling II. Norwegian tunnelling society NFF, Oslo, p 132

Berkey CP, Sanborn JF (1922) Engineering geology of the Catskill water supply Trans Am Soc Civ Eng 48:1029-1595

Bredehoeft JD, Wolff RG, Keys WS, Shuter E (1976) Hydraulic fracturing to determine the regional in situ stress field, Piceance Basin, Colorado Geological Society of America bulletin 87:250

Brekke TL, Ripley BD (1987) Design Guidelines for Pressure Tunnels and Shafts. University of California, Berkeley, U.S.

Broch E (1982) The Development Of Unlined Pressure Shafts And Tunnels In Norway. Paper presented at the ISRM Symposium, Achen, 1982.05.26-28

Bunger AP, Kear J, Dyskin AV, Pasternak E (2014) Interpreting Post-Injection Acoustic Emission in Laboratory Hydraulic Fracturing Experiments. Paper presented at the 48th U.S. Rock Mechanics/Geomechanics Symposium, Minneapolis, Minnesota, 2014.8.18

Chitrala Y, Moreno C, Sondergeld C, Rai C (2011) Microseismic and microscopic analysis of laboratory induced hydraulic fractures. Paper presented at the Canadian Unconventional Resources Conference, Calgary, Canada, 15-17 November

Cornet F (1993) 15 - The HTPF and the Integrated Stress Determination Methods. In: Hudson JA (ed) Comprehensive rock engineering, vol 3. Pergamon, Oxford, pp 413-432. doi:https://doi.org/10.1016/B978-0-08-042066-0.50021-5

Cornet FH, Li L, Hulin JP, Ippolito I, Kurowski P (2003) The hydromechanical behaviour of a fracture: an in situ experimental case study International Journal of Rock Mechanics and Mining Sciences 40:1257-1270 doi:https://doi.org/10.1016/S1365-1609(03)00120-5

Cosgrove JW (1995) The expression of hydraulic fracturing in rocks and sediments Geological Society, London, Special Publications 92:187 doi:https://doi.org/10.1144/GSL.SP.1995.092.01.10

Doe TW, Korbin GE (1987) A Comparison Of Hydraulic Fracturing And Hydraulic Jacking Stress Measurements. Paper presented at the The 28th U.S. Symposium on Rock Mechanics (USRMS), Tucson, Arizona, 1987.1.1

Dusseault MB (2013) Geomechanical Aspects of Shale Gas Development. Paper presented at the ISRM International Symposium - EUROCK 2013, Wroclaw, Poland, 2013/1/1/

Engelder T (1993) Stress Regimes in the Lithosphere. Princeton, New Jersey

Fairhurst C (2003) Stress estimation in rock: a brief history and review International Journal of Rock Mechanics and Mining Sciences 40:957-973 doi:https://doi.org/10.1016/j.ijrmms.2003.07.002

Felsenthal M (1974) Step-rate Tests Determine Safe Injection Pressure on Floods Oil & Gas Journal 72:49-55

Frash L, Gutierrez M, Hampton J (2013) Scale Model Simulation of Hydraulic Fracturing for EGS Reservoir Creation Using a Heated True-Triaxial Apparatus doi:https://doi.org/10.5772/56113

Garshol K Fossmark kraftverk, utlekkasje fra trykksjakt (In Norwegian). In: Berg K, Heltzen AM, Johansen PM, Stenhamar P (eds) Fjellspregningskonferansen, Bergmekanikkdagen, Geoteknikkdagen, Oslo, 1988. Norsk Jord- og Fjellteknisk Forbund, pp 25.21-.25.11

Gederaas TB, Raaen AM (2009) Precise minimum horizontal stress determination from pump-in/flowback tests with drilling mud.

Gehne S (2018) A laboratory study of fluid-driven tensile fracturing in anisotropic rocks. Doctoral, University of Portsmouth

Gudmundsson A (2011) Rock Fractures in Geological Processes. Cambridge University Press, United States of America. doi:https://doi.org/10.1017/CBO9780511975684

Guglielmi Y, Cook P, Soom F, Schoenball M, Dobson P, Kneafsey T (2021) In Situ Continuous Monitoring of Borehole Displacements Induced by Stimulated Hydrofracture Growth Geophysical research letters 48:1-9 doi:https://doi.org/10.1029/2020GL090782

Haimson B (1992) Designing pre-excavation stress measurements for meaningful rock characterization. Paper presented at the ISRM Eurock '92 Symposium on Rock Characterization, London, 4–17 September

Haimson BC (1993) The Hydraulic Fracturing Method of Stress Measurement: Theory and Practice In: Hudson JA (ed) Comprehensive rock engineering, vol 3. Pergamon, Oxford, pp 395-412. doi:https://doi.org/10.1016/B978-0-08-042066-0.50021-5

Haimson BC, Cornet FH (2003) ISRM Suggested Methods for rock stress estimation—Part 3: hydraulic fracturing (HF) and/or hydraulic testing of pre-existing fractures (HTPF) International Journal of Rock Mechanics and Mining Sciences 40:1011-1020 doi:https://doi.org/10.1016/j.ijrmms.2003.08.002

Halvorsen A, Roti JA (2013) Design of unlined headrace tunnel with 846 m head at lower Kihansi, Tanzania. Filling experience. In: Broch E, Grasbakken E, Stefanussen W (eds) Norwegian Hydropower Tunnelling II. Norwegian tunnelling society NFF, Oslo, pp 29-39

Hansen SE, Hanssen TH Hydraulisk splitting (In Norwegian). In: Berg K, Heltzen, A.M, Johansen, P.M., Stenhamar, P. (ed) Fjellspregningskonferansen, Bergmekanikkdagen, Geoteknikkdagen, Oslo, 1988. Norsk Jord- og Fjellteknisk Forbund, pp 26.21-.26.15

Hartmaier HH, Doe TW, Dixon G (1998) Evaluation of hydrojacking tests for an unlined pressure tunnel Tunnelling and Underground Space Technology incorporating Trenchless Technology Research 13:393-401 doi:https://doi.org/10.1016/S0886-7798(98)00082-0

Helwig PC (1987) A theoretical investigation into the effects of water hammer pressure surge on rock stability of unlined tunnels. In: Broch E, Lysne DK (eds) Underground hydropower plants : proceedings of the international conference (Hydropower '87), Oslo, Norway, June 22-25 1987 : Vol. 2, vol Vol. 2. Tapir, Trondheim,

Hubbert MK, Willis DG (1957) Mechanics of hydraulic fracturing Journal of Petroleum Technology:153-168

Hudson JA, Cornet FH (2003) Special Issue on rock stress estimation International Journal of Rock Mechanics and Mining Sciences 40:955 doi:https://doi.org/10.1016/j.ijrmms.2003.08.001

Hudson JA, Cornet FH, Christiansson R (2003) ISRM Suggested Methods for rock stress estimation—Part 1: Strategy for rock stress estimation International Journal of Rock Mechanics and Mining Sciences 40:991-998 doi:https://doi.org/10.1016/j.ijrmms.2003.07.011

Häring MO, Schanz U, Ladner F, Dyer BC (2008) Characterisation of the Basel 1 enhanced geothermal system Geothermics 37:469-495 doi:https://doi.org/10.1016/j.geothermics.2008.06.002

IEA (2021) Hydropower Special Market Report. Paris

IHA (2021) Hydropower Status Report 2021.

Jaeger C (1979) Rock Mechanics and Engineering. Cambridge University Press. doi:10.1017/CBO9780511735349

Jung H, Sharma MM, Cramer DD, Oakes S, McClure MW (2016) Re-examining interpretations of non-ideal behavior during diagnostic fracture injection tests Journal of Petroleum Science and Engineering 145:114-136 doi:https://doi.org/10.1016/j.petrol.2016.03.016

Kehle RO (1964) The determination of tectonic stresses through analysis of hydraulic well fracturing Journal of Geophysical Research 69:259-273 doi:https://doi.org/10.1029/JZ069i002p00259

Lanting G (2021) CC BY 3.0 Wikimedia Commons,

Lavrov A, Larsen I, Bauer A (2016) Numerical Modelling of Extended Leak-Off Test with a Pre-Existing Fracture Rock Mechanics and Rock Engineering 49:1359-1368 doi:https://.doi.org/10.1007/s00603-015-0807-x

Lia L, Jensen T, Stensby KE, Midttømme GH, Ruud AM (2015) The current status of hydropower development and dam construction in Norway International journal on hydropower and dams 22:7

Lu M (1987) A numerical method for the analysis of unlined pressure tunnels in jointed rock. Imperial College London

Mao R, Feng Z, Liu Z, Zhao Y (2017) Laboratory hydraulic fracturing test on large-scale pre-cracked granite specimens J Nat Gas Sci Eng 44:278-286 doi:https://.doi.org/10.1016/j.jngse.2017.03.037

Marulanda A, Ortiz C, Gutierrez R Definition of the use of steel liners based on hydraulic fracturing tests. A case history. In: Stephansson O (ed) Rock stress and rock stress measurements : proceedings of the International Symposium on Rock Stress and Rock Stress Measurements, Stockholm, 1-3 September 1986, Luleå, 1986. Centek Publishers, pp 599-604

Merritt AH (1999) Geologic and geotechnical considerations for pressure tunnel design. Paper presented at the Geo-Engineering for Underground Facilities, University of Illinois, 13-17 June

Neupane B, Panthi KK, Vereide K (2020) Effect of Power Plant Operation on Pore Pressure in Jointed Rock Mass of an Unlined Hydropower Tunnel: An Experimental Study Rock mechanics and rock engineering 53:3073-3092 doi:https://doi.org/10.1007/s00603-020-02090-7

Nolte KG Fracture Design Considerations Based on Pressure Analysis. In: SPE Cotton Valley Symposium, 1982. SPE-10911-MS. doi:https://doi.org/10.2118/10911-ms

Nordal S, Grøv E, Emdal A, L'Heureux JS (2018) Skredene i Tosbotn, Nordland 1. og 2. april 2016. Rapport fra undersøkelsesgruppe satt ned av Nordland Fylkeskommune (In Norwegian). NTNU, Trondheim

Novák P, Moffat AIB, Nalluri C, Narayanan R (2007) Hydraulic structures. 4th ed. edn. Taylor & Francis, London

NVE (2016) Kostnadsgrunnlag for vannkraft (In Norwegian). The Norwegian Water Resources and Energy Directorate, Oslo

Palmstrom A, Broch E (2017) The design of unlined hydropower tunnels and shafts: 100 years of Norwegian experience International journal on hydropower and dams 3:1-9

Philippe V, Eda Q, Milton Assis K, Tom J, Mehmet E (2019) ISRM Suggested Method for the Lugeon Test Rock mechanics and rock engineering 52:4155-4174 doi:https://doi.org/10.1007/s00603-019-01954-x

Price NJ, Cosgrove JW (1990) Analysis of geological structures. Cambridge University Press, Great Britain

Rancourt AJ (2010) Guidelines for preliminary design of unlined pressure tunnels. PhD, McGill University

Rutqvist J, Cappa F, Rinaldi AP, Godano M (2014) Modeling of induced seismicity and ground vibrations associated with geologic CO2 storage, and assessing their effects on surface structures and human perception International Journal of Greenhouse Gas Control 24:64-77 doi:https://doi.org/10.1016/j.ijggc.2014.02.017

Rutqvist J, Stephansson O (1996) A cyclic hydraulic jacking test to determine the in situ stress normal to a fracture International Journal of Rock Mechanics and Mining Sciences and Geomechanics Abstracts 33:695-711 doi:https://doi.org/10.1016/0148-9062(96)00013-7

Rutqvist J, Stephansson O (2003) The role of hydromechanical coupling in fractured rock engineering Hydrogeology Journal 11:7-40 doi:https://doi.org/10.1007/s10040-002-0241-5

Raaen AM (2006) The pump-in/flowback test improves routine minimum horizontal stress magnitude determination in deep wells.

Raaen AM, Skomedal E, Kjørholt H, Markestad P, Økland D (2001) Stress determination from hydraulic fracturing tests: the system stiffness approach International Journal of Rock Mechanics and Mining Sciences 38:529-541 doi:https://doi.org/10.1016/S1365-1609(01)00020-X

Savitski AA, Dudley JW Revisiting Microfrac In-situ Stress Measurement via Flow Back - A New Protocol. In: SPE Annual Technical Conference and Exhibition, 2011. SPE-147248-MS. doi:https://doi.org/10.2118/147248-ms

Schjerven H (1921) Tryktunnelen ved Herlandsfossen (In Norwegian). Den Norske Ingeniør- og Arkitekt-forening og Den Polytekniske Forening, Oslo, Norway

Selmer-Olsen R (1970) Experience with Unlined Pressure Shafts in Norway. Paper presented at the Large Permanent Underground Openings - proceedings of the international symposium, Oslo,

Stanchits S, Surdi A, Gathogo P, Edelman E, Suarez-Rivera R (2014) Onset of Hydraulic Fracture Initiation Monitored by Acoustic Emission and Volumetric Deformation Measurements Rock Mechanics and Rock Engineering 47:1521-1532 doi:https://doi.org/10.1007/s00603-014-0584-y

Svee R (1972) Surge chamber with an enclosed, compressed air-cushion Paper presented at the International Conference of Pressure Surges, Canterbury, England,

USACE (1997) Engineering and Design. Tunnels and shafts in rock. Department of the army. U.S. Army Corps of Engineers, Washington, DC

Vavryčuk V (2014) Earthquake Mechanisms and Stress Field. In: Beer M, Kougioumtzoglou IA, Patelli E, Au IS-K (eds) Encyclopedia of Earthquake Engineering. Springer Berlin Heidelberg, Berlin, Heidelberg, pp 1-21. doi:https://doi.org/10.1007/978-3-642-36197-5_295-1

Vogt JHL, Vogt F (1922) Tryktunneller og geologi (In Norwegian) vol 93. Norges geologiske undersøkelse, Kristiania

Warren WE, Smith CW (1985) In situ stress estimates from hydraulic fracturing and direct observation of crack orientation Journal of Geophysical Research 90:6829-6839 doi:https://doi.org/10.1029/JB090iB08p06829

White L (1913) The Catskill Water Supply. First edn. John Wiley & Sons, Inc., New York

Zang A et al. (2017a) Hydraulic fracture monitoring in hard rock at 410 m depth with an advanced fluid-injection protocol and extensive sensor array Geophys J Int 208:790-813 doi:https://doi.org/10.1093/gji/ggw430

Zang A, Stephansson O, Zimmermann G (2017b) Keynote: Fatigue Hydraulic Fracturing Procedia Engineering 191:1126-1134 doi:https://doi.org/10.1016/j.proeng.2017.05.287

Zangeneh N, Eberhardt E, Bustin RM (2015) Investigation of the influence of natural fractures and in situ stress on hydraulic fracture propagation using a distinct-element approach.(Report) Canadian Geotechnical Journal 52:926 doi:https://doi.org/10.1139/cgj-2013-0366

Zoback MD (2007) Reservoir geomechanics. Cambridge University Press, Cambridge

Zoback MD, Kohli AH (2019) Unconventional reservoir geomechanics : shale gas, tight oil and induced seismicity. Cambridge University Press, Cambridge

Ødegaard H, Nilsen B (2018) Engineering Geological Investigation and Design of Transition Zones in Unlined Pressure Tunnels. Paper presented at the ISRM International Symposium - 10th Asian Rock Mechanics Symposium, Singapore, 29.10-2.11 2018

Ødegaard H, Nilsen B (2021) Rock Stress Measurements for Unlined Pressure Tunnels: A True Triaxial Laboratory Experiment to Investigate the Ability of a Simplified Hydraulic Jacking Test to Assess Fracture Normal Stress Rock Mechanics and Rock Engineering 54:21 doi:https://doi.org/10.1007/s00603-021-02452-9

Ødegaard H, Nilsen B, Barkved H (2020) Design of Unlined Pressure Tunnels in Norway – Limitations of Empirical Overburden Criteria and Significance of In-Situ Rock Stress Measurements. Paper presented at the ISRM International Symposium - EUROCK 2020, physical event not held, 2020/11/4/

Aasen O, Ødegaard H, Palmstrom A (2013) Planning of Pressurized Headrace Tunnel in Albania. In: Broch E, Grasbakken E, Stefanussen W (eds) Norwegian Hydropower Tunnelling II. Norwegian tunnelling society NFF, Oslo, p 132

Paper I

Engineering Geological Investigation and Design of Transition Zones in Unlined Pressure Tunnels

Henki Ødegaard[a]* and Bjørn Nilsen[a]

[a] *Norwegian University of Science and Technology NTNU, Trondheim, Norway*
* henki.odegaard@ntnu.no

Abstract

The transition zone, i.e. where the pressurized water enters the steel lined section of the waterway, is a key component of the entire tunnel system in any underground hydropower project utilizing unlined pressure tunnels. Not only is it important for conveying the pressurized water into the turbine, its positioning also defines the location, length and layout of several other tunnels. The key for deciding on positioning of the transition zone is to identify a place with sufficient in-situ rock mass stress to withstand the internal water pressure generated from the hydraulic head of the pressure tunnel. To prepare complete tender documents, preliminary positioning of the transition zone must be defined before sufficient stress data for final positioning are available. In Norway, such early assessments have often been made on empirical basis with little or no testing. Even though this approach normally is necessary in the preliminary phase of a project development, the final decision on transition zone positioning, must be based on in-situ testing. Recognizing that stress testing is required for safe design of the transition zone, flexibility in both layout and construction schedule should be incorporated in the project. To ensure this flexibility, the tender documents must include a specific plan that describes what ground investigations should be done, where they should be done, what the acceptable criteria for such tests are, and how the results should be adopted in the design. In this paper, a proposal on the outline of such a plan will be presented based on Norwegian experience and practice in investigation, design and construction of the transition zone area for selected projects. The work presented is part of the hydropower research being performed at HydroCen, based at NTNU in Trondheim, Norway.

Keywords: Hydropower tunnels, rock stress, transition zone (cone)

1. Introduction

As water conduits for energy production, rock tunnels constitute an integral part of underground hydropower projects. In Norway, the use of unlined pressure tunnels has become the norm for any underground hydropower project, and the concept has achieved worldwide recognition (Rancourt, 2010). The main motivation for adopting the unlined concept is the potential for very large cost reductions when replacing a steel or concrete lined tunnel with an unlined tunnel. There are, however, several reports of unlined pressure tunnels not performing as expected due to hydraulic failure of the tunnel caused by the internal water pressure, as documented by Broch (1982), Merritt (1999) and Palmstrom and Broch (2017) amongst others. To reduce the risk associated with hydraulic failure of unlined pressure tunnels, knowledge about rock stresses in the area of interest is required. Obtaining such information in due time for preparation of tender documents can be difficult due to the inherent limitations of the stress measuring methods, combined with the often difficult physical access to the investigation point. Therefore, project owners and engineers often have to make their tender stage tunnel design without direct stress measurements, and postpone rock stress measurements to the construction phase. This implies that changes to the tender design must be allowed for, in case insufficient stress levels are identified during construction stage stress measurements (Halvorsen and Roti, 2013).

A specific plan describing the testing- and design methodology for the siting of the transition zone is a useful common basis for both Contractor and Client when deciding the final design. The outline of such a plan is presented herein, based on Norwegian experience and practice in investigation, design and construction of the transition zone area in hard rock conditions. The plan is specially emphasizing the rock stress measurements, though it is recognized that knowledge about the overall rock mass conditions is essential in any underground design.

A key requirement for using unlined pressure tunnels is that, at any point along the pressurized waterway, the rock stress surrounding the tunnel must be larger than the internal water pressure. If not,

the water pressure can lift, or jack, the rock mass so that hydraulic failure and associated large leakages occur. Excessive leakages from the pressure tunnel can cause catastrophic events such as flooding of nearby underground structures and even landslides as reported by Brekke and Ripley (1987), Benson (1989) and Palmstrom and Broch (2017). To avoid such incidents it is absolutely required to ensure that any section of unlined pressure tunnel has sufficiently high rock stresses to accommodate the internal water pressure.

During normal turbine operations, the function of a pressure tunnel is to transmit water from a water reservoir located at a high elevation, downstream into one or several turbines located in a powerhouse, as schematically shown in Fig. 1. At some point upstream of the power station, a steel liner is installed for conveying the water into the powerhouse where the turbines are located. With an unlined concept, the starting point of this steel liner, often called the transition zone, is governed by the in situ rock stress since any tunnel section where the minimum rock stress is less than the internal water pressure must be steel lined.

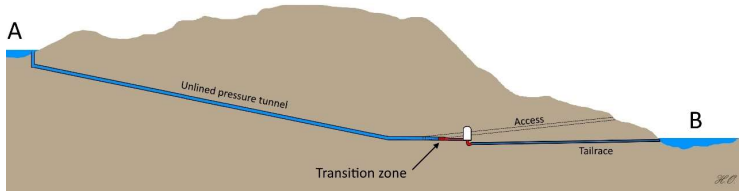

Fig. 1. Idealised long section of a pressure tunnel system

2. Rock stresses

Rock stresses are affected by many factors such as geologic and tectonic history, topography, and heterogeneities causing changes in rock mass E-modulus, such as faults and weakness zones (Fairhurst, 2003). Additionally, the original state of stress is disturbed by any nearby opening in the rock mass, such as an excavation, cave or open joint, where the rock stress locally will rotate and the magnitude change (Hudson et al., 2003). An explicit example of just how much rock stresses can vary over short distances was presented by Martin and Chandler (1993) in their paper describing the rock mass conditions in the Underground Research Laboratory (URL) in Canada. Here it was described how comprehensive rock stress measurements, performed in a relatively homogeneous pluton, showed highly variable stress magnitudes and orientations, as can be seen in Fig. 2.

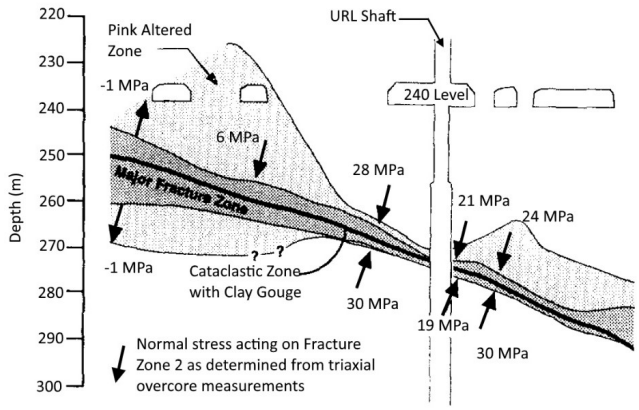

Fig. 2. Figure showing how geological structures can change the stress magnitudes and direction over short distances. Figure modified after Martin and Chandler (1993).

The most commonly adopted stress measurement methods for pressure tunnel design in Norway are hydraulic fracturing tests in addition to some simplified water pressure tests. The great benefit of tests using hydraulic pressure is that they closely simulate what would occur in a pressure tunnel, and that they test a relatively larger area of the rock mass than do various other stress measurement methods based on stress release.

Before direct stress measurements were readily available, engineers needed other means for estimating the rock mass stress at a given location. This was done by using various rules of thumb, or criteria, which represented simple limit equilibrium methods where only the gravitational rock stresses were included (Nilsen and Thidemann, 1993).

2.1. Empirical criteria for assessing rock stresses from weight of overburden

Internationally, one of the most used criteria is the Norwegian Criterion for Confinement, developed by Bergh-Christensen and Dannevig (1971). This criteria state that the stress generated from the weight of the overburden, corrected for slope angle, must exceed the pressure from the water column. Or, by looking at Equation 1, the criterion indicate what the minimum overburden, L, must be for different values of head (H) and slope angle β , see also Fig. 3.

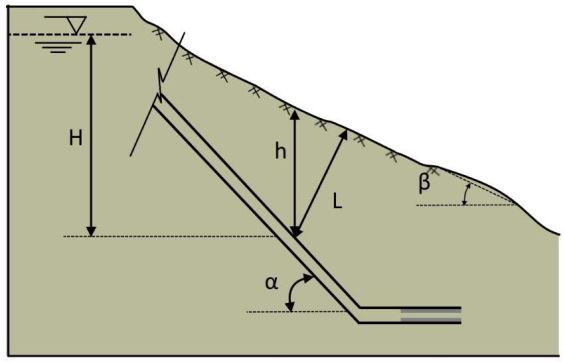

Fig. 3. Norwegian criterion for confinement, figure design based on Bergh-Christensen and Dannevig (1971)

$$L > \frac{\gamma_w \times H}{\gamma_r \times cos\beta} \quad (1)$$

γ_w = Unit weight of water
γ_r = Unit weight of rock

Despite the usefulness of this criterion during early project phases, and the previous widespread use also for final design, it has some major shortcomings that renders its use for final design of unlined pressure tunnels questionable (Merritt, 1999). One such shortcoming is that the criteria assume direct relationship between overburden and rock stresses, whilst it is known that the minimum principal stress do not necessarily correlate with the weight of overlying rock mass, neither do it necessarily increase with increasing overburden. The recent hydraulic failure of the pressure tunnel belonging to Bjørnstokk HPP in Norway further document the inadequacy of this criteria for final design (Palmstrøm and Buen (2017).

2.2. Hydraulic fracturing

The hydraulic fracturing (HF) method for stress determination originates from a technique developed by the petroleum industry to stimulate oil production. It has been used commercially since the early fifties, and the method has since also been developed as one of the most reliable methods for direct measurement of the minimum principal stress of rock masses, σ_3. The test procedure is standardized by ISRM (Haimson and Cornet, 2003) and ASTM (ASTM, 2008).

Referring to Fig. 4, the basic principle of this test can be summarised as follows (Smith and Montgomery, 2014):

1) A borehole is drilled into rock in the direction of one of the principal stresses, in this case assumed drilled horizontally from within a tunnel.
2) A straddle packer is used to isolate the test section.
3) The packer is expanded and fluid (usually water) is pumped into the section at a higher rate than it can escape.
4) At a pressure P_f, the rock breaks, with the borehole splitting along its axis due to tensile hoop stresses generated by the high internal pressure.

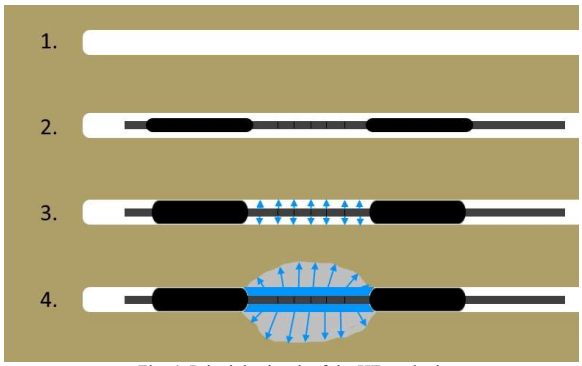

Fig. 4. Principle sketch of the HF method.

Once a fracture is initiated and water enters, it will propagate at a pressure just above the normal compression acting across the fracture. Shutting off the pump and closing the pressure system should allow the fluid to stop flowing in the fracture, so that pressure losses due to flow are eliminated, assuming that leakage into the rock mass can be ignored. This static pressure is known as the Instantaneous Shut-In Pressure (ISIP), or P_S (Fairhurst, 2003). During repeated pressurisation of the same test section, the fracture created from the first pressurisation cycle will re-open at a pressure lower than what was needed to generate the fracture as the tensional strength of the rock no longer needs to be overcome (Haimson and Cornet, 2003). By performing repeated pressurisation cycles in the same section, several values can be obtained. The P_S value, under ideal conditions, can be taken as equal to the minimum principal rock stress, σ_3.

2.3. Simplified water pressure test

A somewhat experimental test method for measuring rock mass stresses has since the eighties been practiced in Norway, as a way of estimating the minor principal rock stress in relation to pressure tunnel design. The method has many variants, and is somewhat similar to more established tests such as the cyclic hydraulic jacking test (Rutqvist and Stephansson, 1996) the step rate test (Smith and Montgomery, 2014) or modified Lugeon test (Houlsby, 1976). An example of this simplified pressure test method is described below. At each measuring locality:

1. Three 15 m long holes are drilled, by percussion drilling, in three different directions at the face of the tunnel in question, trying to intersect all main joint sets.
2. A single mechanical packer, connected to a grouting rod is fixed at a certain depth in the hole, avoiding bypass into the tunnel.
3. The hole is pressurized in several pre-defined increments until a sudden increase of flow is registered (jacking). After jacking occurs, the pressure is reduced in the same increments—thus creating a loop. Each pressure increment is maintained for 2–5 min.
4. After venting the hole after the first cycle, the pressure cycle is repeated at least once for the same hole section.
5. All data for pressure, flow and time are continuously registered during the test.

When plotted on a pressure-flow diagram, as shown in Fig. 5, the first pressure cycle can indicate what pressure is needed to open an existing joint, indicated as "1_Pb" in the figure. Consecutive test cycles will indicate the pressure needed to re-open or shut the joint, in the provided example in Fig. 5 corresponding to approximately 30 bar. In the legend to the right of Fig. 5, the prefix signifies whether it is first or second pressure cycle, whilst "Up" and "Down" relates to increasing or decreasing pressure increments, respectively.

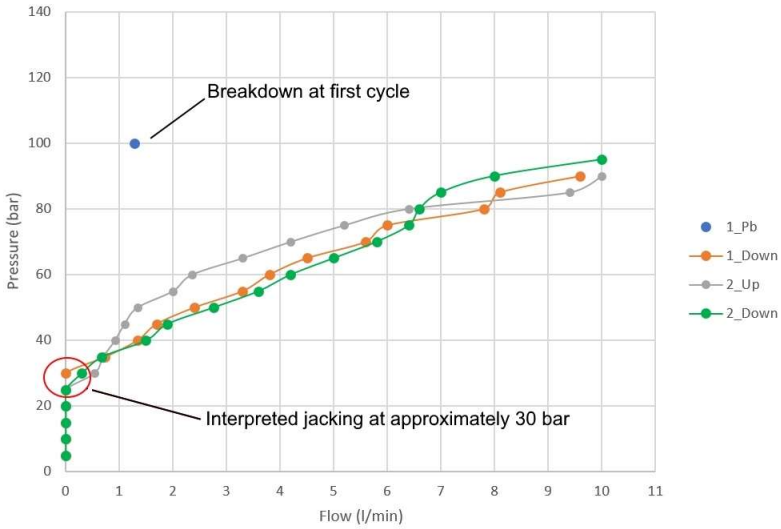

Fig. 5. Example of a field measurement result from a simplified pressure test.

The benefit of this method is that it can be performed without much hindrance to the ordinary excavation cycle; it can be performed by using commonly available equipment available for rock grouting; and if executed properly it indicates what would actually happen in the rock mass during water filling of the tunnel system. Since the necessary equipment for performing this test for the most part is what you would need during ordinary grouting operations, trained tunnelling crew can be used for performing the test. This will reduce costs significantly compared to ordinary HF test. Recent project experience in Norway indicate that the cost of these simplified tests typically can cost around 10–20 % of what standard HF tests cost.

2.4. Recommended stress measurement principle

Though extreme, the URL example provided in Chapter 2 serves as an example of the very large stress variations that can occur over relatively short distances in a rock mass at shallow depths. If left undetected, such large stress variations can have serious effect on unlined pressure tunnels.

If HF measurements are performed in an area of locally high stress, thus leading designers to conclude on satisfactory safety against hydraulic failure, the remaining (untested) section of pressure tunnel might experience lower stress levels, which could represent an unsafe design. Typically, on smaller Norwegian hydroelectric projects, only one or two rounds of measurements are performed due to budget limitations set by the Client. This contrasts the ideal, which would be a continuous log of the least principal stress along the pressure tunnel. One way to get closer to this ideal is to implement the simplified water pressure test as a supplement to the standard HF test. Then, standard HF tests should be performed at key locations, as per the current practice, and these measurements could be supplemented by simplified water pressure tests performed in the tunnel stretches between HF test locations. This would require that a standard procedure for the recommended simplified water pressure tests is established, and that the correlation between the simplified water pressure tests and the standard

HF tests is investigated. Investigating any such correlation and establishing a testing procedure for this simplified pressure test is part of ongoing research associated with the HydroCen project.

Currently, only preliminary data from parallel tests by standard ISRM HF testing and the simplified pressure test performed in the same area are available. These data were gathered as part of the investigation programme for the design of the unlined pressure tunnel belonging to the 22.5 MW New Verma HPP in Central Norway. From the same approximately 40 m long test section in the pressure tunnel the following estimates of the minor principal rock stress were made:

- Standard HF test results show relatively large scatter, indicating σ_3 values between 2.9–7.6 MPa, originating from 24 shut-in values performed in five holes. The largest values originate from tests performed in two holes drilled orthogonally compared to the other three
- Simplified pressure tests in the same area show significantly lower values, in the range of 1–3 MPa, but interpretation of the pressure data is uncertain due to lack of information on testing conditions.
- From overburden assessments using the Norwegian criterion for confinement, σ_3 values in the range of 2.5–2.7 MPa were anticipated

For the time being, not enough information of the testing regime for the simplified pressure tunnel is available for meaningful conclusion on any correlation with the HF tests. Further evaluation of this and other available datasets, together with additional parallel testing at ongoing project and laboratory testing of hydraulic failure, will be performed as part of this PhD project connected to HydroCen.

3. Investigation strategy plan

3.1. Background

Deciding where to locate the transition zone is usually a trade-off between the desire to keep the power station cavern close to the surfacewith reduced costs due to shorter service- and access tunnel length, and the requirement to locate the transition zone where the rock stresses are sufficiently high to avoid hydraulic failure. From a planning and contractual point of view, it is desirable to decide the final position of the transition zone as early as possible, since its position governs the layout and location of the powerhouse complex with appurtenant tunnels. Unfortunately, due to the inherent heterogeneous nature of most rock masses and the limitations of rock stress measuring techniques, the decision on the final position of the transition zone must await the results from rock stress measurements performed in the tunnels close to the transition zone.

3.2. Objective

To verify the tender stage stress assumptions an investigation strategy plan, specifying the ground investigation programme to be performed concurrent with tunnel excavation, must be included in the tender documents. When and where the specified investigations described in the plan can be executed depend on the chosen excavation sequence, something that must be taken into account such that the access to key investigation points is prioritized.

3.3. Main approach

The main purpose of the investigation programme is to find a safe location for the transition zone. At this location, and any location upstream of this, the rock stress requirements must met. The stress requirement must be defined explicitly in the tender documents, as a minimum acceptable value of the least principal stress, σ_3. In Norway the following requirements are often used (Aasen et al., 2013):

- σ_3 should be 20-30 % higher than the maximum dynamic head
- σ_3 should be 30-50 % higher than the static head.

The strategy plan is organised such that some key test-locations in the tunnel system are pre-defined, where set requirements for rock stress, rock mass quality and permeability are given. Focusing on the stress requirements, the following constitute the concept of the plan (see also Fig. 6 and Fig. 7):

1. The first test location, TL1, is typically located a few hundred meters inside the main access leading to the transition zone. Here, a first indication of stress levels is given by standard HF tests is given.
2. After passing TL1, simplified pressure tests are performed regularly to get an continuous log of stress levels, and also to get an early warning in case of unforeseen stress levels, thus allowing early preparation for relocation
3. The second test location TL2, is located close to the transition zone and serves as a verification test site for the tender design, in case TL1 showed satisfactory conditions. Satisfactory results here indicate that the tender design can be maintained, and that the access tunnels to power station, to tailrace and to the headrace can be branched off from the main access.
4. Even after concluding on satisfactory conditions in TL2, thus confirming tender design, regular measurements using the simplified pressure test should be performed in the entire pressurized water way, to investigate any potential low stress zone further upstream.

If the stress measurements show inadequate stress levels, the layout should be designed to allow for an inward shift of the transition zone and power station complex without excessive increase of total tunnel length. The investigation plan should also allow for such changes, as indicated by the TL1(b) location, serving as an additional test location in case TL1 showed unexpectedly low results. As indicated in the idealised longitudinal section in Fig. 7, an inward shift of the transition zone would only increase the access tunnel length, as well as giving a bit longer pressure shaft. The waterway would essentially stay the same length.

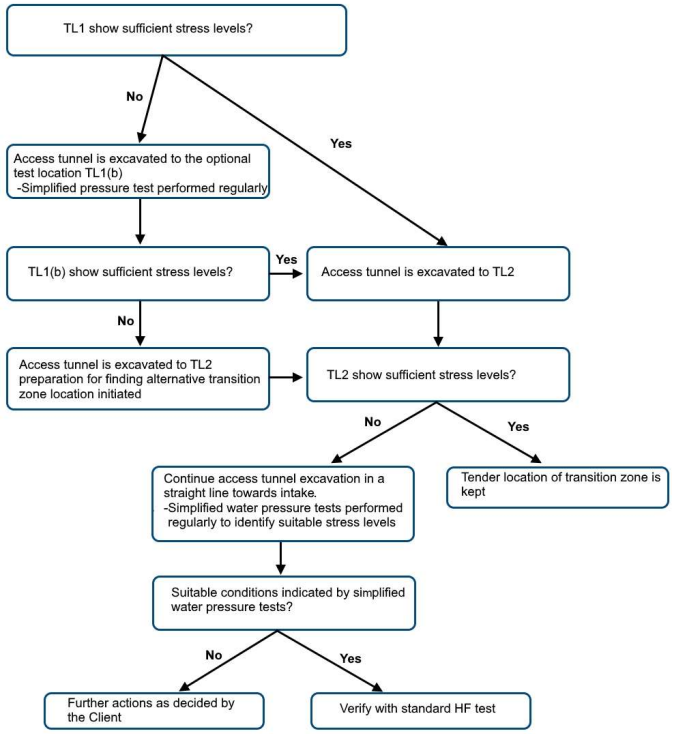

Fig. 6. Flow chart for stress measurement campaign

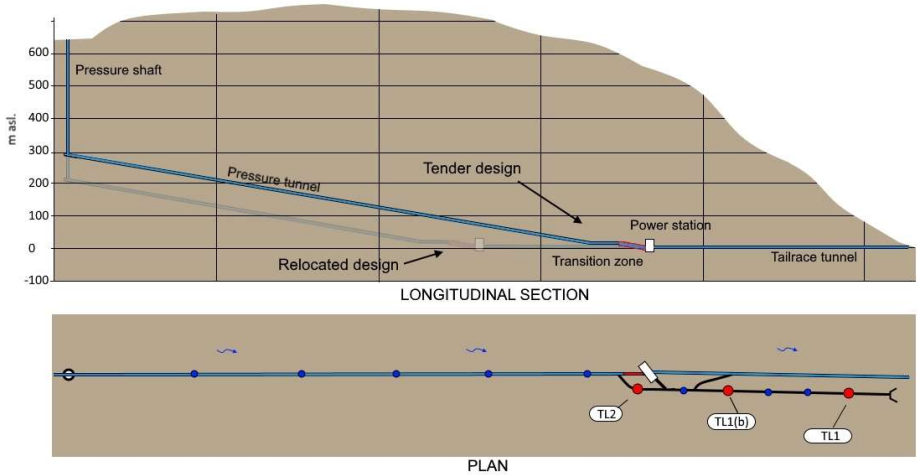

Fig. 7. Idealized overview of a unlined pressure tunnel system. The red circles in the plan drawing indicate hydro fracture (HF) test locations; blue circles indicate test locations for simplified water pressure tests.

3.4. General tender design considerations

By accepting that the tender design might be modified during the construction phase, measures to ease these changes must be included in the tender documents. As a very general starting point, the following five measures are suggested to ease the contractual handling of the foreseen changes:

1. Ensure that all parties engaged in the project (Client, consultants, contractors and government) are aware that tender design of the pressure tunnel system might be changed during construction, state this in relevant tender documents.
2. Ensure that such changes are allowed for in the tender document, e.g. by adopting a unit price and unit time system for the contract (Halvorsen and Roti, 2013).
3. Ensure that relevant access permits allow for necessary relocation of key infrastructure, such as aeriation shafts and access roads to these.
4. Align the access tunnel and pressure tunnel in the same approximate direction, similar to that of increasing overburden, and do not branch off from the access tunnel before the first direct stress measurements have confirmed tender stage assumptions regarding stress state. This reduces the necessary length of tunnel in case relocation of the transition zone is necessary
5. Ensure that excavation of the access tunnel towards the transition zone is given top priority so that final siting of this area can be done as soon as possible. This should be stated in contract documents.

4. Conclusions

To ensure safe and rational design of unlined pressure tunnels, knowledge about the minor principal stress of the rock mass is crucial. This knowledge can only be gained with any confidence by direct stress measurements performed in close proximity to the volume of rock to be investigated. In practice, this means that the tender design must be adjusted to accommodate changes as deemed necessary from detailed investigations during excavation. To minimise the negative effect such changes can have on the project, the tender design layout and contract should be prepared for changes by adopting a flexible layout and a unit price and unit time system for the contract. Furthermore, a plan specifying the details of the planned investigations should accompany the tender documents. This plan must give an indication of the necessary design changes in case of unsatisfactory investigation findings.

To enhance the resolution of stress data, enabling a more continuous “stress-log” of the entire pressure tunnel system, a supplementary stress estimation method, informally called the “simplified pressure test”, is proposed. More research is needed, and planned for in the ongoing HydroCen project (HydroCen, 2018), to develop this method, and to investigate any correlation between the method and the established HF test. Hopefully, this test method could serve as a useful supplement to the established HF test method.

Acknowledgements

The authors wish to thank Rauma Energi AS for granting us access to measurement data from the New Verma HPP. The Research Council of Norway (NFR) is acknowledged for financing this ongoing research through HydroCen.

References

AASEN, O., ØDEGAARD, H. & PALMSTROM, A. 2013. Planning of Pressurized Headrace Tunnel in Albania. *In:* BROCH, E., GRASBAKKEN, E. & STEFANUSSEN, W. (eds.) *Norwegian Hydropower Tunnelling II.* Oslo: Norwegian tunnelling society NFF.

ASTM 2008. Standard Test Method for Determination of In-Situ Stress in Rock Using Hydraulic Fracturing Method. ASTM International.

BENSON, R. P. 1989. Design of unlined and lined pressure tunnels. *Tunnelling and Underground Space Technology incorporating Trenchless Technology Research,* 4**,** 155-170.

BERGH-CHRISTENSEN, J. & DANNEVIG, N. T. 1971. Engineering geological evaluation of the unlined pressure shaft at the Mauranger hydropower plant (in Norwegian). Oslo: GEOTEAM A/S.

BREKKE, T. L. & RIPLEY, B. D. 1987. Design Guidelines for Pressure Tunnels and Shafts. Berkeley, California: University of California, Berkeley.

BROCH, E. 1982. The Development Of Unlined Pressure Shafts And Tunnels In Norway. *ISRM Symposium.* Achen: International Society for Rock Mechanics and Rock Engineering.

FAIRHURST, C. 2003. Stress estimation in rock: a brief history and review. *International Journal of Rock Mechanics and Mining Sciences,* 40**,** 957-973.

HAIMSON, B. C. & CORNET, F. H. 2003. ISRM Suggested Methods for rock stress estimation—Part 3: hydraulic fracturing (HF) and/or hydraulic testing of pre-existing fractures (HTPF). *International Journal of Rock Mechanics and Mining Sciences,* 40**,** 1011-1020.

HALVORSEN, A. & ROTI, J. A. 2013. Design of unlined headrace tunnel with 846 m head at lower Kihansi, Tanzania. Filling experience. *In:* BROCH, E., GRASBAKKEN, E. & STEFANUSSEN, W. (eds.) *Norwegian Hydropower Tunnelling II.* Oslo: Norwegian tunnelling society NFF.

HOULSBY, A. C. 1976. Routine interpretation of the lugeon water-test. *Q J Engng Geol,* 9**,** 303-313.

HUDSON, J. A., CORNET, F. H. & CHRISTIANSSON, R. 2003. ISRM Suggested Methods for rock stress estimation—Part 1: Strategy for rock stress estimation. *International Journal of Rock Mechanics and Mining Sciences,* 40**,** 991-998.

HYDROCEN. 2018. *Norwegian Research Centre for Hydropower Technology* [Online]. Available: www.ntnu.edu/hydrocen [Accessed April 16th 2018].

MARTIN, C. D. & CHANDLER, N. A. 1993. Stress heterogeneity and geological structures. *International Journal of Rock Mechanics and Mining Sciences & Geomechanics Abstracts,* 30**,** 993-999.

MERRITT, A. H. 1999. Geologic and geotechnical considerations for pressure tunnel design. *In:* FERNANDEZ, G. & BAUER, R. A. (eds.) *Geo-Engineering for Underground Facilities.* University of Illinois: ASCE.

NILSEN, B. & THIDEMANN, A. 1993. *Rock engineering,* Trondheim, Norwegian Institute of Technology. Department of Hydraulic Engineering.

PALMSTROM, A. & BROCH, E. 2017. The design of unlined hydropower tunnels and shafts: 100 years of Norwegian experience. *International journal on hydropower and dams,* 3**,** 1-9.

PALMSTRØM, A. & BUEN, B. 2017. Leirskred forårsaket av brudd i kraftverkstunnel. *Geo,* 20**,** 38-40.

RANCOURT, A. J. 2010. *Guidelines for preliminary design of unlined pressure tunnels.* Doctor of Philosophy PhD, McGill University.

RUTQVIST, J. & STEPHANSSON, O. 1996. A cyclic hydraulic jacking test to determine the in situ stress normal to a fracture. *International Journal of Rock Mechanics and Mining Sciences and Geomechanics Abstracts,* 33**,** 695-711.

SMITH, M. B. & MONTGOMERY, C. T. 2014. *Hydraulic Fracturing,* Hoboken, CRC Press.

Paper II

Norwegian Group for Rock Mechanics
ISBN: 978-82-8208-072-9
C.C. Li, H. Ødegaard, A.H. Høien, J. Macias (Eds.)

ISRM International Symposium
Eurock 2020 – Hard Rock Engineering
Trondheim, Norway, 14-19 June

Design of unlined pressure tunnels in Norway – limitations of empirical overburden criteria and significance of in-situ rock stress measurements

H. Ødegaard & B. Nilsen
Norwegian University of Science and Technology, Trondheim, Norway
henki.odegaard@ntnu.no

H. Barkved
Multiconsult, Stavanger, Norway

Abstract

A key requirement for unlined pressure tunnels is confinement, i.e. that the minimum principal stress must exceed the internal water pressure. Failure to meet this requirement can cause hydraulic jacking of the rock mass, leading to excessive leakages. Before reliable methods for measuring the minimum principal stress were available, engineers designing unlined pressure tunnels used various overburden criteria to assess rock stresses based on an assumed link between the weight of overburden and the minimum principal rock stress. Despite the usefulness of overburden criteria during a preliminary project phase, their simplifications and assumptions strongly limit their reliability for final design of pressure tunnels. Rock stress data from 15 modern Norwegian Hydropower plants presented in this paper show how the minimum principal stress magnitude, as estimated from overburden criteria, can differ significantly from the stress magnitude originating from *in-situ* measurements.

The recognition that overburden is no reliable indicator of *in-situ* stress has emphasized the need for performing rock stress measurements. In Norway, hydraulic methods have been preferred for measuring stress related to pressure tunnel design since the early 1980s. Due to budgetary limitations testing is typically limited, however, to one or two critical locations. This is an unsatisfactory situation given the potentially large variability of stresses over relatively short distances. It is therefore proposed to investigate alternative methodologies to establish a more "continuous" stress log along the pressure tunnel. To achieve this, we plan to further develop the "simplified jacking test", a cost-effective method occasionally applied in Norway to get a crude estimate of the jacking pressure. The aim is to develop this method into more standardized forms and to investigate a potential correlation to the more established ISRM hydraulic fracturing and jacking tests.

The research presented in this paper is part of the Norwegian hydropower research centre HydroCen, based at NTNU in Trondheim, Norway.

Keywords

Hydropower tunnels, rock stress, hydraulic fracturing

ISRM

NBG

1 Introduction

Norway's climate, topography and geology represent ideal conditions for the development of hydroelectric energy, and have formed the basis for the very large portion of Norway's electric energy production stemming from hydropower, estimated to about 95 % of the total electric energy produced. The total installed capacity of Norwegian hydropower plants reached 31 GW in 2016, producing 144 TWh (IHA, 2017), ranking Norway as number one in Europe and number eight in the World.

From a rock engineering perspective, one of the major contributions from the more than 100 years of hydropower development in Norway is the extensive use of unlined pressure tunnels and shafts, some of which with hydraulic heads exceeding 1,000 m. Since the sixties, most Norwegian plants have been designed with unlined pressure tunnels and shafts, leaving only small fractions of the total tunnel length steel lined or equipped with penstocks. It was the record breaking Tafjord K3 Plant, utilising 286 m head in an unlined shaft, which initiated this development and marked the transition from a steel lined to an unlined concept in Norwegian hydropower. The main motivation for the unlined design was economics, since significant time and costs can be saved by replacing steel liners and penstocks with unlined tunnels.

A crucial premise for this design is that the *in-situ* minimum principal stress, σ_3, must exceed the internal water pressure in the unlined part of the tunnel, i.e. that there is sufficient confinement. Failure to meet this requirement can cause hydraulic jacking of the rock mass, leading to excessive leakages and potentially catastrophic flooding of nearby underground structures and even landslides. Numerous failures have been reported around the world, and in Norway alone nine cases have been reported since 1919, the latest incident as recent as in 2016, see Table 1.

Table 1 Overview of Norwegian hydroelectric plants where hydraulic failure of unlined pressure tunnel has occurred.

Plant	Year	Reference
Herlandsfoss	1919	(Schjerven, 1921)
Skar	1920	(Vogt and Vogt, 1922)
Byrte	1968	(Selmer-Olsen, 1970)
Brokke	1968	(Bergh-Christensen, 1982)
Åskåra	1970	(Bergh-Christensen, 1974)
Bjerka	1971	(Valstad, 1981)
Holen	1981	(Selmer-Olsen, 1981)
Fossmark	1986	(Garshol, 1988)
Bjørnstokk	2016	(Nordal et al., 2018)

At none of the listed cases of hydraulic failure of pressure tunnels had stresses been measured prior to the first filling of the system. Before reliable stress measurement techniques were available, engineers designing unlined pressure tunnels used various overburden criteria to assess the ability of the rock mass to withstand the internal water pressure. These criteria do, however, suffer from some serious shortcomings rendering their use for final design questionable, and many authors have warned against their use for final design (US Army Corps of Engineers, 1997), (Merritt, 1999) and (Rancourt, 2010).

A thorough review of all relevant design criteria for pressure tunnel design cannot be covered within the limited space allowed for this paper, and for more details the interested reader is therefore referred to Brekke and Ripley (1987), Merritt (1999) and Aasen et al. (2013).

2 Empirical overburden criteria

As mentioned in the introduction, stress estimation for unlined pressure tunnel design has traditionally been based on overburden criteria linking the weight of the overlying column of rock, corrected for topographical effects, with the minimum principal stress magnitude, σ_3.

Internationally, one of the most used criteria is the Norwegian Criterion for Confinement, introduced by Bergh-Christensen and Dannevig (1971). This criterion defines the limit equilibrium between the water pressure and the weight of rock for a displacement towards the free surface shown in Eq. (1) and Figure 1.

$$L > \frac{\gamma_w \times H}{\gamma_r \times cos\beta} \qquad (1)$$

Where γ_w and γ_r respectively are the unit weights of water and rock (N/m^3), L is the minimum distance to the hillside/rock surface (m), H the static head (m) and β the average angle of the hillside slope.

To find a safe location for the unlined section of the pressure tunnel based on this method, a representative profile of the overlying rock surface is drawn, and the shortest allowable distance between this surface and the pressure tunnel or -shaft is found by calculating L in Eq. 1. As shown by Figure 1, the stabilising force ($\gamma_w \times L \times \cos\beta$), for this L-value will balance the pressure from the hydraulic head ($\gamma_w \times H$) which tends to displace the rock mass towards the nearest free surface, i.e. the rock surface. As can be seen from Eq. 1 the stabilising contribution will depend upon the terrain slope, such that a horizontal surface will provide a stabilizing contribution identical to the weight of overburden.

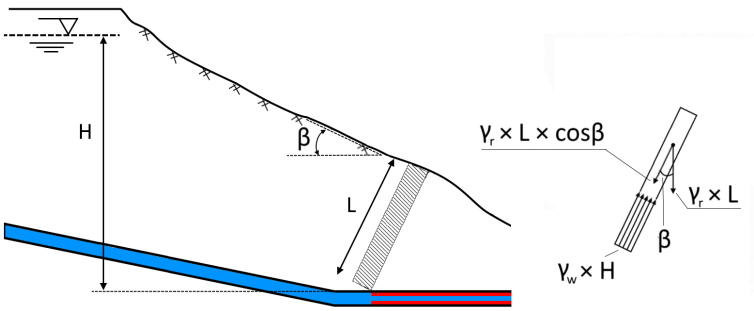

Figure 1: Norwegian criterion for confinement, modified after Bergh-Christensen (1982).

Despite their previous widespread use for design of unlined pressure tunnels, such criteria suffer from the inherent assumptions of the minimum principal stress being governed only by weight of the overlying rock mass and local topography, and that this direction actually is the σ_3 direction. Although rather special, cases where buckling can lift part of the overburden load and thus creating a condition where a stress is subtracted from the vertical component of stress have been reported (Engelder, 1993).

To further substantiate our argument that overburden criteria cannot be used for safe pressure tunnel design, we have performed a comparison of stress measurement data with data from overburden criteria for 15 modern Norwegian hydropower plants. This comparison, presented in Chapter 3, clearly demonstrates how simple overburden criteria fail to provide a reliable assessment of the minimum principal stress suitable for pressure tunnel design.

3 The Norwegian Criterion versus stress measurements

A recent review presented in Barkved (2018) documented stress measurement data from 15 Norwegian hydropower plants constructed between 1994 and 2018. The purpose of the review was to compare *in-situ* values of σ_3 with the values obtained from the empirical overburden criteria. The 15 plants were selected based on the following criteria:

1. Construction completed after 1990.
2. Static head in the unlined section more than 200 m.

3. Rock stress measurements performed.

To enable this comparison, it was necessary to use the location where the stress measurements were performed as basis for measuring the distance to the nearest rock surface, i.e. L in Eq. 1. Available terrain data were used to find the representative slope angle, β, including correction for protruding ridges as suggested by Broch (1984). Where available, rock density data was gathered from each project- If not available, characteristic values for the local rock type were used. The main findings from the comparison is presented in Figure 2.

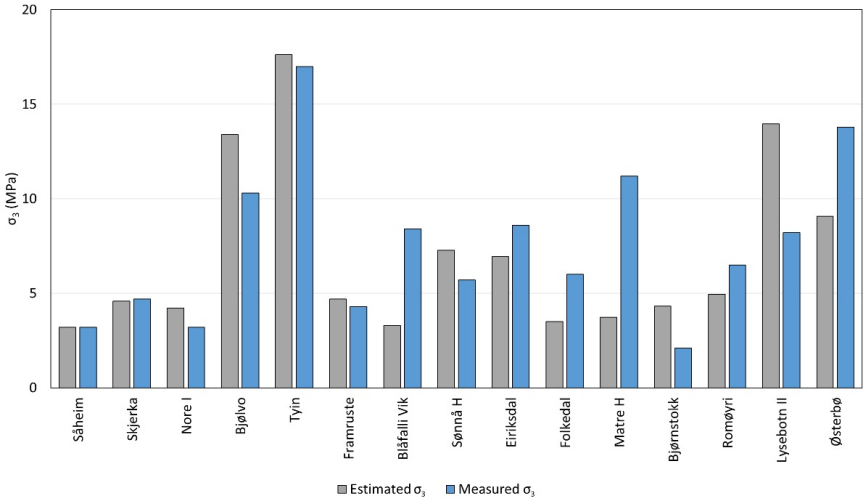

Figure 2: Magnitude of minimum principal stress from overburden criteria versus measured values.

As can be seen in Figure 2, the empirical criterion overestimated the measured minimum principal stress in seven out of the 15 investigated hydroelectric projects. Opposite, the overburden criteria significantly underestimated stresses at several of the plants. These findings demonstrate the limitations of overburden criteria as tools for predicting σ_3, and that rock stress data obtained from such criteria can differ substantially from the actual stress.

There is no doubt that these overburden criteria historically have been very valuable tools, but seeing that they still are being used for final design of unlined pressure tunnels, at least until recently, it should in our opinion be warned against such a practice.

For preliminary assessments of σ_3 we do believe that the overburden criteria may still serve as a simple and useful tool, and the current practice of assigning a factor of safety (FoS) to such calculations is sensible. There is, however, reason to adopt a somewhat higher FoS than the commonly used range of 1.3 to 1.5. From a comprehensive numerical analysis of different scenarios, Rancourt (2010) proposed a FoS ranging from 1.1 to 1.9. Even higher values than 1.9 might be warranted by looking at the stress data comparison presented above.

4 Proposed strategy for stress measurements

Acknowledging the heterogenous and rather unpredictable nature of rock stresses, a rational design approach for unlined pressure tunnels is to perform a preliminary rock stress assessment to delimit the underground region where it is considered likely that σ_3 will be higher than the design hydraulic head. These preliminary assumptions must then be controlled by performing in situ stress measurements during the construction stage. This approach requires a clear plan for the investigations as well as contractual flexibility, the principles of which are outlined in Ødegaard and Nilsen (2018). In the following an aspect related also to the verification of the tender design stress assumptions, will be addressed — namely how many measurements are needed and where should we measure?

The current practice in Norway is to perform stress measurements at or near the planned location of the transition zone (transition between unlined and steel lined tunnel). Often ISRM HF testing is the

preferred method, with testing limited to one or two measuring locations, each location typically only covering a few tens of meter of tunnel. This leaves the remaining upstream length of pressure tunnel, which can be several kilometres long, with no measurements. Since plant layouts normally are such that the overburden increases along the pressure tunnel in the upstream direction, designers assume a corresponding stress increase. From the above discussion it should be clear that this is not a safe approach, as also emphasized by Haimson (1992). To resolve this unsatisfactory situation, we propose to aim for a stress log along the entire unlined section of pressure tunnel, rather than the current practice of a few point measurements.

To achieve this, we suggest that the current tradition of performing ISRM HF tests at a few critical locations is maintained, but that these measurements are supplemented with many simplified jacking tests distributed along the entire length of the pressure tunnel. For this approach to be technically and economically viable, a simplified version of the hydraulic jacking test with the following main characteristics is envisaged:

- Testing must be performed concurrent with and without hindrance to other activities near the excavation face.
- The test must not require specialised equipment other than what is usually available at the tunnel site.
- Tests must be performed in holes drilled at various orientations to ensure that the population of fractures oriented normal or close to normal to σ_3 are intersected. Failure to do so can potentially cause the interpretation of stress magnitude to be too high.
- No downhole tool for fracture delineation is needed.
- Tests are performed in small diameter boreholes, typically 51 mm or 64 mm holes, suitable for effective drilling and rod handling with commonly available drilling equipment.
- Testing is to be performed in a section of the borehole not affected by influence from the tunnel.
- Mechanical single packers fixed on connectable rigid rods are used to isolate the test section, as shown in Figure 3.
- Test holes are pressurised to at least the design head, plus a suitable factor of safety.
- Simple and fast interpretation of test data, requiring no advanced calculations, is needed.

Figure 3 Mechanical packers used to isolate the test section

To develop the proposed simplified jacking tests into a test method useful for design of unlined pressure tunnels there are two main issues which need attention:

1. A standardised test procedure must be developed, including instructions on the interpretation of test data.
2. A correlation between the values obtained from the simplified jacking test and the ISRM HF test needs to be established.

These issues constitute the main research items associated with the first authors ongoing PhD work, and the current plans for this work is presented below.

5 Planned laboratory and field campaign

For the test procedure, we are planning to use some of the already existing jacking tests as basis, and combined with planned field and laboratory work the intention is to develop a new test procedure enabling fast, cheap and robust estimates of jacking pressures. Many variants of hydraulic jacking tests have been described, and some of the most relevant are the cyclic hydraulic jacking test (Rutqvist and Stephansson, 1996) the step rate test (Smith and Montgomery, 2014), the modified Lugeon test (Houlsby, 1976) and a jacking test described by Hartmaier et al. (1998). The hydraulic jacking procedures already practised in Norway will also be relevant.

For the laboratory campaign, hydraulic fracturing and hydraulic jacking tests will be performed in a newly designed apparatus enabling testing on 300 mm cubical rock specimens in true triaxial confinement up to 20 MPa. A high flow dual piston reciprocating pump is used to induce the water pressure in drill holes in the sample. The laboratory equipment is shown in Figure 4. So far only preliminary function tests have been performed, and no test results are yet available. The first tests are planned in 2020.

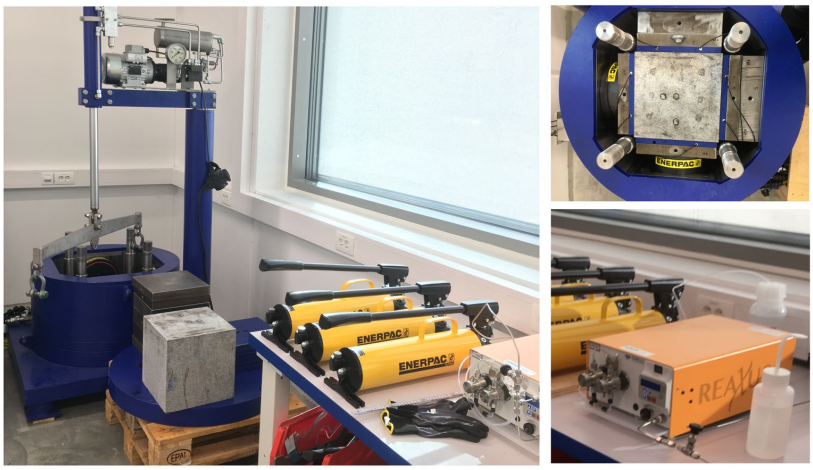

Figure 4: Overview of the newly developed true triaxial rig for hydraulic jacking and fracturing tests.

To investigate a possible correlation between the simplified jacking tests, both laboratory and field trials are planned. The field campaign is to be based on the execution of simplified jacking tests at underground locations where stress data from ISRM HF tests already are available, and the first field trials have already been performed.

6 Summary and Conclusions

Despite the obvious shortcomings of the overburden criteria in assessing σ_3, the principles behind them are deeply rooted in the hydropower industry. This creates some challenges where:

- Clients, used to rock engineers relying on overburden criteria (seemingly cheap), oppose the prospects of spending money on stress measurements.
- Clients arguing that their project has so marginal profitability that they cannot afford stress measurements, and that overburden criteria has worked in the past (partially true!).
- Engineers accepting a bare minimum of stress measurements due to the relatively high cost combined with low willingness to pay from the Clients side.
- Engineers and clients being satisfied with measuring stresses at one or two locations, leaving many kilometres of pressure tunnels essentially untested.

These challenges might be solved if it is clearly shown that measurements are absolutely required, and if we are able to develop and standardise a simplified hydraulic jacking test which is correlated with the established ISRM HF test.

7 Acknowledgements

The authors wish to thank Agder Energi, Hydro, E-CO Energi, Sweco Norge, Sunnhordland Kraftlag, Saudefaldene, Spilde Entreprenør, BKK, Småkraft, Lyse Energi and Sogn og Fjordane Energi for granting us access to measurement data from their plants. We also want to thank Magne Sollie for the design assistance and excellent manufacturing of our true triaxial rig. The Research Council of Norway (NFR) is acknowledged for financing this ongoing research through HydroCen.

8 References

Aasen, O., Ødegaard, H. & Palmstrom, A. 2013. Planning of Pressurized Headrace Tunnel in Albania. *In:* Broch, E., Grasbakken, E. & Stefanussen, W. (eds.) *Norwegian Hydropower Tunnelling II.* Oslo: Norwegian tunnelling society NFF.

Barkved, H. 2018. Gjennomgang av designgrunnlag for utvalgte betongpropper/overgangssoner i nyere norske vannkraftanlegg (in Norwegian). Trondheim, Norway: NTNU (Unpublished).

Bergh-Christensen, J. Brudd i uforet trykktunnel ved Åskåra kraftverk (In Norwegian). *In:* Broch, E., Heltzen, A. M. & Johannessen, O., eds. Fjellspregningskonferansen, Bergmekanikkdagen, Geoteknikkdagen, 1974 Oslo. Norsk Jord- og Fjellteknisk Forbund, 15.1-15.8.

Bergh-Christensen, J. 1982. Design Of Unlined Pressure Shaft At Mauranger Power Plant Norway. *ISRM International Symposium.* Aachen, Germany: International Society for Rock Mechanics and Rock Engineering.

Bergh-Christensen, J. & Dannevig, N. T. 1971. Engineering geological evaluation of the unlined pressure shaft at the Mauranger hydropower plant (in Norwegian). Oslo: GEOTEAM A/S.

Brekke, T. L. & Ripley, B. D. 1987. Design Guidelines for Pressure Tunnels and Shafts. Berkeley, California: University of California, Berkeley.

Broch, E. 1984. Unlined high pressure tunnels in areas of complex topography. *Water Power & Dam Construction,* 36:11**,** 21-23.

Engelder, T. 1993. *Stress Regimes in the Lithosphere*, Princeton, New Jersey.

Garshol, K. Fossmark kraftverk, utlekkasje fra trykksjakt (In Norwegian). *In:* BERG, K., HELTZEN, A. M., Johansen, P. M. & Stenhamar, P., eds. Fjellspregningskonferansen, Bergmekanikkdagen, Geoteknikkdagen, 1988 Oslo. Norsk Jord- og Fjellteknisk Forbund, 25.1-.25.11.

Haimson, B. 1992. Designing pre-excavation stress measurements for meaningful rock characterization. *In:* Hudson, J. A. (ed.) *ISRM Eurock '92 Symposium on Rock Characterization.* London: British Geotechnical Society.

Hartmaier, H. H., Doe, T. W. & Dixon, G. 1998. Evaluation of hydrojacking tests for an unlined pressure tunnel. *Tunnelling and Underground Space Technology incorporating Trenchless Technology Research,* 13**,** 393-401.

Houlsby, A. C. 1976. Routine interpretation of the lugeon water-test. *Q J Engng Geol,* 9**,** 303-313.

Iha. 2017. *Norway statistics* [Online]. Available: https://www.hydropower.org/country-profiles/norway [Accessed November 5th 2019].

Merritt, A. H. 1999. Geologic and geotechnical considerations for pressure tunnel design. *In:* Fernandez, G. & Bauer, R. A. (eds.) *Geo-Engineering for Underground Facilities.* University of Illinois: ASCE.

Nordal, S., Grøv, E., Emdal, A. & L'Heureux, J. S. 2018. Skredene i Tosbotn, Nordland 1. og 2. april 2016. Rapport fra undersøkelsesgruppe satt ned av Nordland Fylkeskommune (In Norwegian). NTNU.

Rancourt, A. J. 2010. *Guidelines for preliminary design of unlined pressure tunnels.* Doctor of Philosophy PhD, McGill University.

Rutqvist, J. & Stephansson, O. 1996. A cyclic hydraulic jacking test to determine the in situ stress normal to a fracture. *International Journal of Rock Mechanics and Mining Sciences and Geomechanics Abstracts,* 33**,** 695-711.

Schjerven, H. 1921. Tryktunnelen ved Herlandsfossen (In Norwegian). *Teknisk Ukeblad.* Den Norske Ingeniør- og Arkitekt-forening og Den Polytekniske Forening.

Selmer-Olsen, R. 1970. Experience with Unlined Pressure Shafts in Norway. *In:* Brekke, T. L. & Jörstad, F. A. (eds.) *Large Permanent Underground Openings - proceedings of the international symposium.* Oslo: Universitetsforlaget.

Selmer-Olsen, R. 1981. Betraktninger over store vannlekkasjer i dyptliggende tunneler (In Norwegian). *Fjellspregningskonferansen, Bergmekanikkdagen, Geoteknikkdagen.* Trondheim: Tapir.

Smith, M. B. & Montgomery, C. T. 2014. *Hydraulic Fracturing,* Hoboken, CRC Press.

US Army Corps of Engineers 1997. Engineering and Design. Tunnels and shafts in rock. Washington, DC: Department of the army. U.S. Army Corps of Engineers.

Valstad, T. 1981. Uforete vanntunneler og -sjakter : vannutbrudd fra tilløpstunnelen til Bjerka kraftverk (In Norwegian). *Rapport (Norges geotekniske institutt : trykt utg.).* Oslo.

Vogt, J. H. L. & Vogt, F. 1922. *Tryktunneller og geologi (In Norwegian),* Kristiania, Norges geologiske undersøkelse.

Ødegaard, H. & Nilsen, B. 2018. Engineering Geological Investigation and Design of Transition Zones in Unlined Pressure Tunnels. *ISRM International Symposium - 10th Asian Rock Mechanics Symposium.* Singapore: International Society for Rock Mechanics and Rock Engineering.

Paper III

Rock Mechanics and Rock Engineering (2021) 54:2995–3015
https://doi.org/10.1007/s00603-021-02452-9

ORIGINAL PAPER

Rock Stress Measurements for Unlined Pressure Tunnels: A True Triaxial Laboratory Experiment to Investigate the Ability of a Simplified Hydraulic Jacking Test to Assess Fracture Normal Stress

Henki Ødegaard[1] · **Bjørn Nilsen**[1]

Received: 23 October 2020 / Accepted: 19 March 2021 / Published online: 27 March 2021

Abstract
To avoid hydraulic failure of unlined pressure tunnels, knowledge of minimum principal stress is needed. Such knowledge is only obtainable from in situ measurements, which are often time-consuming and relatively costly, effectively limiting the number of measurements typically performed. In an effort to enable more stress measurements, the authors propose a simplified and cost-effective stress measuring method; the Rapid Step-Rate Test (RSRT), which is based on existing hydraulic testing methods. To investigate the ability of this test to measure fracture normal stresses in field-like conditions, a true triaxial laboratory test rig has been developed. Hydraulic jacking experiments performed on four granite specimens, each containing a fracture, have been performed. Interpretation of pressure-, flow- and acoustic emission (AE) data has been used to interpret fracture behaviour and to assess fracture normal stresses. Our experimental data suggest that the proposed test method, to a satisfactory degree of reliability, can measure the magnitude of fracture normal stress. In addition, a clear correlation has been found between fracture closure and sudden increase in AE rate, suggesting that AE monitoring during testing can serve as a useful addition to the test. The rapid step-rate test is also considered relevant for field-scale measurements, with only minor adaptions. Our findings suggest that the RSRT can represent a way to get closer to the ideal of performing more testing along the entire length of pressure tunnel, and not only at key locations, which requires interpolation of stress data with varying degree of validity.

Keywords Hydropower · Unlined pressure tunnels · Hydraulic jacking · Rock stress measurements · True-triaxial testing

1 Introduction

The main objective of experiments described in this paper is linked to a general challenge encountered during final design of pressure tunnels in hydropower; how can the magnitude of minimum principal rock stress be assessed, to a satisfactory degree of reliability, along several kilometres of unlined pressure tunnel? In the early 1900s, prior to the establishment of reliable methods for measuring the underground state of stress, engineers designing the first pressure tunnels made their stress estimations based on simple calculation of overburden weight, as described by Schjerven (1921) and Berkey and Sanborn (1922). This approach, assuming a nearly hydrostatic stress field with all three principal stresses similar and corresponding to the overburden weight is not generally true—as convincingly demonstrated in the landmark paper written by Hubbert and Willis (1957). Still, as thoroughly described in Rancourt (2010), the tradition of using overburden weight as input for stress estimation, the so-called *overburden criteria*, persists in various design guidelines. Though useful for preliminary assessment of rock stress, overburden criteria in general suffer from assumptions and over-simplifications making them unsuitable for reliable estimate of minimum principal stress (USACE 1997; Merritt 1999; Rancourt 2010).

Today, it is generally accepted that reliable data on the magnitude of minimum principal rock stress is absolutely required to ensure a safe design of unlined pressure tunnels, and that in situ stress measurements are essential in providing such information. In connection with investigations for unlined pressure tunnels, hydraulic fracturing (HF) and hydraulic testing of pre-existing fractures (HTPF) have

✉ Henki Ødegaard
henki.odegaard@ntnu.no

[1] Norwegian University of Science and Technology, Trondheim, Norway

become common test methods. These tests, both standardized by the ISRM (Haimson and Cornet 2003), can under ideal testing conditions provide highly reliable estimates of the magnitude of minimum principal stress. Still, the relatively high testing cost, combined with the economical sensitivity of most hydropower projects, limit the number of tests that can be justified, often leaving long stretches of the pressure tunnel essentially untested. In some extreme cases, stress measurements are omitted altogether and design is based on empirical overburden criteria alone. This is indeed a risky approach, as experienced for instance in the recent failure of the Bjørnstokk HPP in Norway (Nordal et al. 2018).

To mitigate some of the risk associated with the current practice of performing few, but high quality, measurements at test locations relatively far apart, often requiring stress interpolation of uncertain validity, the authors believe it is required to distribute measurement locations and at the same time increase the number of measurement locations. For such an approach to be practically and economically viable, stress measurements need to be cost-effective, relatively fast and uncomplicated to execute, with a minimum requirement for specialized equipment and crew. Various types of hydraulic jacking tests have been performed regularly by parties engaged in the final design of unlined pressure tunnels both in Norway and abroad. These tests are typically borehole tests where existing fractures of unknown orientation are hydraulically stimulated to find the pressure at which the fracture opens, slips (if it supports some amount of shear stress) and closes. The basic idea behind performing such hydraulic jacking tests is to find the population of fractures oriented perpendicularly to the minimum principal stress, σ_3. This requires a large number of tests, performed in boreholes of various orientations. The lower bound values obtained from these tests in a given volume of rock is considered representative of the minimum principal stress (Hartmaier et al. 1998). The main advantage of this approach is the relatively large number of individual measurements, providing better insight into the stress variability, and potentially detecting regions of lower than expected stresses, rather than the absolute accuracy of which the minimum principal stress can be measured.

Based on the authors involvement in stress measurements for many hydroelectric projects, with observation of various challenges encountered with the execution and interpretation of hydraulic jacking tests, we have designed a laboratory experiment to investigate the ability of hydraulic jacking tests to measure fracture normal stress. Two variants of hydraulic jacking tests have been tested as part of this study and are presented in Sect. 4.1. Both test types are inspired by existing hydraulic jacking test methods but are still novel by the simplification of test procedure, limiting the requirements of specialized crew and equipment. To make the laboratory experiments as representative as possible for in situ testing conditions, efforts have been made to ensure that conditions in the lab closely resemble what is common in the field, including true triaxial confinement of the tested rock specimens.

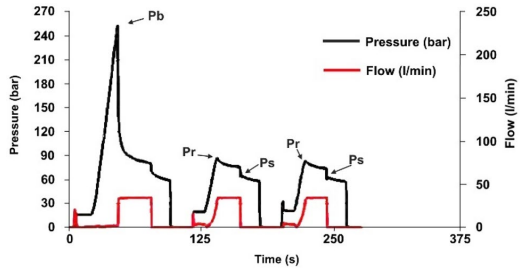

Fig. 1 Typical pressure–time curve obtained from a HF test conducted as part of the investigations for a Norwegian hydroelectric plant. (Average P_s from the two reopening cycles was interpreted at 69 bars)

Laboratory scale hydraulic fracturing experiments under true triaxial confinement have been widely studied by researchers working in the petroleum industry (Haimson and Fairhurst 1969; Ishida et al. 1997; Chitrala et al. 2011; Rasouli 2013; Stanchits et al. 2014; Huang and Liu 2017), by researchers working with deep geothermal projects (Frash et al. 2015; Hampton et al. 2018; Zhuang et al. 2020), and for field-scale rock stress measurements (Ikeda and Tsukahara 1982; Cheung and Haimson 1989; Ishida 2001). The study described in this paper is, to the authors' knowledge, the first time that laboratory-scale hydraulic fracturing experiments under true triaxial confinement have been used in connection with investigations for design of unlined hydropower tunnels.

2 Conventional Hydraulic Tests for Measuring the Underground State of Stress

2.1 Hydraulic Fracturing

The HF test method includes the pressurization, usually by water, of a short, isolated section of borehole, devoid of fractures, until a fracture is created. The pressures at which the borehole ruptures, termed the breakdown pressure (P_b), the pressure required to reopen the fracture at consecutive pressure cycles (P_r) and the pressure measured immediately after pumping stops, termed the instantaneous shut-in pressure (P_s) are all recorded throughout the test, see Fig. 1.

The in situ state of stress can be assessed from such measurements by applying the classical hydraulic fracturing criterion, introduced by Hubbert and Willis (1957):

$$P_b = T + 3\sigma_3 - \sigma_1 - P_0$$

or

$$\sigma_1 = T + 3\sigma_3 - P_b - P_0 \quad (1)$$

where T is the tensile strength of the rock, P_0 the initial pore pressure in the rock and σ_1 and σ_3 are the maximum and minimum principal stresses, respectively. Guidelines on how to measure the tensile strength of the rock, T, are provided in Haimson and Cornet (2003), including laboratory tests on extracted core, such as the hollow cylinder test or the Brazilian test, or, when core is not available, by looking at the difference between breakdown pressure in the first pressure cycle, P_b, and the reopening pressure, P_r, found during subsequent cycles.

Calculation of the magnitude of σ_1 based on Eq. (1) has proven rather uncertain due to the difficulty in assessing the tensile strength from such tests (Zoback 2007). Magnitude of σ_3, however, require no calculation since in the classical interpretation of the HF test, it is assumed that the created fracture opens normal to the minimum principal stress, and consequently that:

$$P_s = \sigma_3 \quad (2)$$

Several techniques for assessing the minimum principal stress from analysis of hydraulic fracturing tests are described in the literature, and reference is made to Zoback and Kohli (2019) for an overview of such methods.

When a fracture has been created, it can be assumed that for consecutive pressurization cycles $T = 0$, and that P_b in Eq. (1) can be replaced by the reopening pressure, P_r such that (Bredehoeft et al. 1976):

$$P_r = 3\sigma_3 - \sigma_1 - P_0$$

or

$$\sigma_1 = 3P_s - P_r - P_0 \quad (3)$$

There is also some uncertainty related to this method of calculating σ_1, mainly due to the difficulty of picking the exact pressure at which the fracture re-opens (Ito et al. 1999). In addition, in cases with negative tangential stresses around the borehole, i.e. where $3\sigma_3 < \sigma_1$, the fracture will never completely close, and no meaningful estimate on reopening pressures can be identified (Haimson 1992).

An important requirement for the proper execution and interpretation of the HF test is that the borehole axis is in the same direction as one of the principal stresses, or at least deviating less than 15° from it. Tests performed in deviating boreholes invalidate the classical method of interpreting results, potentially causing considerable error (Warren and Smith 1985). This requirement necessitates, in principle, reliable information of the stress directions, which for hydroelectric projects—often situated at relatively shallow depths in mountainous regions, would require 3D stress measurements since the in situ stress orientation might vary considerably over short distances. The additional cost and time required for 3D stress measurements limit the applicability of the HF test in such cases.

2.2 Hydraulic Testing of Pre-existing Fractures

To circumvent some of the limitations associated with the HF method, the HTPF test was developed by Cornet and Valette (1984). The objective of the HTPF method is to determine the normal stress supported by pre-existing fracture planes with known orientations and, by inversion of the test results, determining the complete stress field.

The magnitude of normal stress is found in much the same way as done for assessing σ_3 during the HF test, i.e. by assessing shut-in pressure after full fracture opening. However, since the stimulated fracture is not necessarily oriented normal to σ_3, Eq. (2) can be rewritten as follows:

$$P_s = \sigma_n \quad (4)$$

where σ_n is the normal stress acting across the fracture. The HTPF test is performed by pressurizing the test section at a pre-determined constant flow until fracture opening, followed by a shut-in phase, similar to the HF test. After this first cycle is either: (1) a stepwise increase (forward-step) in flow rate conducted until full fracture opening, followed by another shut-in phase; or (2) an initial forward-step flow increase followed by a stepwise flow decrease (backward-step). By plotting pressure data vs. flow rate from the step-rate tests can a bilinear curve be obtained, the intersection of which can be taken as the normal stress (Haimson and Cornet 2003). Determining the regional stress field is then done by finding a best fit function to the measured normal stresses, together with the fracture orientation, as presented by Cornet (1993).

Testing a minimum of eight individual fractures of various orientation is required for a complete stress determination with the HTPF test. Since each tested fracture needs to be isolated it is further a requirement that the rock mass cannot be too fractured (Amadei and Stephansson 1997). The number of tests required can, however, be reduced by combining the HF test with the HTPF test, provided ideal testing conditions (Cornet 2016). The relatively large number of tests combined with the extensive formulae required to find the complete stress field is arguably

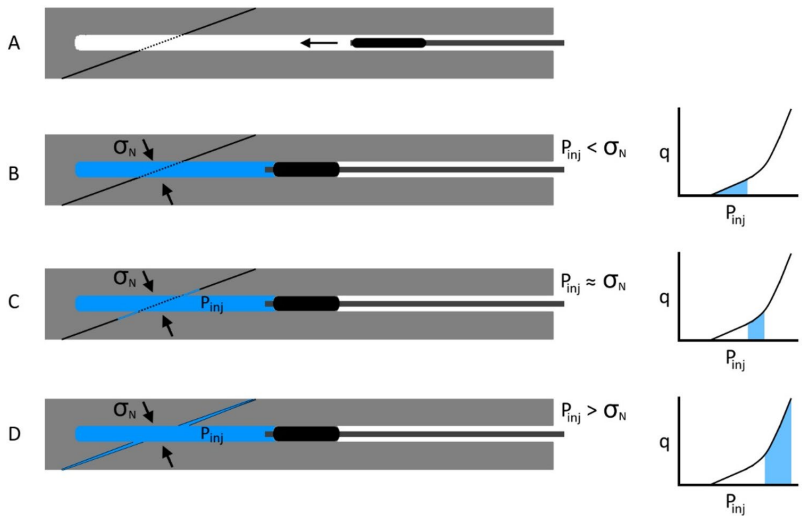

Fig. 2 Schematic view of a borehole intersected by a fracture supporting a normal stress σ_n at various stages of the hydraulic jacking test. **a** Installation of single packer at predetermined depth, **b** pressurization of the test section, with the corresponding, idealized, linear trend in the qP_{inj}-plot, **c** onset of hydraulic jacking of the fracture, indicated by the transition between linear to gradual qP_{inj} development to the right and **d** full hydraulic jacking

the main drawback of the HTPF method in the context of assessing σ_3 for unlined pressure tunnel design purposes.

2.3 Hydraulic Jacking Tests

The basic principle of the various hydraulic jacking tests is to pressurize a section of a borehole intersected by one or several pre-existing fractures, and by monitoring fluid pressure and flow to find the fluid pressure at which the fracture can be kept opened. This pressure is taken as a measure of the normal stress acting across the stimulated fracture, since once the fracture is opened, the stress concentration which previously surrounded the borehole is reduced and the pressure, P_{inj}, required to hold the fracture open is equal to that of the in situ normal stress across the fracture (Hubbert and Willis 1957).

According to Rutqvist and Stephansson (2003), the first hydraulic jacking tests were performed during the investigation of the Malpasset dam failure in the 1960s. During these investigations, it was demonstrated how the permeability of the rock mass was affected by the effective normal stresses on the fractures, with permeability decreasing with increasing effective stress (Londe and Sabarly 1966). These tests thus provided some of the first insights on the hydromechanical (HM) coupling in fractured rock masses. Many variants of hydraulic jacking tests have since been developed, including: the step-rate test (Felsenthal 1974); the aforementioned HTPF test (Cornet and Valette 1984); a hydraulic jacking test developed specifically for pressure tunnel investigations (Brekke and Ripley 1987); the cyclic hydraulic jacking test (Rutqvist and Stephansson 1996) and; though not strictly a hydraulic jacking test, the modified Lugeon test (Philippe et al. 2019).

Hydraulic jacking tests are considered highly relevant for assessing stresses in connection with unlined pressure tunnel design since they are relatively simple to execute and they simulate the effect imposed on the rock mass by the pressurized water (Doe and Korbin 1987; Benson 1989; Broch et al. 1997; Merritt 1999). Testing is commonly performed during the constructional phase of hydroelectric projects, with number and location of tests based on local conditions.

The normal testing procedure is to drill boreholes in various directions into the rock mass surrounding the tunnel, and then install a single packer at a depth where stress influence from the tunnel can be ignored, to isolate a section of borehole. This borehole section, which typically is 5–15 m long, is then injected by water until the water pressure (P_{inj}) exceeds the in situ normal stress acting across the fracture most favourably oriented for opening, effectively providing a single measure of the magnitude of normal stress supported by the stimulated fracture, see Fig. 2. Tests are typically pressure controlled with pressure increments of 0.3–1 MPa, and with each increment held a few minutes until steady-state conditions are achieved. Each test cycle consist of a stepwise pressure increase followed by stepwise decrease with the same pressure increments. Testing in several holes and repeated cycles in each hole are commonly performed to improve the reliability of the measurements.

The interpretation of hydraulic jacking tests traditionally has been based on assumption of a distinct fracture opening or closure when P_{inj} equals or just barely exceeds the normal stress acting across the fracture. This assumption is, however, not necessarily valid, since it has been found that

fracture opening and closure are gradual, rather than distinct, which affects the interpretation of test results (Rutqvist and Stephansson 1996). Still, the pressure at the transition from a gradual to a linear pressure decline might serve as a reasonable, lower bound, normal stress estimate (Hartmaier et al. 1998).

3 Experimental Setup

The experiments reported in this article have been performed in a newly developed true triaxial test rig, designed specifically for performing these experiments. In the current laboratory setup, we know in advance the magnitude of normal stress acting across the tested fractures, and it is, therefore, possible to assess how well various testing procedures can predict this "true" value under various testing configurations. This, in turn, may provide input on how field-scale hydraulic jacking tests should be performed to provide a sound estimation of normal stresses across fractures, while at the same time keeping the test as simple and cost-effective as possible. To investigate this, a number of laboratory-scale hydraulic jacking experiments on cubical rock blocks subjected to true triaxial confinement have been performed. Confinement of the rock specimen has been achieved by placing the specimen inside a stiff test frame and pressurizing the specimen sides from three orthogonal directions, the magnitude in each direction individually adjustable between 0 and 20 MPa.

3.1 Test Rig

The test rig, shown in Fig. 3, consists of the following main units: a custom built true triaxial test frame with an integrated crane; a monitoring system for monitoring fluid pressure, fluid flow and acoustic emission (AE) signals, and a high-pressure reciprocating injection pump.

The modular test frame, made to order by Sollie Solutions AS, is made of structural steel (S355) and consists of a quadratic bottom plate on which a circular spacer element and the main steel body rests, see Fig. 4. The main steel body has an outer diameter of 820 mm and the minimum material thickness is 80 mm. On top is an 80-mm-thick lid which can be hoisted with the integrated hydraulic crane. The top lid is fixed with four Ø60 mm high strength (S165M) tension bolts running from the bottom plate through the top plate. Three 30 mm openings, angled 0°, 15° and 30° from the vertical, run through both top lid and the upper sensor platen, enabling drilling into the specimen under confinement and used also for installation of the injection packer into a confined specimen. The rock specimen is located centrally in the loading frame, surrounded by platens of different thicknesses, including six 19 mm sensor platens, housing

Fig. 3 Overview of the test rig. From left to right is **a** the test frame, **b** the integrated hydraulic crane, **c** one of the granite specimens resting on the top lid, **d** three hand pumps used for pressurizing the hydraulic pistons, **e** the high-pressure pump used to pressurize the test section, and the desktop computer where tests are controlled and monitored

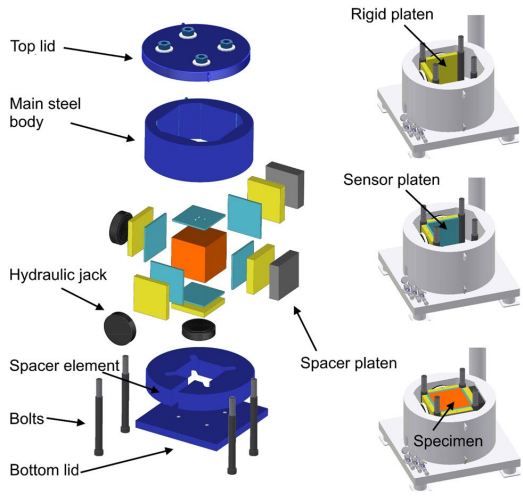

Fig. 4 Assembly drawing of the test rig to the left, and the rig at various stages of assembly to the right

acoustic emission (AE) sensors; five 40-mm-thick rigid platens, ensuring even load transfer from the cylinder to the specimen; and two 60 mm dummy platens, serving as rigid spacer elements, see Fig. 4. All platens are 290 mm wide, slightly smaller than the specimen width, to avoid contact between neighbouring platens during testing. Three hydraulic cylinders were used to load the specimen sides. Each cylinder is pressurized with a hand pump, allowing for individual control of the three stress directions according to the desired stress configuration. Since the stresses are intended to simulate a tectonic stress situation, no adjustment of stress

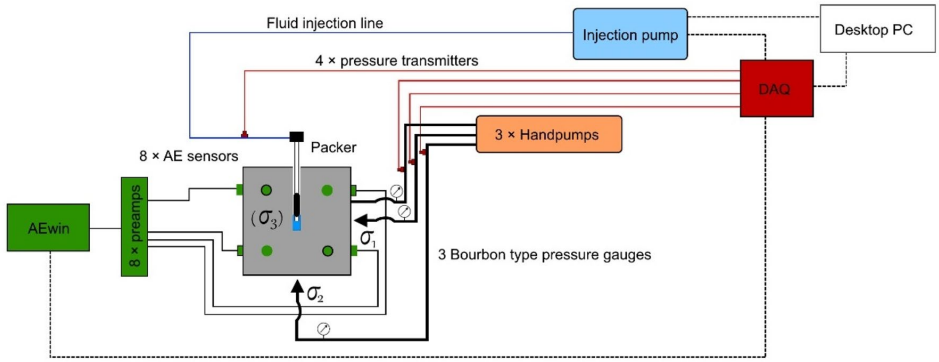

Fig. 5 Schematic overview of the monitoring system (side view). σ_3 in brackets indicate that it is the stress in the direction normal to the paper plane

was made during the test. The hydraulic cylinders have an integrated tilting function, where the plunger can be tilted up to 4° from the loading axis, thus accommodating minor rotations between the moving and stationary parts of the cylinder to prevent uneven loading, similar to the effect of spherical seats. To enhance load transfer was the diameter of the hydraulic piston was chosen such that it would be close to that of the specimen. Similar design choices for true triaxial rigs have been described by Zhang and Fan (2014) and Shi et al. (2013).

Confining pressures (P_{jack}) and injection pressures (P_{inj}) were monitored by four pressure transmitters, each having a 1 kHz sampling rate. The pressure data were displayed real-time throughout testing and data was stored for post-test analysis and processing. As a backup, the fluid pressure in the hydraulic lines could also be monitored by separate gauges, in the form of a 10 Hz pressure transmitter integrated with the injection pump, and three Bourdon pressure gauges for the confining pressures. A simplified overview of the monitoring system is shown in Fig. 5.

A dual piston reciprocating pump capable of providing 28 MPa injection pressure, at a maximum flow of 100 ml/min, was used to pressurize the borehole test section. The pump was factory configured to flow-control mode. The flow was controlled through a programme developed in LabVIEW, and was adjustable in 0.1 ml/min increments within the full flow range from 0.1 to 100 ml/min. A high-pressure stainless steel fluid injection line was used to transfer water from the pump to the packer, where the water entered the test section via the packer rod. Return flow, when needed, was directed through a separate return line equipped with two autoclave needle valves marked as "A" and "B" in Fig. 6. This valve arrangement serves the dual purpose of venting the system as well as enabling flow-back over a constant choke by fixing valve "B" at a pre-determined choke and shutting the flow on and off with valve "A" (though this latter option was not been employed for the experiments described in this paper). The total water volume in the tubing and test section was approximately 44 ml, distributed between the high-pressure tubing (10 ml), the packer rod (14 ml) and the open-hole sections (20 ml).

Fig. 6 Injection pump and packer assembly. Top: pump with valve configuration enabling flow-back. Unbroken arrow indicates flow direction during injection, dotted arrow shows direction during flow-back and venting. The lower left picture shows the injection packer with scale indicated. Note, the in-house modification of the upper part of the packer rod, incorporating an eye bolt for secure anchoring of the packer during testing. The expansion loop in the steel pipe is shown in the lower right photo

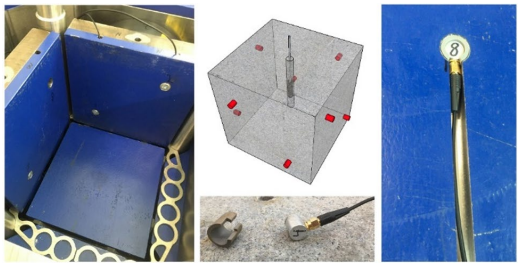

Fig. 7 AE sensor-mounting overview, showing sensor platens to the left, the AE sensor arrangement with two sensors placed in contact with each of the four sensor sides at the top middle, the loose rubber jacket used to protect the AE sensor from noise at the lower middle, and the sensor when mounted in the sensor platen (rear-side view) to the right

A 19 mm high-pressure, mechanical injection packer was used to isolate the test section during testing. This kind of packer is structurally similar to the single-use packers commonly used for both field-scale hydraulic jacking tests and rock mass grouting, and has the advantage of being easy to handle, durable and highly efficient in sealing the borehole. The injection line tubing was connected to the packer by a sliding coupling connection, enabling a fast and watertight connection. The downstream section of steel tubing was given an expansion loop to ensure better manoeuvrability of the tubing when connecting to the packer. The packer and steel pipe with the sliding connection are shown in Fig. 6.

3.2 AE Monitoring

AE monitoring was used as an aid in the analysis of pressure and flow data, enabling linking of AE activity with the mechanical behaviour of the stimulated fractures during hydraulic testing. The orientation of the fracture could also be mapped by 3D event localization, where each hypocentre represented a single point in a point cloud representing the fracture. During all tests, AE signals were monitored using eight broadband AE sensors with a 500 kHz operating frequency. The sensors, AE-HTRX type, were connected to an AE measurement system consisting of eight 2/4/6 voltage preamplifiers and an eight-channel acoustic emission PCI card configured with AEwin software, version E5.90. The preamplifiers gain was set to 40 dB for all channels.

Two holes for the AE sensors, with appurtenant grooves for the AE cables, were machined in each sensor platen to protect the sensors from the cylinder load. This arrangement enabled direct contact with the specimen side without damaging the specimen, see Fig. 7. Each AE sensor is 18.7 mm high with 22.2 mm diameter. Each sensor was wrapped with a 3-mm-thick rubber jacket to minimize acoustic contact between the side of the sensor and the steel platen. In addition, on the passive side of each sensor, a penny-shaped piece of rubber was placed to ensure that a gentle pressure was transmitted from the rigid platen to the sensor, promoting good acoustic coupling with the specimen.

Table 1 Typical values of some index properties of the Iddefjord granite

Property	Value
Density (kg/m^3)	2630
Poisson's ratio	0.30
Porosity (%)	<1
Sound velocity, V_p (m/s)	4000
Uniaxial compressive strength (MPa)	230
Brazilian tensile strength (MPa)	9

3.3 Rock Specimens

The specimens used in all experiments were cubes of Iddefjord granite, cut from a quarry in south-eastern Norway. The approximately 920 Ma old granite was chosen due to its homogeneity, low permeability, and availability. The side lengths of the tested rock cubes were 300 mm $\pm$ 0.5 mm. Opposing sides of the cubical specimens were sawn parallel to $\pm 0.4°$, as measured by a precision protractor. Main index properties of the Iddefjord granite are given in Table 1.

3.4 Test Preparation

Each rock specimen was visually inspected for damage before testing, and the P-wave sound velocity (V_P) measured. A vertical, 180-mm-deep borehole was drilled with a hand-held percussion drill from the top centre of the specimen through the specimen centroid such that a 60 mm open-hole test section could be established in the middle of the sample, as shown in Fig. 8. After drilling, the borehole was flushed thoroughly with water until clear return water could be observed. The selected 20 mm hole diameter was considered an optimal dimension as it is large enough to be comparable to field-scale operations (Haimson and Zhao 1991), but at the same time small enough to avoid stress perturbation away from the borehole.

To facilitate the hydraulic jacking tests, a new fracture had first to be made in the initially intact rock specimens. This was done by confining the specimen inside the rig and hydraulically fracturing it, using the same equipment used for later hydraulic jacking tests. To promote the development of a vertical fracture a stress configuration with $\sigma_H > \sigma_v > \sigma_h$ was chosen. Despite omitting, any pre-slotting of the borehole to control the fracture direction the fractures developed fairly planer and close to vertical, in a classic bi-wing (i.e. to both sides of the borehole) manner.

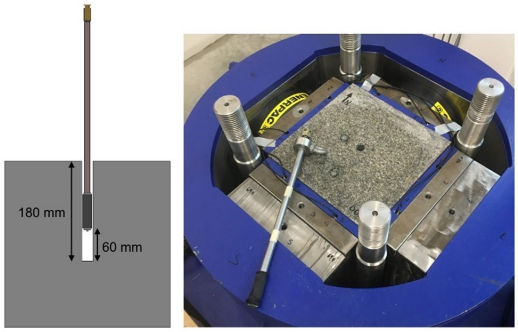

Fig. 8 Overview of packer and packer placement, with the location of the packer elements inside the specimen shown to the left and the packer resting on top of the mounted specimen to the right

Before lowering the specimen inside the test frame, a thin layer of acoustic couplant was applied to the active side of the AE sensors, i.e. the surface in contact with the specimen. A paving slab lifter was used to clamp the specimen as it was lowered into the test frame using the integrated crane. Once the specimen had been placed inside the test frame, and the four sensor platens placed in contact with the specimen, the remaining platens could be installed, ensuring both a snug fit and that the specimen was maintained centrally in the test frame, as shown in Fig. 8. An initial check of the acoustic coupling was then made by first confining the specimen to 1 MPa in both horizontal directions, and then performing a pencil-lead test to ensure satisfactory acoustic contact between specimen and sensor.

For all tests, the true triaxial stress field, with $\sigma_H = 7$ MPa, $\sigma_h = 3$ MPa and $\sigma_v = 4$ MPa, was kept constant throughout the test. The chosen stress magnitudes were considered representative for stress conditions at typical depths of Norwegian hydroelectric projects where, due to the predominantly compressional tectonic regime in Norway, the maximum horizontal stress commonly exceeds the magnitude of the vertical stress. The stress directions were set to promote hydraulic jacking of the existing hydraulic fracture, and not creating new fractures, i.e. by ensuring that the direction of minimum horizontal stress was closest to normal to the fracture, and that the maximal horizontal stress was closest to parallel to the fracture. The stress directions, stress magnitude and fracture orientation for all specimens are shown in Fig. 9.

After confinement of the specimen, the packer could be installed and tightened, thus representing the actual field condition. The packer rod was topped off with water and the injection line thoroughly flushed prior to connecting the high-pressure injection line to the packer, to avoid trapped air in the system. Low-pressure injection into the test section was performed prior to each test to check for any leaks, causing the fracture to be wetted prior to testing. The specimen

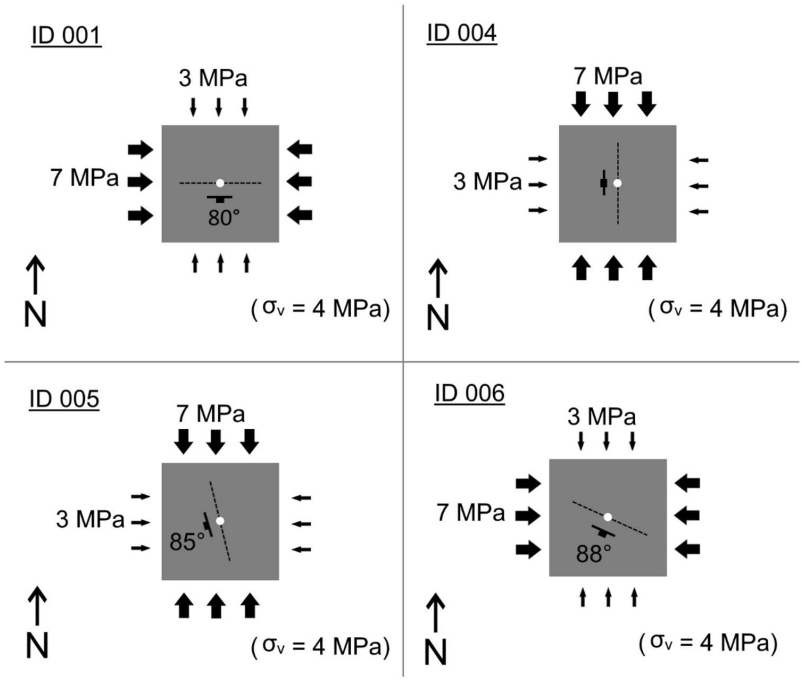

Fig. 9 Stress field and fracture orientation for the tested specimens, topside views

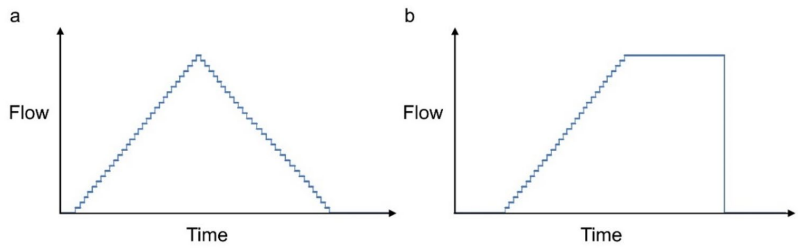

Fig. 10 Overview of test types, RSRT to the left, Type B to the right

itself was unsaturated prior to testing. Ordinary tap water at ambient temperatures was used in all tests. Any water reaching the sample boundaries during testing is effectively drained along the sensor platen–specimen interface before being drained out of the test rig. The packer rod was anchored to the crane yoke prior to testing, a final safety measure to avoid sudden release and ejection of the packer during testing.

4 Experimental Results

4.1 Test Procedure

Two types of hydraulic jacking experiments have been conducted as part of this study. The first is a rapid variant of the step-rate test, hereafter termed the rapid step-rate test (RSRT), where water is injected in a series of pre-determined flow steps, and the corresponding response in injection pressure, P_{inj} is registered. The test starts with forward-step flow increments until hydraulic jacking occurs, interpreted in the test as a distinct deviation from the initial linear stage in the pressure–time plot. After hydraulic jacking, the test continues with backward-step flow reduction down to zero flow, similar to that of the *Fracture reopening—option 3* of the HTPF method (Haimson and Cornet 2003).

The stepwise flow change, and relatively small flow increment of each step, ensures that the pressure in the test interval can be raised steadily, even when the initial permeability of the test section is unknown.

For the second test type, termed Type B, the first part of the procedure is basically identical with the RSRT, using the same ascending flow increments. In the second half of the test follows a brief period of constant flow before the pump is stopped without venting the injection line, similar to that of the *Fracture reopening—option 2* of the HTPF method (Haimson and Cornet 2003). It should be noted that, due to the experimental setup, no traditional shut-interpretation to assess the fracture normal stress is intended, since it is believed that the leaky periphery (fracture extending to specimen edges) would cause gradual fracture closure and thus indistinct shut-in pressure interpretation (Rutqvist and Stephansson 1996). The shut-in phase is instead performed to investigate the acoustic emission (AE) response to fracture closure. The idealized, flow/time curves for the two test types are shown in Fig. 10.

An important feature of both test procedures is that the flow change for each step, and the duration of which each flow step is maintained, is kept constant throughout the test. For the experiments presented in this paper, each flow step is fixed at 1 ml/min, and the duration of each flow step is 1 s, giving a flow rate change of 1 ml/min/s. Consecutive tests on the same specimen were made without removing the specimen from the test rig between tests. The RSRT was performed first, and, after waiting a minimum of 0.5 h, Test B was performed.

4.2 Fracture Orientation

To enable calculation of the normal stress across the different fractures, the orientation of each fracture had to be known. This was done by investigating the AE hypocentre location from 3D AE data and, where applicable, by direct measurements of visible fracture trace on the specimen sides. Though the fracture itself rarely was visible to the naked eye, it could be traced on the specimen sides either by post-test injection of water with methylene blue, a water-soluble dye, or from the colour contrast from the wetted fracture against the otherwise dry specimen. This combined fracture mapping provided an efficient and non-destructive means of identifying the fracture orientation and shape. To illustrate the ability of the AE system to locate the fracture, an AE hypocentre plot has been draped on a photo of the actual specimen immediately after removing the sample from the test rig after testing, see Fig. 11.

The fracture surfaces were not perfectly planar, and one single value for the orientation had to be chosen for the normal stress calculation. This orientation is termed the *Representative Dip/dip-direction*. The combined uncertainty due to variation in fracture orientation (the fact that the fracture is not entirely planar), and due to inaccuracy of orientation measurement, is estimated to be max $\pm 5°$ for dip-direction and $\pm 2°$ for dip, representing a max. error of about 0.28 MPa in the normal stress calculation. The dip- and dip-direction

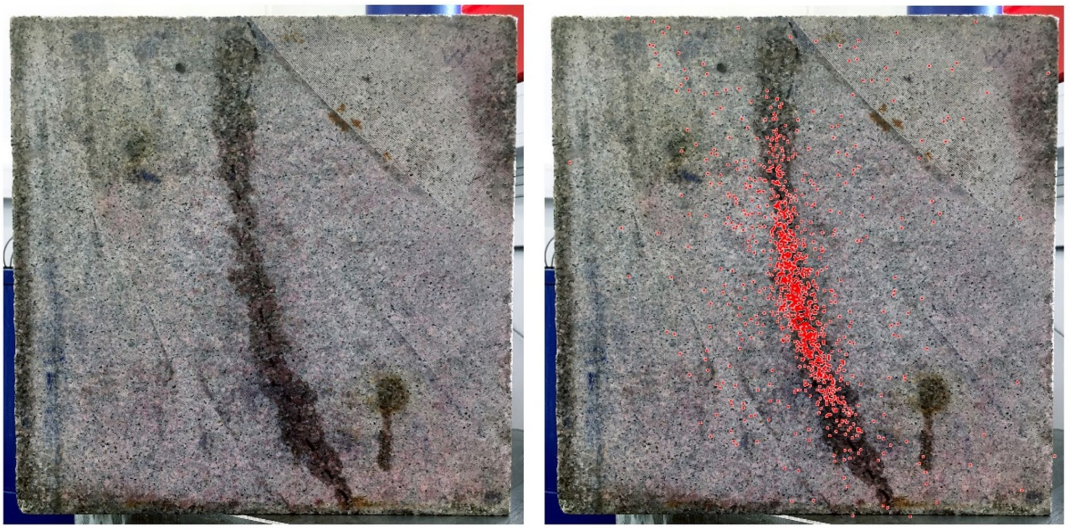

Fig. 11 Correlation between AE hypocentre locations and hydraulic fracture. Granite specimen (ID 001) after hydraulic stimulation shown to the left, with the wetted fracture trace shown as a dark line running vertically from the top centre, curving slightly to the right. To the right is a compiled view of the same specimen photo, draped with the AE hypocentre locations (red dots) originating from hydraulic jacking test. The two dark dots visible in the lower right and upper left are caused by residue from the acoustic couplant

Table 2 Fracture orientation for the tested specimens

Specimen ID	Representative dip/dip-direction	Comment
001	80/180	Bi-winged fracture. The fracture is fairly planar, but slightly curved towards south in the lower parts of the fracture
004	90/090	Bi-winged vertical fracture. The northern branch in planar, striking exactly N–S and the southern branch deviating slightly towards the S–SE
005	85/255	Bi-winged planar fracture developed mainly in the specimen's upper half
006	90/205	Bi-winged and fairly planer fracture, but with the south-eastern branch deviating slightly from that of the north-western

for each fracture, relative to the local north (see Fig. 9), is provided in Table 2, together with a brief description of the fracture.

4.3 Rapid Step-Rate Tests

4.3.1 Pressure–Time Plots

Four tests using the RSRT procedure, tests 001-A, 004-A, 005-A and 006-A, have been performed as part of this study. The injection pressures and flow rates are plotted as function of time in Fig. 12. For all tests, an initial linear trend can be observed in the ascending pressure–time curve, representing the combined effect of minor fluid leakage to the specimen and elastic deformation of the test system, the latter caused primarily by compression of the water and the rubber packer. The observed variation of initial pressure development, as seen for the different specimens, reflect the unique hydraulic properties of the stimulated fractures, of which the residual aperture is believed to be the predominant. The point on the ascending pressure–time curve where the initial linear trend deviates from linearity, indicate increased fluid leak-off and marks the onset of hydraulic jacking. Opposite, in the descending pressure–time curve, the start of a linear pressure decay indicates fracture closure and corresponding reduced fluid leak-off.

Starting with test 001-A in Fig. 12, a linear pressure increase can be observed until deviation at $P_{\mathrm{inj}} = 3.8$ MPa, suggesting leak-off. From the start of the descending flow steps, at $t = 83$ s, a non-linear pressure decline can be

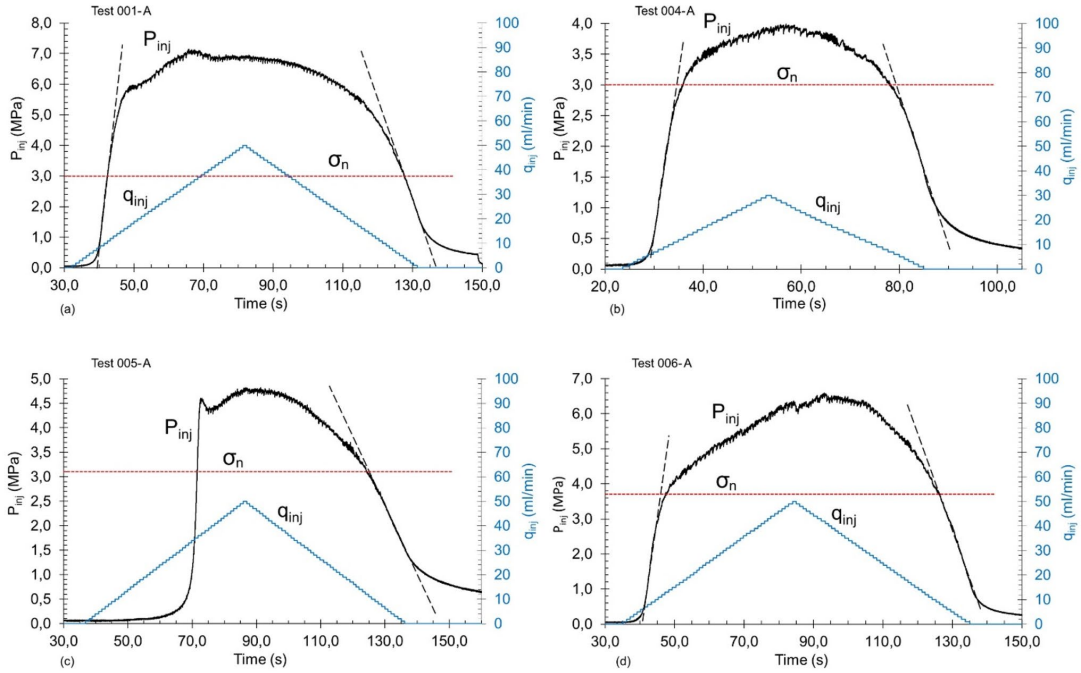

Fig. 12 Injection pressure variation as a function of time and flowrate for tests 001-A, 004-A, 005-A and 006-A. The horizontal, red line indicates the magnitude of the calculated normal stress acting across each respective fracture. Where applicable, a dashed line has been drawn to highlight the deviation from the linear trend in the pressure–time curve

observed until $P_{inj} = 3.2$ MPa, followed by a linear pressure decay, indicating fracture closure. A similar pattern can be observed for test 004-A, with deviation from the linear trend starting at $P_{inj} = 2.6$ MPa, suggesting fracture opening. Then, following a gradual pressure decay after reversal of flow steps, a linear pressure decay can be observed at $P_{inj} = 2.6$ MPa, suggesting closure. The ascending pressure curve of Test 005-A differs from 001-A and 004-A by, following an initial linear pressure increase, a distinct breakdown at $P_{inj} = 4.6$, suggesting minimal fluid leak-off and a rather sudden fracture opening. After reversal of flow steps, a gradual pressure decay, similar to that of the preceding two tests, can be observed until $P_{inj} = 3$ MPa, from where a linear pressure decay takes place—suggesting fracture closure. For Test 006-A, deviation from linearity of the ascending pressure–time curve occurs at $P_{inj} = 3.2$ MPa. As for the previous three tests, a gradual pressure decline is then followed by a linear decay, in this case starting at $P_{inj} = 3.8$ MPa. For some of the tests, a pressure increase can be observed even after flow step reversal, causing the local P_{inj} peak to occur after the q_{inj} peak. This only reflects that, even though the flow rate is being reduced, the volume of fluid being injected still exceeds that which is leaking out.

From these observations, it seems clear that the pressure at which fracture closure occurs is in close agreement with the normal stress. The pressure observed at fracture opening, however, does not show similar agreement with fracture normal stresses, with apparent fracture opening occurring at pressures both higher and lower than the fracture normal stress. A summary of the interpreted opening and closure pressures for the four tests is given in Table 3.

During testing, can a small, but distinct, increase of the confining pressure (P_{jack}), in the direction normal to the fracture, be observed, see Fig. 13. The onset of this pressure increase occurs prior to any clear signs of hydraulic jacking in the P_{inj}–t plot, and well below the fracture normal stress. This clearly indicate that some fluid enters the fracture prior to hydraulic jacking, causing minor fracture opening and a corresponding push-back on the confining pressure. This is believed to be related to the mechanism discussed in Sect. 2.3, where it is shown how minute fracture opening at fluid pressures lower than the fracture normal stress, can be one of the reasons why reopening (and closing) of a pressurized fracture is believed to be gradual, rather than distinct, causing some ambiguity in the interpretation of fracture

Table 3 Summary of interpreted opening and closing pressures for the step-rate tests, compared to the normal stress on the stimulated fractures

Test ID	Pressure–time plots		*qP*-plots		Calculated normal stress across fracture (MPa)
	$P_{inj\ (opening)}$ (MPa)	$P_{inj\ (closure)}$ (MPa)	$P_{inj\ (opening)}$ (MPa)	$P_{inj\ (closure)}$ (MPa)	
001-A	3.8	3.2	3.7	3.2	3.0
004-A	2.6	2.6	2.4	2.6	3.0
005-A	N/A*	3.0	N/A*	3.0	3.1
006-A	3.2	3.8	2.9	3.7	3.7

*Instantaneous pressure drop

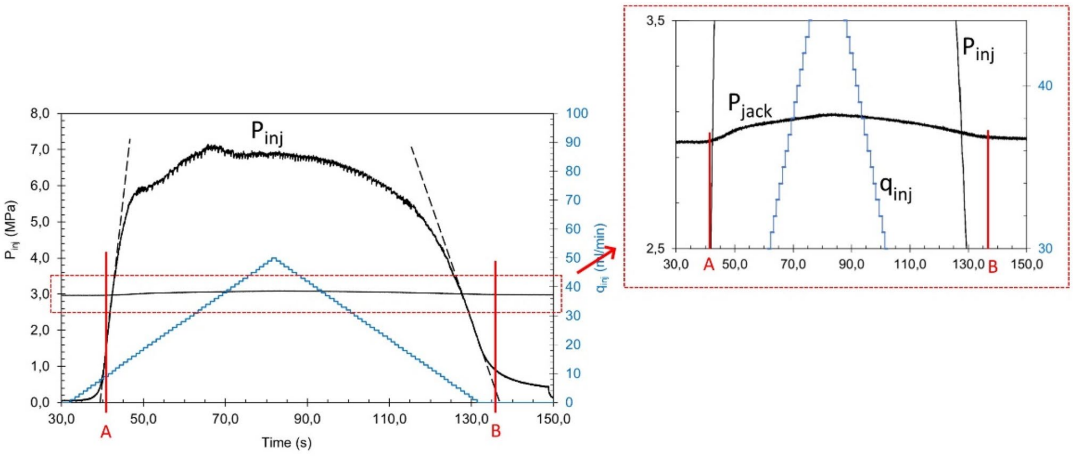

Fig. 13 Two plots of pressure and flow versus time from the same test (001-A), with the original pressure scale to the left, and a detailed view to the right, the latter highlighting the confining pressure. The time of onset of the elevated confining pressure is highlighted with the red line marked as "A", and the time at which it ceases indicated with the red line marked "B"

opening and closure in hydraulic jacking tests (Rutqvist and Stephansson 1996).

A similar, but much smaller, pressure response can be observed in all three confining stress directions when injecting unfractured specimens, indicating that there is some minute outward expansion of the specimen caused by the load from the pressurized water acting on the borehole walls, and to a lesser extent, from any water penetrating into microcracks in the specimen imposing an additional outward pressure (Evans et al. 1988).

4.3.2 Flow Versus Pressure (qP-Plots)

Hydraulic jacking test data, initially presented as real-time plots of pressure and flow vs. time in Fig. 12, are frequently presented in flow vs. pressure (*qP*-plots), as was schematically presented in Fig. 2. We have adopted a similar way of assessing the test data in *qP*-plots as proposed by Hartmaier et al. (1998), where the transition from linear to non-linear trend in the *qP*-plot is interpreted as onset of fracture dilation (jacking). However, instead of looking at the fracture-opening stage only, we use the same approach also for the fracture closure stage, interpreting the pressure at the transition from a non-linear to a linear trend in the *qP*-plot as fracture closure pressure. In Fig. 14, the corresponding graphs are presented for the four tests.

As can be seen, the interpreted fracture closure pressures in Fig. 14 are in close agreement with the interpretation made from the pressure–time plots in Fig. 12, and with the actual normal stress magnitudes. The interpreted fracture-opening pressures, however, both over- and underestimates the respective actual normal stresses. A summary of the interpreted opening and closure pressures found from the *qP*-plots is given in Table 3.

4.3.3 Pressure–Time Plots with Acoustic Emission (AE) Rate

For further assessment of the hydromechanical response of the fractures to the step-rate tests (shown in Fig. 12),

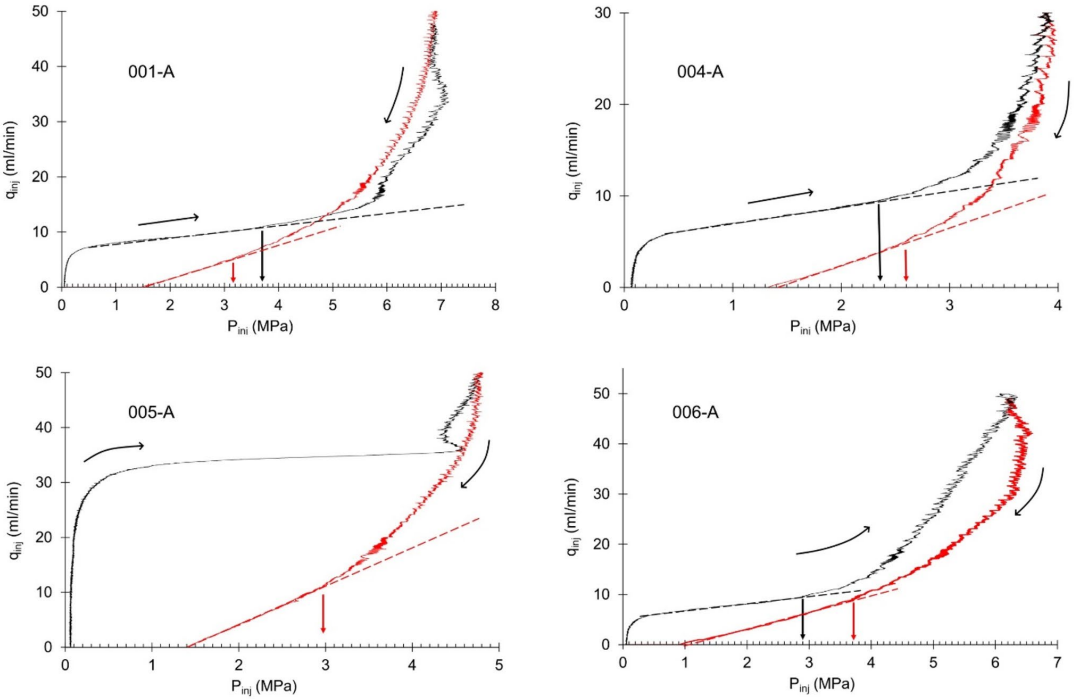

Fig. 14 Injection pressure versus flowrate for tests 001-A, 004-A, 005-A and 006-A (running average). The pressures at which the curves deviate from the linear trend (dotted line) are indicated with a vertical arrow. The graph is given two colours to differentiate the increasing flow steps (black) and the decreasing flow steps (red)

and to investigate potential correlation between AE activity and fracture opening or closure, AE event rates have been plotted together with the step-rate test results. The resulting combined graphs are shown in Fig. 15.

As indicated by Fig. 15, certain correlations exists between the fracture behaviour and the Acoustic Emission event rate. Particularly worth mentioning are: (1) there is little or no AE activity prior to leak-off, indicating that the gradual fracture opening occurs at pressures well below the fracture normal stress, is aseismic, or generating too weak AE signals to be detected; (2) fracture reopening can generate a distinct AE response, with onset coinciding fairly well with the point of leak-off, and finally; (3) a distinct burst of AE activity is associated with fracture closure.

4.4 Type B Hydraulic Jacking Test

A total of four tests based on the Type B test procedure have been performed. Injection pressures, flow rates and AE event rates from these tests are plotted as functions of time in Fig. 16. The event rate activity during the first half of each test evidently is lower than what observed for the RSRT (cf. Fig. 15), even though the initial flow stage for each test type is identical. The reason for this difference in AE behaviour may be associated with the gradual reduction of acoustic contact, caused by partial removal of the water-soluble acoustic couplant, and possibly also with changes in how well the two surfaces fit together, i.e. the fracture surface matedness. Despite this, a strong correlation between fracture closure during the shut-in period and AE activity was observed for all tests, as shown by Fig. 16.

Starting with test 001-B in Fig. 16, an initial linear pressure increase can be observed until $P_{inj} = 3.6$ MPa, from where deviation from linearity indicates leak-off. Full hydraulic jacking can be seen from about $t = 27$ s. No distinct AE response is observed prior to shut-in, but a very distinct AE response can be seen after shut-in when the fracture starts to close at $t = 55.7$ s, when $P_{inj} = 4.5$ MPa. An AE activity peak can then be seen at $t = 57$ s, when $P_{inj} = 3.8$ MPa. The AE event rate then gradually fades out as the pressure drops further and the fracture closes. For

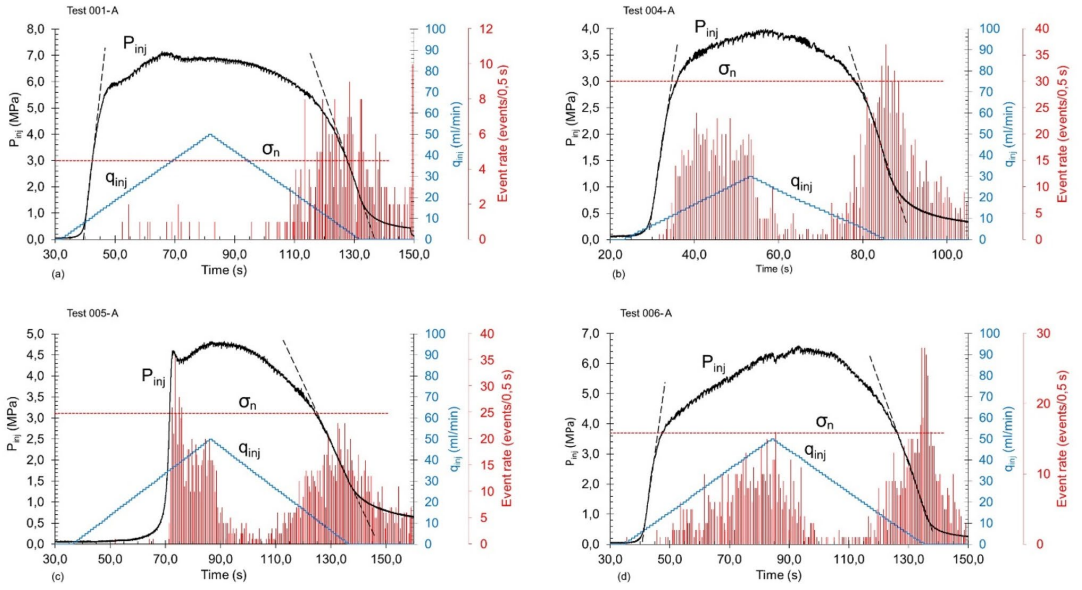

Fig. 15 Injection pressure variations as function of time, flowrates and AE event rates for tests 001-A, 004-A, 005-A and 006-A. The horizontal red lines indicate the magnitude of the calculated normal stress acting across each respective fracture. Where applicable, a dashed line has been drawn to indicate the point of deviation from the straight line in the pressure–time curve

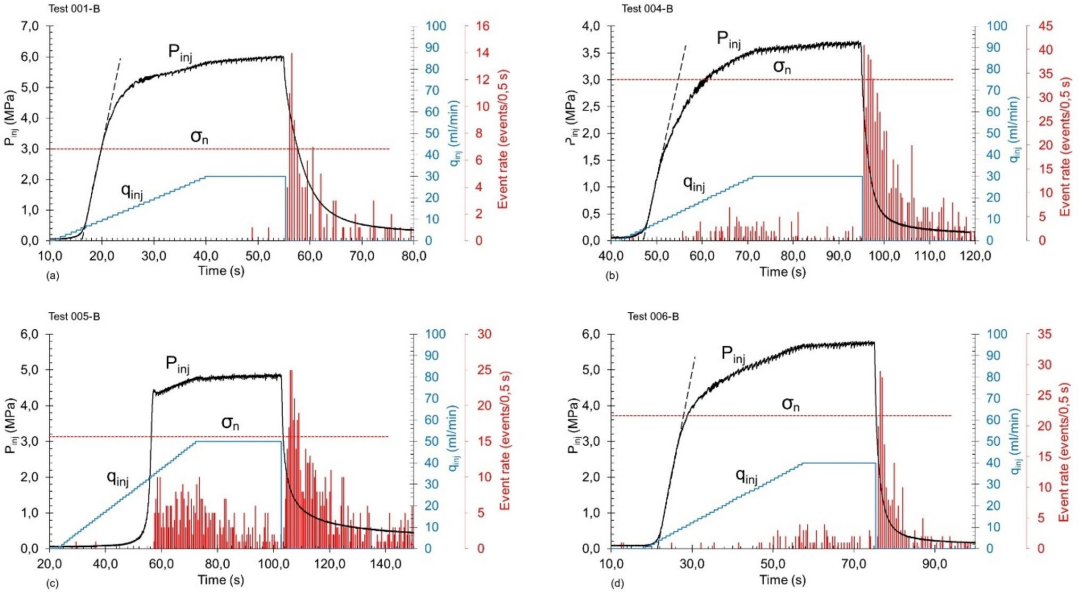

Fig. 16 Injection pressure variations as a function of time, flowrates and AE event rates for tests 001-B, 004-B, 005-B and 006-B. The horizontal red, dotted line indicates the magnitude of the calculated normal stress acting across each respective fracture. Where applicable, a dashed black line has been drawn to highlight the deviation from the linear trend in the pressure–time curve

Table 4 Summary of P_{inj}-results for fracture opening, AE activity onset and AE activity peak

Test ID	$P_{inj\ (opening)}$ (MPa)	$P_{inj\ (AE\ onset)}$ (MPa)	$P_{inj\ (AE\ peak)}$ (MPa)	Calculated normal stress across fracture
001-B	3.6	4.5	3	3.0
004-B	1.6	2.4	2.4	3.0
005-B	N/A*	2.4	1.7	3.1
006-B	3.4	2.9	2.0	3.7

Calculated normal stresses are shown for comparison

*Instantaneous pressure drop

test 004-B a gradual deviation from the initially linear pressure–time curve can be seen from $P_{inj} = 1.6$ MPa, but with no corresponding AE activity. Full hydraulic jacking can be seen from about $t = 63$ s, when $P_{inj} = 3.1$ MPa. Immediately following shut-in a distinct AE response be observed at $t = 95.5$ s, also marking the event rate peak occurring at $P_{inj} = 2.4$ MPa. The AE event rate then gradually fades out as the pressure drops further and the fracture closes. For test 005-B a distinct breakdown, occurring at $P_{inj} = 4.4$ MPa can be observed after an initial linear pressure increase. A clear AE response to the breakdown can be seen with a sudden onset of AE activity. Some AE activity persists all the way to the shut-in phase, but a distinct increase in AE event rate can be observed after shut-in, the onset of which occurring at $t = 104$ s and $P_{inj} = 2.4$ MPa. The AE activity peak occurs at $t = 106$ s, when $P_{inj} = 1.7$ MPa. In test 006-B a gradual deviation from the linear pressure–time curve can be seen when $P_{inj} = 3.4$ MPa, but with no AE activity. Full hydraulic jacking can be seen from about $t = 37$ s, when $P_{inj} = 4.7$ MPa. Immediately following shut-in a distinct AE response can be observed from $t = 76$ s when $P_{inj} = 2.9$ MPa. Immediately afterwards follows the AE event rate peak at $t = 76.5$ and $P_{inj} = 2$ MPa, before the AE activity gradually fades out when the fracture closes. A summary of the pressure observed at the fracture opening, AE activity onset and AE activity peak for Type B tests is presented in Table 4.

From the above observations, it can be inferred that fracture closure is associated with a distinct AE response, but that AE data alone cannot be used to pinpoint the magnitude of normal stress, since the distinct AE response seems to appear when the fluid pressure is below the normal stress.

5 Discussion

5.1 Assessment of Fracture Normal Stress

The hydraulic jacking experiments presented in this paper are aimed at investigating the ability of a simplified hydraulic jacking test to assess fracture normal stresses in an effort to facilitate more frequent stress measurements for the final design of unlined pressure tunnels. The results from the laboratory-scale hydraulic jacking experiments performed as part of this study, have indicated that the magnitude of normal stresses acting across fractures in rock can be measured efficiently, and to a reasonable level of accuracy, by the rapid step-rate test. The RSRT procedure is similar to ordinary step-rate tests but differ by the relatively small flow increments combined with the short and fixed duration of each step, enabling rapid and semi-automated testing. This represents a major benefit for field-scale operations since the time for testing can be reduced to minutes for individual tests rather than hours as sometimes can be seen in field tests.[1] The semi-automated testing procedure can further reduce operator bias and make testing more efficient since the fixed steps easily can be programmed in a computer-controlled pump. Therefore, it is believed that the RSRT can serve as one way to approach to the ideal of measuring stress regularly along the pressure tunnel rather than at a few locations only, following up the idea outlined in Ødegaard and Nilsen (2018). The short duration of each flow step does not guarantee steady-state conditions during the RSRT, but this does not invalidate the test approach since step-rate tests can be performed without reaching stabilized pressures at each step, provided that equal step-durations are used throughout the test, as discussed by several authors, e.g. (Nolte 1982; Singh et al. 1987; Economides and Nolte 2000; Lizak et al. 2006; Smith and Montgomery 2014).

The experimental results suggests that the most accurate estimate of fracture normal stresses is made by assessing data from the backward-step phase, i.e. the fracture closure phase. These findings are in qualitative agreement with those presented by Rutqvist and Stephansson (1996), who found that reopening pressures were influenced by gradual opening of the fractures—and that interpretation of fracture normal stresses from hydraulic jacking tests should be made from the fracture closure stages to avoid effects of non-linear fracture stiffness.

An additional argument for assessing normal stress from the fracture closure stages is the fact that fractures can dilate

[1] Unpublished test results from hydraulic jacking tests performed at the Verma HPP, Injeksjonsteknikk (2017).

at hydraulic pressures lower than the fracture normal stress due to shear movement (Rancourt 2010). Even though this can affect the interpretation of the fracture-opening pressure, the shear stress will be released upon fracture opening, and a stiffness contrast can still be observed during the fracture closure stage.

On a pressure–time plot of the fracture closure phase, the normal stress can then be estimated from the transitional point between gradual pressure decline and linear decline. In a plot of flow vs. pressure, a *qP*-plot, the same pressure can be found by picking the transitional point between a gradual to a linear trend when flow- and pressure data are plotted for the fracture closure phase. This interpretation can be linked to the idea of system stiffness, originally proposed by Raaen et al. (2001), where the slope of the pressure–time graph observed prior to fracture closure represents the less stiff system associated with an open fracture, and the succeeding, steeper, linear pressure decline represents the system stiffness when the fracture is closed, as discussed in further detail in Sect. 5.2. The same way of reasoning has been presented by Thörn et al. (2015), who proposed that stiffness difference also could be associated with the matedness of fracture surfaces, where poorly fitted surfaces have low normal stiffness whilst well-mated fractures large normal stiffness. This difference in matedness might explain the observed reduction of system stiffness represented by the difference of slope between the pre-opening and post-closure stages for all four hydraulic jacking tests, see Fig. 12. The same mechanism can also explain the observed distinct difference in fracture opening pressure between tests 004-A and 004-B, which would otherwise be expected to be similar since the pressurization rate and confining pressures were identical. This assumed change in matedness might have been caused by minor shear dislocation of the fracture during testing, or by particles dislodged from the fracture surface during the hydraulic jacking, as has been suggested by Chitrala et al. (2011).

5.2 Determination of Fracture Closure

Fracture closure following hydraulic stimulation can be described as a three-stage process (Hayashi and Haimson 1991): stage 1, hinge-like fracture closure, i.e. closure by width reduction but at constant fracture length; stage 2, fracture starting to close at the tip and gradual fracture length reduction, and ultimately; stage 3, where the fracture closes fully, or to its residual aperture depending on the fracture characteristics, see Fig. 17. This understanding of fracture closure behaviour has been used by Raaen et al. (2001) to explain the different stages of pressure decline during flow-back tests. Referring to Fig. 17, the essence of their interpretative model is that the initial linear pressure decay (stage 1) represents the system stiffness when the fracture is

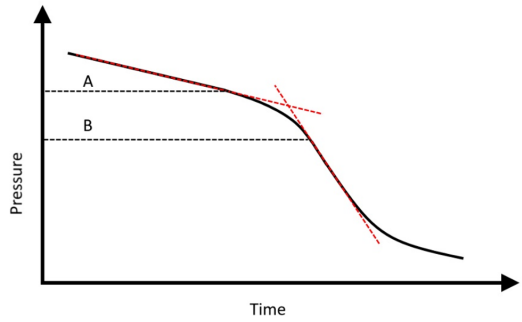

Fig. 17 The three stages of fracture closure shown in an idealized pressure–time plot for the step-down stage of a RSRT: first, a linear pressure decline is observed when the fracture closes in a hinge-like manner, until point A, where deviation from linearity indicates onset of fracture closure (asperities start to touch). As the fracture closes, it will progressively increase its stiffness until point B, where the fracture is closed. Modified after Savitski and Dudley (2011)

open, and when the asperities of the fracture surfaces start to touch (point A), there is a gradual increase in system stiffness (stage 2), until the fracture finally closes (point B) and a new linear pressure decay is observed (stage 3), representing the system stiffness with a closed fracture.

There has been some debate as to which of the two inflection points best represents fracture closure and corresponding fracture normal stress. Arguments have been put forward for picking the point of first inflection (*A*) (Raaen et al. 2001), picking the intersection point of the lines drawn through the two linear segments (Plahn et al. 1997) and (Jung et al. 2016), or picking the lower inflection point (B) (Shlyapobersky 1989) and (Savitski and Dudley 2011).

In the experimental data, it has been found that the pressure at the lower inflection point corresponds reasonably well with the expected normal stress, as discussed in Sect. 4.3.1. An initial linear pressure decline, corresponding to stage 1 of Fig. 17, cannot be identified in the pressure–time graphs of tests 001-A and 004-A, but is partially visible for tests 005-A and 006-A, as can be seen in Fig. 12. This might suggest that picking the upper inflection point would overestimate the normal stress.

Picking the inflection points presented in Fig. 12 was done by fitting straight lines to the linear trend of each graph, to find the point of deviation. This approach, common in field applications, will introduce some subjectivity to the fracture closure determination. To reduce this subjectivity, plots of the time derivative of pressure versus time have been used, since the time derivative of pressure is linear when the system stiffness is constant, and stiffness changes thus may be detected from such plots (Raaen et al. 2001). However, since the pressure–time graphs are quasi-linear, the derivative plots offer only limited guidance on finding the exact

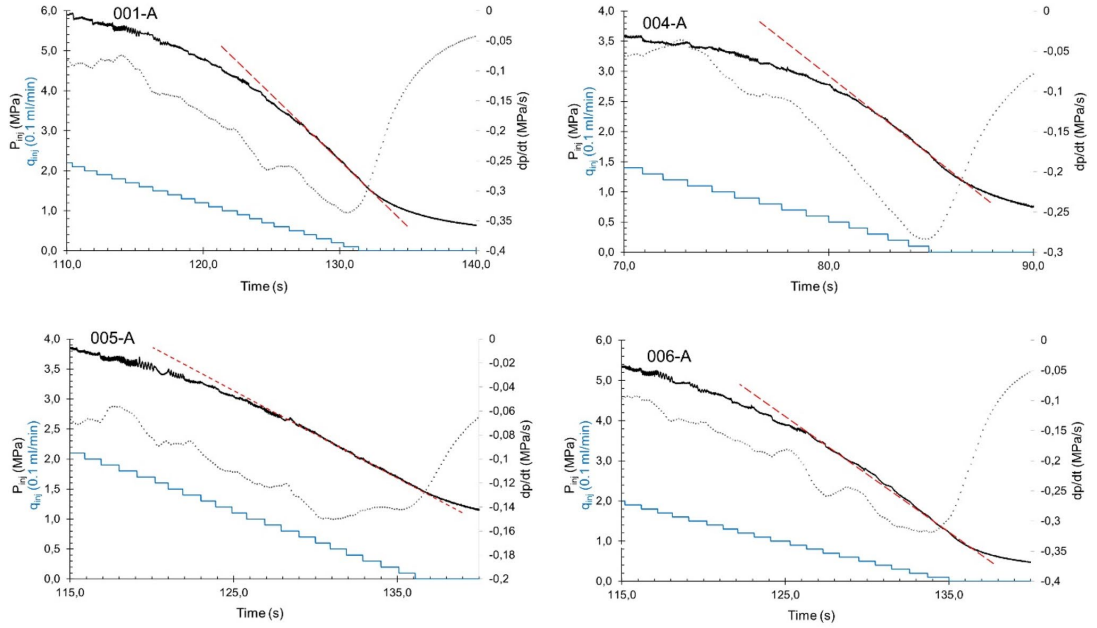

Fig. 18 Injection pressure variation as a function of time and flowrate, including the time derivative of the pressure (dotted line) for the closure stage of tests 001-A, 004-A, 005-A and 006-A

inflection points, as no distinct breaks in the derivative plot can be found, see Fig. 18.

The authors believe that simple graphical methods for finding the inflection point, as illustrated in Figs. 12 and 14, are well suited for the purpose as they can provide estimates of fracture normal stresses that are reasonably accurate, whilst at the same time maintaining the intended simplicity of the RSRT procedure.

5.3 Fracture Behaviour and AE Response

The observed link between AE response and the mechanical behaviour of the fracture represents a useful supplement to hydraulic jacking tests, potentially enabling a more robust assessment of fracture normal stresses. Similar observations of AE events associated with fracture closure have been reported by several authors (Ishida et al. 1997, 2012; Chitrala et al. 2011; Zhuang et al. 2020). Upon investigating the reported link between AE activity and fracture closure Bunger et al. (2014), however, did not find the same correlation during unconfined laboratory experiments, and concluded that it was not appropriate to link post shut-in AE events with fracture closure. From our experiments, we firmly believe that such a link does exists, and that the reported absence of AE events might be linked to the unconfined conditions of which the test was performed.

The AE event rate response does not seem to be sufficiently distinct to assess the exact moment of fracture closure, and the fracture normal stress, hence, could not be assessed from AE data alone. It is believed that the indistinct AE response primarily is caused by the repeated dynamic contact of fracture wall asperities, caused by the dilated fractures response to the incremental flow steps. In addition, when fluid percolates through the fracture there can be local and temporal pressure fluxes caused by repeated cycles of pressure build-up and deflation. Still, AE monitoring during hydraulic jacking tests is considered highly promising, not only for identifying the moment of fracture closure, but also to delineate the orientation of the stimulated fracture, as originally suggested by Tanaka et al. (1997), and later demonstrated by (Zang et al. 2017). The "tail" of AE events observed long after the fracture appears to be closed is believed to be associated with the further, slow, closure of the fracture as water without hydraulic connection to the test section slowly is drained from the fracture.

5.4 Relevance to Field-Scale Stress Measurements

Investigation of hydraulic fracturing processes at laboratory scale requires proper scaling to adequately represent field conditions (De Pater and Weijers 1994). Results obtained from laboratory-scale hydraulic jacking experiments are, however, more easily transferred to field conditions as no material strength parameters, such as fracture toughness need to be considered. Still, some adaptions must be made when upscaling the proposed test procedure to field conditions, mainly related to the equipment used during testing, as will be discussed in the following.

First, is it required that the pump can be operated in flow-control mode without significant pressure pulses, so that the test sequence can be programmed to the desired flow steps and that fluid flow and pressure can be accurately measured and logged. A potential limiting factor for hydraulic jacking tests may be represented by the flow capacity of the pump, especially in the case of high rock mass permeability. One example is what was experienced at the Kihansi HPP in Tanzania, where measurements performed in an extensional tectonic regime required a pump capable of delivering 100 l/min at 20 MPa (Dahlø et al. 2003). Sufficient pumping capacity has also been addressed by Benson (1989), and the practical reason is clear: should the pumping capacity be too low for a given test hole, no pressure build-up can be achieved, and hence, no meaningful estimate of fracture normal stresses can be made. A common practical mitigating measure to this problem is simply to shorten the test section by deeper packer placements, or alternatively omitting holes with too high permeability altogether, moving to the next. Should still the permeability be too high can either shorter holes be drilled, or viscosity adjustments made to the injection fluid (Dr. B. Buen, personal communication May 2019).

During the laboratory experiments described in this paper, it has been found that the native 1 kHz sampling rate of the pressure transmitters should be downsampled to reduce noise, in line with the findings of Kakurina et al. (2020). By looking at the data at various degrees of downsampling, it seems that 100 Hz sampling rate would be optimal, and that sampling rates lower than 10 Hz should be avoided, since important details are lost. Therefore, we recommend sampling rates ranging from 10 to 100 Hz for field-scale hydraulic jacking tests. The transmitter itself should ideally be located as close to the test section as possible to minimize the effect of friction losses, especially at high flow rates (Wandke and Cooper 2016).

To enhance the sensitivity to minor changes in system stiffness during hydraulic testing it has been suggested to minimize the fluid volume used during testing, and to use a piping system with high stiffness (Ito et al. 2006). Even though this theoretically can enhance the sensitivity, it is hard to realize in the field due to the minimum requirements of the borehole dimensions, causing the bulk of the fluid volume to be in the open-hole section and only a fraction in the tubing/piping.

In the introduction, it was argued that distributed measurements along the entire length of a pressure tunnel can provide better insight regarding stress variability, and thus reduce the risk of hydraulic failure. To enable timely adjustments of the tunnel design (if stresses are too low), these measurements should be performed not too far behind the advancing excavation front. This requires that the measurements can be made quite regularly, such that they in a sense are an integral part of the tunnelling activities—and not as per current practice an occasional specialist activity requiring planned stops in other tunnelling activities. Performing standardized HF/HTPF tests regularly along the pressure tunnel would be prohibitively costly, due to the specialist nature of such tests. Though relatively cost-effective, the simplified hydraulic jacking tests commonly used as an alternative to HF/HTPF tests are somewhat impractical due to the long test duration (typically ~ 1–2 h for each test), causing undesirable hindrance to other tunnelling activities. The semi-automated and rapid nature of the proposed RSRT enable highly efficient tests (minutes, rather than hours), and since operator bias can be minimized—there is no strict requirement for specialist crews.

6 Conclusions

A simplified hydraulic jacking test variant, termed the rapid step-rate tests, has been proposed as an alternative to the commonly adopted methods to assess the magnitude of minimum principal stress for the final design of unlined pressure tunnels. The ability of this test to assess the magnitude of normal stress acting across fractures in rock has been confirmed by laboratory experiments, demonstrating good agreement between measured and anticipated values of normal stress. The experimental data suggest that interpretation of test data should be made based on the fracture closure phase only, as data from the fracture-opening phase indicate fracture-opening pressures both much higher and lower than the anticipated magnitude of normal stress.

AE monitoring during hydraulic jacking tests has proven a valuable tool for delineating the fracture orientation, and a clear correlation between fracture closure and AE activity has been demonstrated. The exact moment of fracture closure has, however, not been possible to detect in the AE data alone.

To further assess the field applicability of the proposed Rapid Step-Rate Test, a field verification is needed. Some initial field tests have already been performed, the

preliminary results of which have been used when preparing the RSRT procedure. Additional field tests are under planning.

The link between fracture closure and AE event rate has turned out as a highly promising path in laboratory testing and should be further investigated for use in the field. By pursuing the original idea suggested by Tanaka et al. (1997) with a downhole AE-sonde deployed in the same hole as that which is being tested, improved detection of AE events might be attained. This, in turn, might enable linking the moment of fracture closure, detected from AE data, with the fracture orientation, also found from AE data—potentially providing more accurate rock stress estimation from hydraulic jacking and fracturing tests.

Acknowledgements The Research Council of Norway (NFR) is acknowledged for financing this ongoing research through the Norwegian Research Centre for Hydropower Technology (HydroCen). The authors would like to thank Professor Marte Gutierrez and PhD candidate Ketan Arora for sharing their experience with the design and use of their true-triaxial test rig during our visit to the Colorado School of Mines in the U.S. The excellent craftsmanship demonstrated by Magne Sollie, constructing the test frame, and his practical and efficient solutions to certain initial design challenges is also highly appreciated. Lars Nordø is thanked for his curiosity and interest of hydraulic jacking and AE monitoring, resulting in valuable contributions in the laboratory through his MSc-project. Finally, we would like to express our gratitude to the laboratory staff at the Department of Geoscience and Petroleum at NTNU: Noralf, Steffen, Roger, Terje, Gunnar, Jon, and in particular, Torkjell Breivik for his considerable effort in developing the software needed for the monitoring and control of our experiments.

Funding Open access funding provided by NTNU Norwegian University of Science and Technology (incl St. Olavs Hospital - Trondheim University Hospital).

Declarations

Conflict of interest The authors confirm that there are no known conflicts of interest associated with the publication of this article, and that are no financial or non-financial interests that has affected the outcome of this work.

References

Amadei B, Stephansson O (1997) Rock stress and its measurement. Springer, Berlin. https://doi.org/10.1007/978-94-011-5346-1

Benson RP (1989) Design of unlined and lined pressure tunnels. Tunn Undergr Space Technol 4:155–170. https://doi.org/10.1016/0886-7798(89)90049-7

Berkey CP, Sanborn JF (1922) Engineering geology of the Catskill water supply. Trans Am Soc Civ Eng 48:1029–1595

Bredehoeft JD, Wolff RG, Keys WS, Shuter E (1976) Hydraulic fracturing to determine the regional in situ stress field, Piceance Basin, Colorado. Geol Soc Am Bull 87:250

Brekke TL, Ripley BD (1987) Design guidelines for pressure tunnels and shafts. University of California, Berkeley

Broch E, Dahlø TS, Hansen SE (1997) Hydraulic jacking tests for unlined high pressure tunnels. In: Broch E, Lysne DK, Flatabø N, Helland-Hansen E (eds) Hydropower '97. A. A. Balkema, Rotterdam, pp 581–611

Bunger AP, Kear J, Dyskin AV, Pasternak E (2014) Interpreting post-injection acoustic emission in laboratory hydraulic fracturing experiments. In: Paper presented at the 48th US rock mechanics/geomechanics symposium, Minneapolis, Minnesota, 2014.8.18

Cheung LS, Haimson BC (1989) Laboratory study of hydraulic fracturing pressure data—how valid is their conventional interpretation? Int J Rock Mech Min Sci Geomech Abstr 26:595–604. https://doi.org/10.1016/0148-9062(89)91440-X

Chitrala Y, Moreno C, Sondergeld C, Rai C (2011) Microseismic and microscopic analysis of laboratory induced hydraulic fractures. In: Paper presented at the Canadian Unconventional Resources Conference, Calgary, Canada, 15–17 November

Cornet F (1993) 15—The HTPF and the integrated stress determination methods. In: Hudson JA (ed) Comprehensive rock engineering, vol 3. Pergamon, Oxford, pp 413–432. https://doi.org/10.1016/B978-0-08-042066-0.50021-5

Cornet FH (2016) Hydraulic testing in boreholes for a robust and complete in situ stress determination. In: Paper presented at the ISRM international symposium on in-situ rock stress, Tampere, Finland, 2016.1.1

Cornet FH, Valette B (1984) In situ stress determination from hydraulic injection test data. J Geophys Res 89:11527–11537. https://doi.org/10.1029/JB089iB13p11527

Dahlø T, Evans KF, Halvorsen A, Myrvang A (2003) Adverse effects of pore-pressure drainage on stress measurements performed in deep tunnels: an example from the Lower Kihansi hydroelectric power project, Tanzania. Int J Rock Mech Min Sci 40:65–93. https://doi.org/10.1016/S1365-1609(02)00114-4

De Pater CJ, Weijers L (1994) Experimental verification of dimensional analysis for hydraulic fracturing. SPE Prod Facil. https://doi.org/10.2118/24994-PA

Doe TW, Korbin GE (1987) A comparison of hydraulic fracturing and hydraulic jacking stress measurements. In: Paper presented at the the 28th US symposium on rock mechanics (USRMS), Tucson, Arizona, 1987.1.1

Economides MJ, Nolte KG (2000) Reservoir stimulation. Wiley, Chichester

Evans KF, Scholz CH, Engelder T (1988) An analysis of horizontal fracture initiation during hydrofrac stress measurements in granite at North Conway, New Hampshire. Geophys J 93:251–264. https://doi.org/10.1111/j.1365-246X.1988.tb02000.x

Felsenthal M (1974) Step-rate tests determine safe injection pressure on floods. Oil Gas J 72:49–55

Frash L, Gutierrez M, Hampton J (2015) Laboratory-Scale-model testing of well stimulation by use of mechanical-impulse hydraulic fracturing. SPE J 20:536–549. https://doi.org/10.2118/173186-PA0

Haimson B (1992) Designing pre-excavation stress measurements for meaningful rock characterization. In: Paper presented at the ISRM Eurock '92 symposium on rock characterization, London, 4–17 September

Haimson BC, Cornet FH (2003) ISRM suggested methods for rock stress estimation—Part 3: hydraulic fracturing (HF) and/or hydraulic testing of pre-existing fractures (HTPF). Int J Rock Mech Min Sci 40:1011–1020. https://doi.org/10.1016/j.ijrmms.2003.08.002

Haimson B, Fairhurst C (1969) In-situ stress determination at great depth by means of hydraulic fracturing. In: Paper presented at the The 11th US symposium on rock mechanics (USRMS), Berkeley, California, 1969.1.1.

Haimson BC, Zhao Z (1991) Effect of borehole size and pressurization rate on hydraulic fracturing breakdown pressure. In: Paper presented at the the 32nd US symposium on rock mechanics (USRMS), Norman, Oklahoma, 1991.1.1

Hampton J, Gutierrez M, Matzar L, Hu D, Frash L (2018) Acoustic emission characterization of microcracking in laboratory-scale hydraulic fracturing tests. J Rock Mech Geotech Eng. https://doi.org/10.1016/j.jrmge.2018.03.007

Hartmaier HH, Doe TW, Dixon G (1998) Evaluation of hydrojacking tests for an unlined pressure tunnel. Tunn Undergr Space Technol 13:393–401. https://doi.org/10.1016/S0886-7798(98)00082-0

Hayashi K, Haimson BC (1991) Characteristics of shut-in curves in hydraulic fracturing stress measurements and determination of in situ minimum compressive stress. J Geophys Res Solid Earth 96:18311–18321. https://doi.org/10.1029/91JB01867

Huang B, Liu J (2017) Experimental investigation of the effect of bedding planes on hydraulic fracturing under true triaxial stress. Rock Mech Rock Eng 50:2627–2643. https://doi.org/10.1007/s00603-017-1261-8

Hubbert MK, Willis DG (1957) Mechanics of hydraulic fracturing. J Pet Technol 210:153–168

Ikeda R, Tsukahara H (1982) Acoustic emissions detected by hydrophone during hydraulic fracturing stress measurement. In: Paper presented at the workshop XVII—hydraulic fracturing stress measurements, California, 2–5 December

Injeksjonsteknikk (2017) Testresultater fra jekketesting ved Verma kraftverk pel 50-60 (In Norwegian). Unpublished field data

Ishida T (2001) Acoustic emission monitoring of hydraulic fracturing in laboratory and field. Constr Build Mater 15:283–295. https://doi.org/10.1016/S0950-0618(00)00077-5

Ishida T, Chen Q, Mizuta Y (1997) Effect of injected water on hydraulic fracturing deduced from acoustic emission monitoring. Pure Appl Geophys 150:627–646. https://doi.org/10.1007/s000240050096

Ishida T, Aoyagi K, Niwa T, Chen Y, Murata S, Chen Q, Nakayama Y (2012) Acoustic emission monitoring of hydraulic fracturing laboratory experiment with supercritical and liquid CO_2. Geophys Res Lett. https://doi.org/10.1029/2012GL052788

Ito T, Evans K, Kawai K, Hayashi K (1999) Hydraulic fracture reopening pressure and the estimation of maximum horizontal stress. Int J Rock Mech Min Sci 36:811–826. https://doi.org/10.1016/S0148-9062(99)00053-4

Ito T, Igarashi A, Kato H, Ito H, Sano O (2006) Crucial effect of system compliance on the maximum stress estimation in the hydrofracturing method: theoretical considerations and field-test verification Earth. Planets Space 58:963–971. https://doi.org/10.1186/BF03352601

Jung H, Sharma MM, Cramer DD, Oakes S, McClure MW (2016) Re-examining interpretations of non-ideal behavior during diagnostic fracture injection tests. J Petrol Sci Eng 145:114–136. https://doi.org/10.1016/j.petrol.2016.03.016

Kakurina M, Guglielmi Y, Nussbaum C, Valley B (2020) Situ direct displacement information on fault reactivation during fluid injection. Rock Mech Rock Eng. https://doi.org/10.1007/s00603-020-02160-w

Lizak KF, Bartko KM, Self JF, Izquierdo GA, Al-Mumen M (2006) New analysis of step-rate injection tests for improved fracture stimulation design. In: SPE international symposium and exhibition on formation damage control, SPE-98098-MS. https://doi.org/10.2118/98098-ms

Londe P, Sabarly F (1966) La distribution des perméabilités dans la fondation des barrages voûtes en fonction du champ de contrainte. In: Paper presented at the 1st ISRM Congress, Lisbon, Portugal, 1966.1.1

Merritt AH (1999) Geologic and geotechnical considerations for pressure tunnel design. In: Paper presented at the geo-engineering for underground facilities, University of Illinois, 13–17 June

Nolte KG (1982) Fracture design considerations based on pressure analysis. In: SPE cotton valley symposium, SPE-10911-MS. https://doi.org/10.2118/10911-ms

Nordal S, Grøv E, Emdal A, L'Heureux JS (2018) Skredene i Tosbotn, Nordland 1. og 2. april 2016. Rapport fra undersøkelsesgruppe satt ned av Nordland Fylkeskommune. NTNU, Trondheim (**In Norwegian**)

Ødegaard H, Nilsen B (2018) Engineering geological investigation and design of transition zones in unlined pressure tunnels. In: Paper presented at the ISRM international symposium—10th Asian rock mechanics symposium, Singapore, 29.10–2.11 2018

Philippe V, Eda Q, Milton Assis K, Tom J, Mehmet E (2019) ISRM suggested method for the Lugeon Test. Rock Mech Rock Eng 52:4155–4174. https://doi.org/10.1007/s00603-019-01954-x

Plahn SV, Nolte KG, Miska S (1997) A quantitative investigation of the fracture pump-in/flowback test. SPE J 12:20–27. https://doi.org/10.2118/30504-pa

Raaen AM, Skomedal E, Kjørholt H, Markestad P, Økland D (2001) Stress determination from hydraulic fracturing tests: the system stiffness approach. Int J Rock Mech Min Sci 38:529–541. https://doi.org/10.1016/S1365-1609(01)00020-X

Rancourt AJ (2010) Guidelines for preliminary design of unlined pressure tunnels. PhD, McGill University

Rasouli V (2013) A true triaxial stress cell (TTSC) used for simulations of real field operations in the lab. In: Kwasniewski M (ed) True triaxial testing of rocks, vol 4. CRC Press, London, pp 311–319

Rutqvist J, Stephansson O (1996) A cyclic hydraulic jacking test to determine the in situ stress normal to a fracture. Int J Rock Mech Min Sci Geomech Abstr 33:695–711. https://doi.org/10.1016/0148-9062(96)00013-7

Rutqvist J, Stephansson O (2003) The role of hydromechanical coupling in fractured rock engineering. Hydrogeol J 11:7–40. https://doi.org/10.1007/s10040-002-0241-5

Savitski AA, Dudley JW (2011) Revisiting microfrac in-situ stress measurement via flow back—a new protocol. In: SPE annual technical conference and exhibition, SPE-147248-MS. https://doi.org/10.2118/147248-ms

Schjerven H (1921) Tryktunnelen ved Herlandsfossen. Den Norske Ingeniør- og Arkitekt-forening og Den Polytekniske Forening, Oslo (**In Norwegian**)

Shi L, Li B, Bai Q, Feng X (2013) Numerical analysis of loading boundary effects in Mogi-type true triaxial tests. In: Kwaśniewski M, Li X, Takahashi M (eds) Geomechanics research series, vol 4. CRC Press, London, pp 19–33

Shlyapobersky J (1989) On-site interactive hydraulic fracturing procedures for determining the minimum in situ stress from fracture closure and reopening pressures. Int J Rock Mech Min Sci Geomech Abstr 26:541–548. https://doi.org/10.1016/0148-9062(89)91432-0

Singh PK, Agarwal RG, Krase LD (1987) Systematic design and analysis of step-rate tests to determine formation parting pressure. In:

Paper presented at the SPE annual technical conference and exhibition, Dallas, Texas, 1987/1/1/

Smith MB, Montgomery CT (2014) Hydraulic fracturing. Emerging trends and technologies in petroleum engineering. CRC Press, Hoboken

Stanchits S, Surdi A, Gathogo P, Edelman E, Suarez-Rivera R (2014) Onset of hydraulic fracture initiation monitored by acoustic emission and volumetric deformation measurements. Rock Mech Rock Eng 47:1521–1532. https://doi.org/10.1007/s00603-014-0584-y

Tanaka M, Kuwabara K, Honma M, Ishida T, Mizuta Y, Kanagawa T (1997) Determination of crack direction in hydraulic fracutring by borehole acoustic emission sonde. In: Paper presented at the rockbursts and seismisicty in mines, Kraków, Poland, 11–14 August

Thörn J, Ericsson LO, Fransson Å (2015) Hydraulic and hydromechanical laboratory testing of large crystalline rock cores. Rock Mech Rock Eng 48:61–73. https://doi.org/10.1007/s00603-013-0538-9

USACE (1997) Engineering and design. Tunnels and shafts in rock. U.S. Army Corps of Engineers, Washington

Wandke L, Cooper K (2016) Application and analysis of step-rate testing to determine fracture pressure in injection wells. In: Underground injection control conference, Denver, CO, 23–25 February 2016. Ground Water Protection Council, pp 1–23

Warren WE, Smith CW (1985) In situ stress estimates from hydraulic fracturing and direct observation of crack orientation. J Geophys Res 90:6829–6839. https://doi.org/10.1029/JB090iB08p06829

Zang A et al (2017) Hydraulic fracture monitoring in hard rock at 410 m depth with an advanced fluid-injection protocol and extensive sensor array. Geophys J Int 208:790–813. https://doi.org/10.1093/gji/ggw430

Zhang G-Q, Fan T (2014) A high-stress tri-axial cell with pore pressure for measuring rock properties and simulating hydraulic fracturing. Measurement 49:236–245. https://doi.org/10.1016/j.measurement.2013.11.001

Zhuang L et al (2020) Laboratory true triaxial hydraulic fracturing of granite under six fluid injection schemes and grain-scale fracture observations. Rock Mech Rock Eng 53:4329–4344. https://doi.org/10.1007/s00603-020-02170-8

Zoback MD (2007) Reservoir geomechanics. Cambridge University Press, Cambridge

Zoback MD, Kohli AH (2019) Unconventional reservoir geomechanics: shale gas, tight oil and induced seismicity. Cambridge University Press, Cambridge

Paper IV

Simplified hydraulic jacking test to assess fracture normal stress for unlined pressure tunnels—a field experiment using the Rapid Step-Rate Test

Henki Ødegaard[a], Bjørn Nilsen[b]

Department of Geoscience and Petroleum, Norwegian University of Science and Technology, Trondheim, Norway

Abstract

This paper describes an experimental field campaign where a simplified hydraulic jacking test, the Rapid Step-Rate Test (RSRT), has been investigated in a full-scale field setting. The test, originally developed to assess rock stresses for pressure tunnel considerations, had in an earlier laboratory study demonstrated a promising ability to estimate the magnitude of fracture normal stress. The field campaign presented herein was therefore aimed at assessing the field applicability of this test. The field experiments were conducted inside the pressure tunnel of the Løkjelsvatn Hydroelectric Power Plant in Norway, under field conditions identical to those for which the test originally was developed. A total of 29 individual tests were conducted in 7 boreholes, providing 20 test cycles with interpretable test results. The stress estimates made from the test cycles not affected by the near-field stress of the tunnel showed good correlation with the magnitude of minimum principal stress found from a preceding hydraulic fracturing and overcoring stress measurement campaign. The experience from the field campaign suggests that the RSRT can represent an efficient and reliable method to assess the magnitude of minimum principal stress, particularly useful for the final design of unlined pressure tunnels.

Keywords Hydropower, Field testing, Unlined pressure tunnels, Hydraulic jacking, Rock stress measurements

[a] Corresponding author at: Norwegian University of Science and Technology, S.P. Andersens veg 15a, 7031 Trondheim, Norway

e-mail addresses: henki.odegaard@ntnu.no (H. Ødegaard), bjorn.nilsen@ntnu.no (Bjørn Nilsen).

[b] Norwegian University of Science and Technology, Trondheim, Norway

1 Introduction

Assessing the magnitude of minimum principal stress, σ_3, is highly important for the design of unlined pressure tunnels since it governs the maximum allowable water pressure that the tunnel can sustain without failing (Benson (1989); Merritt (1999)). The basic design idea is to locate the section of unlined pressure tunnel in a volume of rock mass σ_3 exceeds the internal water pressure. This will minimize construction costs by limiting the length of steel liner to a relatively short section of tunnel upstream the power station, where it in any case is needed to ensure the controlled conveyance of water into the turbine. The main length of tunnel, from intake to the start of the steel liner, can thus be kept essentially unlined, as schematically shown in Fig. 1a. This design concept represents a highly cost-efficient design solution for the conveyance of pressurised water in hydropower projects, but only if hydraulic failure is avoided. Naturally, there are other design requirements which also need consideration before choosing an unlined concept, but in this paper main emphasis is given to the stress requirement, which in most cases is the key design issue. For an in-depth review of the general design process of unlined pressure tunnels, reference is made to the significant contribution of Brekke and Ripley (1993).

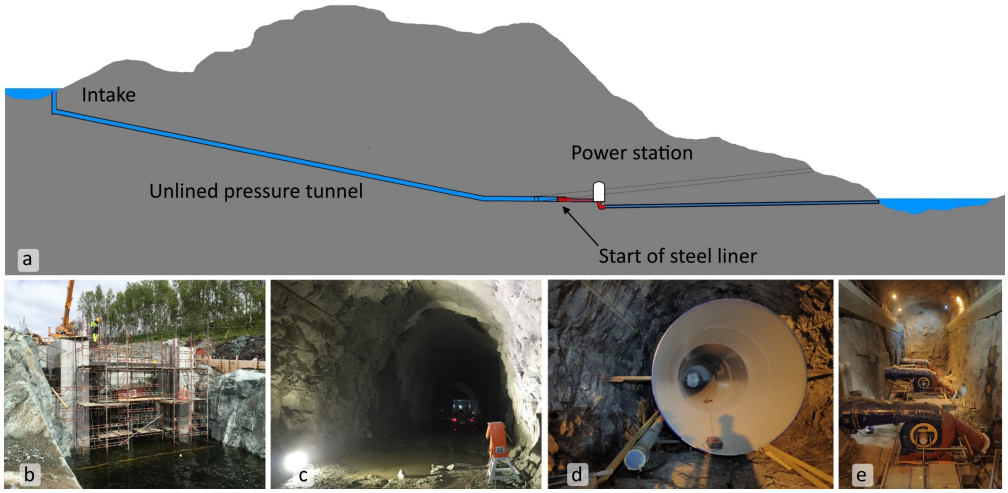

Fig. 1: Conceptual overview of main elements of a hydroelectric plant using unlined pressure tunnels, including picture examples from various HPPs. **a** idealized long section showing the water tunnels, with the unlined sections shown in blue and the steel-lined sections in red, **b** intake structure, **c** section of unlined tunnel, **d** start of steel liner and, **e** power station with horizontal Francis turbines

The significance of stress estimates for safe pressure tunnel design is now well established amongst engineers working with the design of unlined pressure tunnels, and stress measurement techniques based on hydraulic methods are commonly employed, such as the hydraulic fracturing (HF) test (Hubbert and Willis 1957), the hydraulic testing of pre-existing fractures (HTPF) test (Cornet and Valette 1984), as well as other variants of hydraulic jacking tests (Brekke and Ripley (1993); Rutqvist and Stephansson (1996); Quirion and Tournier (2010)).

Typically, stress measurements are performed only at a few key test locations, aimed at verifying design and the tender assumption on stress magnitudes. Once these assumptions are verified, by measurements performed at the selected locations, further testing is often limited, leaving hundreds, or even thousands, of tunnel metres without any stress measurements. One reason for the relatively limited scope of stress measurements is certainly related to costs, but based on the authors' experience, it can also be attributed to an inherent overconfidence on the reliability of stress estimates based on overburden weight. With relatively few test sites, often located far apart, the designer has to make assumptions on the stress gradient beyond measurement locations, leaving the untested sections of pressure tunnel at risk of hydraulic failure. This is an unsatisfactory situation owing to the fact that *in-situ* rock stress can vary significantly over short distances, independently of the surface topography above the point of observation (Marulanda et al. (1986); Haimson (1992); Amadei and Stephansson (1997); Martin and Chandler (1993); Christiansson and Janson (2003); Ødegaard et al. (2020)).

To mitigate this undesirable situation, the authors believe that the number of measurement locations should be increased compared to current practice, to achieve a better coverage and distribution of stress measurement locations along the entire length of the unlined tunnel, as also suggested in Ødegaard and Nilsen (2018). Though it can be argued that it is economically and practically unfeasible to get a continuous stress log along the pressure tunnel, the authors believe that it is still possible to get closer to this goal, by adopting a simplified and cost-effective method for assessing stresses. One test method which potentially could make more testing possible is the Rapid Step-Rate Test (RSRT), developed specifically with the goal of enabling such simple stress assessments (Ødegaard and Nilsen 2021). As the RSRT in laboratory controlled conditions demonstrated a promising ability to assess fracture normal stresses, it was considered of great interest to investigate how the test protocol would perform in the field. The aim of the field campaign described in this study was therefore to assess the field applicability of the RSRT, by performing testing in a full-scale field setting.

The main field campaign of this study includes hydraulic testing in 7 boreholes drilled from the unlined section of the pressure tunnel of Løkjelsvatn hydroelectric power plant (HPP), currently under construction in southern Norway. These field experiments, comprising 29 individual test cycles, were designed in such a way that a comparison could be made between the stress estimates obtained from the RSRT experiments and stress estimates originating from the more well-established hydraulic fracturing (HF) and overcoring (OC) stress measurements. This was possible since HF and OC tests had already been conducted at the same location as part of the plant Owners final design considerations. These preceding tests had been performed by an independent specialist company, SINTEF Community, and access to the test report were granted by the plant Owner, Sunnhordaland Kraftlag AS, SKL.

Originally, it was intended to include data from hydraulic jacking tests performed at another plant, the Leikanger HPP, owned by Leikanger Kraft A/S, but equipment failure unfortunately made these tests unsuccessful. The experience gained during the initial field trials at the Leikanger plant did,

however, prove valuable for the planning of the subsequent field campaign at Løkjelsvatn HPP, and some detail from these failed tests will therefore be included in Chapter 2.1.

The experiments performed at the Løkjelsvatn HPP are, to the authors best knowledge, the first time the Rapid Step-Rate Test protocol have been executed in field-scale conditions.

2 Description of the test sites and test procedures

2.1 Initial field trials - Leikanger HPP

The Leikanger HPP is a is a run-of-river hydroelectric plant located 116 km north-east of Bergen, in the region of Western Norway. The plant has an underground powerhouse equipped with a single Pelton turbine and the installed capacity is 77 MW, with a planned yearly production of 208 GWh once the last stage of development is completed by 2021. The tests, comprising 13 individual test cycles, were performed in 5 different boreholes, all drilled from within the access tunnel of the plant, close to Chainage 550, see Fig. 2. Access to the test site was granted by the plant owner, Sognekraft AS.

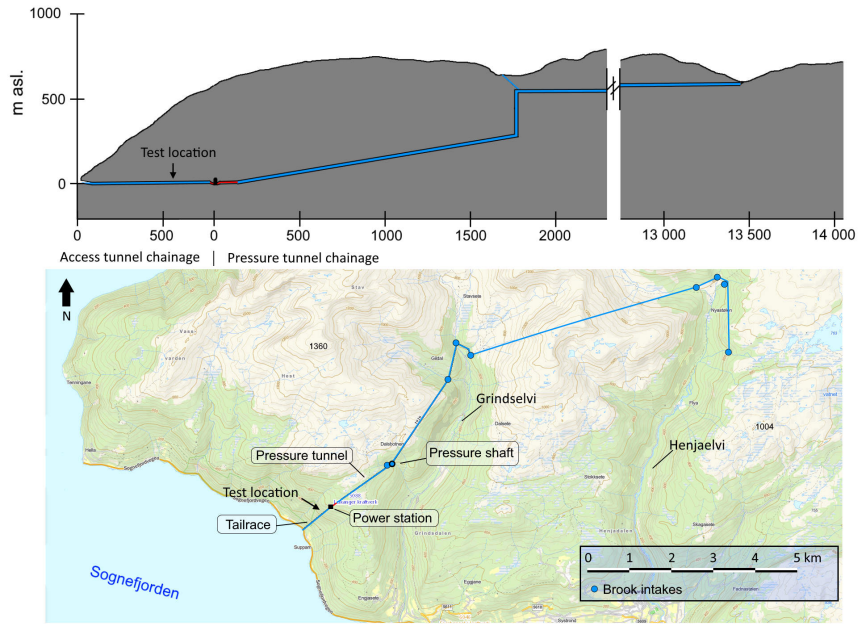

Fig. 2: Leikanger HPP long section (top) and plan view (bottom). The long section has been shortened to promote the visibility of the downstream high-pressure section of the water tunnels. Note that plan view and long section have different scales. Background map after NVE (2020)

The tests were performed with a custom-built, dual-piston, reciprocal pump, using pressure-controlled hydraulic jacking test protocol, similar to the test approach of Doe and Korbin (1987). The test protocol included the stepwise increase in pressure, in a series of rapid 0.1 MPa pressure increments, until hydraulic jacking (or fracturing) occurs, and then reducing the pressure following the same steps

down to ambient pressure while continuously monitoring the resulting pressure and flow. Analysis of the test data was, however, inhibited by excessive flow- and pressure pulsations. The pulsations were caused by a significant drop in flowrate occurring at each piston reversal, causing a corresponding drop in pressure. When the pressure dropped below the set-point, the control system of the pump would immediately try to compensate for the loss of pressure, resulting in even more pulsations. Attempts of manually operating the pump, to override the PID (proportional–integral–derivative controller) of the pump, did not succeed. To worsen the situation, it was also discovered that the ordered hydraulic packers did not have the proper pressure rating, rendering them useless for the tests. Ordinary mechanical grouting packers found at site had therefore to be used, but packer seating depth was limited to 6 m (maximal length of the available grouting rods), considered too short to stay away from the perturbed stress field surrounding the 6.5 m wide access tunnel.

In summary, the test results from the Leikanger HPP could not be used for any meaningful assessment of *in-situ* stresses, but the challenges faced during the pressure-controlled tests did influence the later development of the flow-controlled RSRT protocol, where no PID-control is needed.

2.2 Main field trials - Løkjelsvatn HPP

The main field experiments were all conducted inside the tunnel system of the Løkjelsvatn HPP, a storage hydroelectric plant currently under construction some 90 km south of the city of Bergen, Norway. The plant is equipped with a single 60 MW vertical Francis turbine placed in an underground powerhouse and will, once in operation, provide an annual production of 163 GWh. Planned commissioning of the plant is 2022.

The Løkjelsvatn plant was deemed well-suited for the planned field experiments since the field conditions corresponded well with typical conditions for which the test was originally developed, i.e. measurements performed inside unlined pressure tunnels during the construction stage. A longitudinal section and plan layout of the plant is presented in Fig. 3, and the main components of the tunnel system will be briefly described in the following.

From the intake at the Løkjelsvatn reservoir, shown to the right in the plan overview, the water will be conveyed through a short horizontal headrace tunnel before entering the 480 m deep vertical pressure shaft. A 300 m long pressure tunnel connects the shaft bottom with the start of the steel liner. From this point, the transition zone between the unlined tunnel and the steel-lined, the water is conveyed through an approximately 60 m long section of concrete embedded steel liner before entering the turbine. The 3 200 m long tailrace leads the water to the lower Litledalsvatnet reservoir, shown to the left in the plan overview in Fig. 3. The maximum water pressure sustained by the unlined section of the tunnels is 548 m, equivalent to 5.4 MPa.

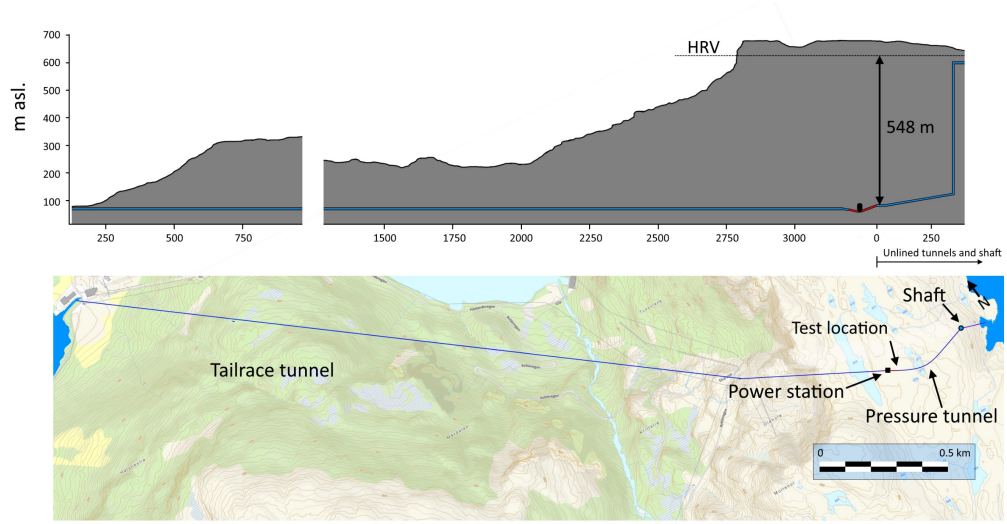

Fig. 3: Løkjelsvatn HPP; longitudinal section (top) and plan view (bottom). The longitudinal section has been shortened to enhance the legibility. Note that plan view and long section have different scales. Background map after NVE (2020)

The test location, where all RSRT experiments were conducted, can be found at the lower end of the pressure tunnel, immediately upstream of the planned steel liner start, as shown in Fig. 3.

2.2.1 Rock mass conditions

According to the tender stage geological map the tunnels of Løkjelsvatn HPP were expected to pass mainly through Cambro-Silurian phyllites and mica schists. Some Precambrian amphibolite was also expected, mainly in the western reaches of the project. At the test location only phyllite was observed, see Fig. 4. The rock mass quality was generally good, with no signs of weathering. In addition to random joints, two joint sets were observed: the foliation, with a typical orientation (dip/dip direction) of 30/170, though with the dip locally varying between 20-50°, and a steep joint set with orientation 80/060. Only minor leaks and drips could be observed at the test location, though significantly larger leakages could be observed in the upper parts of the access tunnel.

Generally, the rock mass conditions at the test site were considered excellent for the D&B excavation, allowing for full round lengths (~5 m) and full face excavation, which is standard for most hard rock tunnelling in Norway. The rock support in the water tunnels consisted mainly of scaling, spot bolting and occasional application of steel fibre reinforced sprayed concrete.

Fig. 4: Examples of phyllite encountered at the lower parts of the pressure tunnel. To the left is the excellent tunnel contour observed at the test location, and to the right a core specimen of the rock. Note the distinct foliation and thin white bands of quartz, characteristic for the rock type

Core- and block samples of phyllite were collected at the test site for laboratory testing of mechanical properties. The resulting index properties are shown for reference in Table 1.

Table 1 Selected index properties of the phyllite found at the test location. All testing was done at the NTNU rock mechanics laboratory, courtesy of Erlend Andreassen

Property	**Value**
Density (kg/m³)	2820 ± 1
Poisson's ratio	0.35 ± 0.01
Sound velocity[1], Vp (m/s)	4900 ± 250
Sound velocity[2], Vp (m/s)	5700 ± 280
Uniaxial compressive strength (MPa)	67 ± 7
Young's Modulus (GPa)	33 ± 4
Brazilian Tensile Strength (MPa)	8 ± 1

[1]Measured normal to foliation
[2]Measured parallel to foliation

The underground state of stress at the test location had been assessed during the aforementioned HF and OC stress measurements. The σ_3 estimates made from these tests are summarised here, based on the test report (Sintef Community 2021):

- σ_3 from HF: 7.3 MPa, based on picking the lowest shut-in (P_{ISIP}) value from a total of 11 tests performed in boreholes H1, H3 and H4.
- σ_3 from OC tests: 9.4±1.0 MPa, based on tests in borehole H7

The magnitude of all three principal stresses, as estimated from the OC tests are presented in Table 2, and an overview of all boreholes at the test location is provided in Fig. 10.

Table 2: Stress values found from 3D overcoring stress estimation performed in borehole H7 (Sintef Community 2021)

Stress	Magnitude (MPa)	Trend	Plunge
σ_1	18.0±0.4	264	72
σ_2	16.1±1.8	163	3
σ_3	9.4±1.0	72	18

The likely range of minimum principal stress σ_3 at the test location, based on the HF and OC stress estimation, would therefore be about 7–9.5 MPa. It can be noted that, according to the OC tests, the major principal stress σ_1 is close to vertical and has a magnitude that corresponds fairly well with that which can be calculated based on pure gravitational loading from the weight of the 591 m column of rock above the test site.

It should also be noted that, even though it is concluded that the minimum principal stress found from the HF measurements is 7.3 MPa, the test report offers no explanation for the considerable spread in shut-in estimates, with P_{ISIP} values varying between 7.3–17.3 MPa.

2.2.2 RSRT test procedure

The RSRT protocol involves injection of water into a sealed-off section of borehole, using pre-determined flow-stages, or steps, while monitoring the corresponding response in water pressure, P_{inj}. The test starts with increasing flow steps, the *forward-step* stage, which is continued until a sudden pressure drop or a distinct deviation from the initial linear stage in a pressure–time plot can be observed, indicative of the creation or re-opening of a fracture, respectively. After fracture opening is the forward-step continued for a certain period before the flow steps are reversed to a stage of decreasing flow steps, termed the *backward-step* stage. The backward-step stage is then continued down to zero flow. By analysis of the resulting pressure development during the backward-step stage can fracture normal stress be assessed according to the principles described in Chapter 2.2.3.

The RSRT protocol is defined by the two parameters step height, Δq (l/min), and the step duration, Δt, which together define the rate of flow-rate change (l/min×s^{-1}), see Fig. 5. The rate of flow-rate change is positive, i.e. increasing, in the forward-step stage, and negative during the backward-step stage.

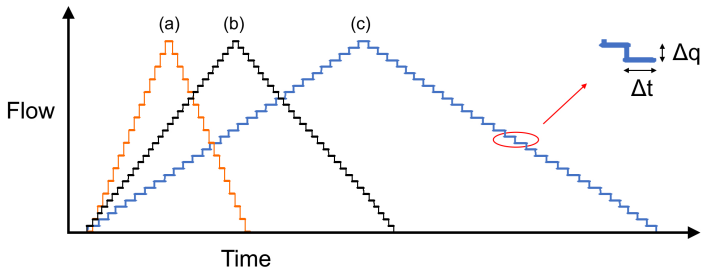

Fig. 5: Conceptual overview of different RSRT flow steps. The rate of flow change can be adjusted by individually changing the flow rate, Δq, or flow step duration, Δt, as shown schematically by graphs a–c

Once the test parameters are defined the test sequence can be run automatically, only requiring the operator to reverse the flow steps after fracture opening, simply by pressing a single button on the touch-screen display of a PLC, an industrial-type computer. The required operator intervention is thus limited to defining the timing of flow reversal and to find the proper Δq and Δt values. Typical values for the tests performed at the Løkjelsvatn HPP were step heights ranging from 0.05–0.2 l/min and a step duration between 2–4 s. As the RSRT interpretation is based on an assessment of fracture behaviour during the backward-step stage, there is no strict requirement on how the pressurisation rate during the forward step-cycle is designed, as long as a fracture is created and opened against the normal stresses acting across it. For simplicity it was, however, decided to maintain the same rate of flow change for both forward- and backward stages within each test cycle, though with some exceptions.

An overview of the test setup including the borehole, the hydraulic packer assembly, fluid lines, pump and monitoring system is shown in Fig. 6. The pump used to pressurize the borehole is a CAT 550 pump, a plunger–type, positive-displacement pump configured to flow-control mode. The simplicity of flow-controlled tests, where no flowmeter or PID-control systems are required, was considered a benefit compared to pressure-controlled tests. Not only is the cost directly reduced when omitting the flowmeter, but the test system is also considered more robust and simpler to operate and maintain. The pump is computer controlled and can be operated and monitored through a touchscreen PLC. A pressure transmitter with a sampling rate of 5 Hz was used to monitor the test pressure, P_{inj}, during testing, and the flowrate, q_{in}, was calculated directly from the rotational speed of the electromotor driving the pump. As can be seen in Fig. 6 a flowmeter was connected to the hydraulic lines, but this was only for use in pressure-controlled tests, and thus not used during the tests at Løkjelsvatn HPP. The maximal flow capacity, 20 l/min according to specifications, was occasionally exceeded by the operator by increasing the RPM of the electromotor beyond the recommended speed. The 20 MPa maximal pressure rating of the hydraulic system was, however, never exceeded.

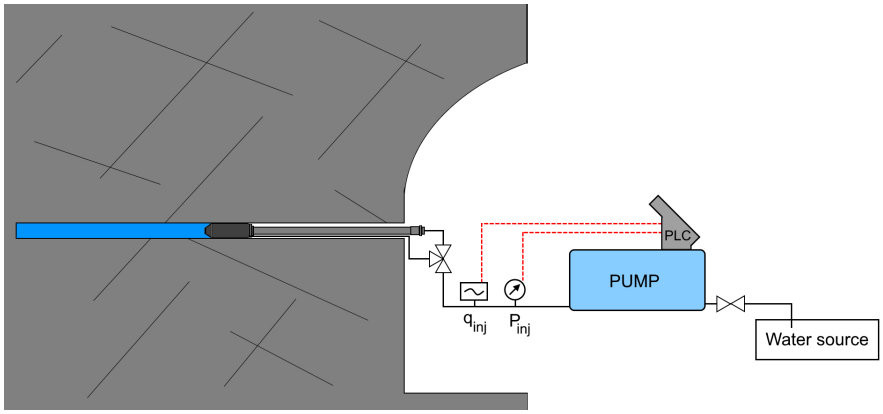

Fig. 6: Schematic overview of the experimental setup for the hydraulic jacking tests using the RSRT protocol

All boreholes were visually inspected for leakage prior to testing, to be able to have a reference to detect any cross-hole leaks during testing. The following general test procedure was then followed:

1. thorough flushing of the borehole, to remove cuttings and particles left after the drilling
2. connecting the packer to the hydraulic tubes, placing packer at the desired depth
3. connecting the packer assembly to the pump with hydraulic hoses
4. packer inflation, to seal off the test section
5. Starting test protocol with the forward-step stage, continuing until a fracture is formed or re-opened. If P_{inj} still increased after fracture opening, the forward-step stage was continued until it exceeded the opening pressure by about 30 %, and then
6. a constant flow was maintained for a brief period before
7. reversing the test such that a backward-step cycle was followed all the way down to zero flow, and finally
8. testing was terminated and the test section vented.

For consecutive cycles in the same borehole steps 5 through 8 were repeated.

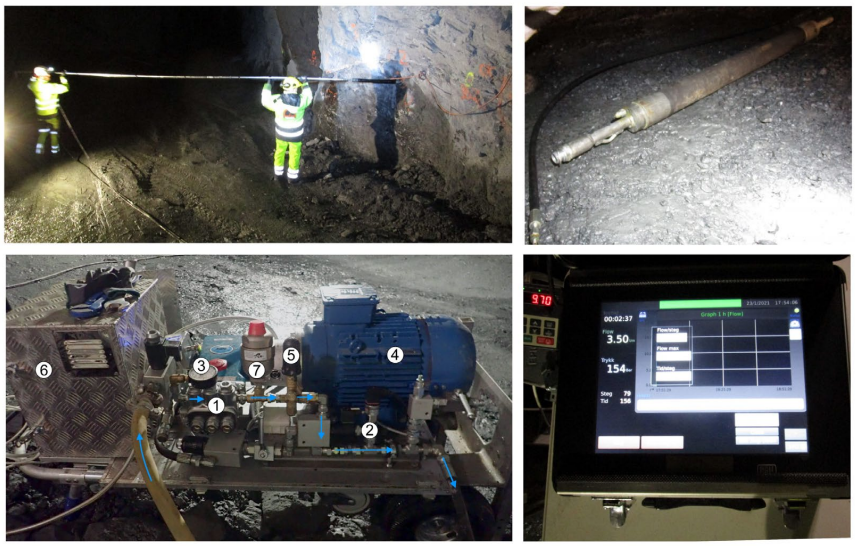

Fig. 7 Overview of the main components for the tests. Installation of the packer assembly (upper left), the hydraulic single packer (top right), the pump (lower left) and the PLC (lower right). In the lower left photo, the following components can be seen: (1) the pump head, (2) pressure transmitter, (3) Bourdon gauge, (4) the electromotor, (5) pressure relief valve, (6) the connection box, and (7) an accumulator tank. The direction of flow is indicated with small arrows

As a safeguard against the consequences of sudden packer ejection, known to have caused fatal accidents during similar stress measurement campaigns (Evans et al. 2003), no personnel were allowed in front of the borehole during testing. In field settings where passage in front of the borehole cannot be forbidden, anchoring of the rod directly to the tunnel wall has to be performed. In Norway, mechanical anchoring of grouting rods has become a mandatory safety measure during all rock mass grouting operations. The effectiveness of even simple mechanical anchorage was experienced during the initial field trials at the Leikanger HPP, where the packer assembly was prevented from shooting out of the hole following a sudden release of the mechanical-type rubber packer. The kinetic energy, and potential risk, associated with such events, should be evident from looking at the example in Fig. 8.

Fig. 8: Example of packer anchoring. Upper photograph showing how the packer rod is mechanically secured to the tunnel wall using expansion anchors and a chain. The lower photo shows how a packer rod was bent after a sudden packer release

During the RSRT experiments attempts were initially made to save time by omitting the push-rods and only using the hydraulic hose itself to push the packer into the hole, but these attempts were not successful. Even though it worked fine in downward slanting boreholes, it was not possible to push the packer to the desired depth in upwards slanting boreholes without the use of rods.

The total length of hydraulic hose, as measured from the rods to the pump, is 36 m, and the total volume in the sealed off system, prior to starting the pump, is about 70-90 litres, depending on the packer placement depth. The open borehole constitutes the bulk of the volume, with the hose and rod together only accounting for 10-15% of the total. All tests were conducted with water at ambient temperatures, using the same water source as used for service water in various tunnelling operations, which for the purpose of a hydraulic jacking test, could be characterised as clean water.

The volume or rock being tested, roughly some tens of meters outside the tunnel periphery, was effectively drained by the tunnel itself, thus the tests were performed in drained conditions.

2.2.3 Fracture closure determination from the RSRT

Determining fracture closure is of great interest when assessing the underground state of stress since it has been shown that the hydraulic pressure required to keep the fracture open will be equal to the in-situ normal stress acting across it (Hubbert and Willis 1957). Since fracture closure is not instant, interpretative techniques are required to find the pressure which best represents the actual normal stress across the fracture. The technique adopted for the assessment of fracture closure from the RSRT is based on the *system stiffness approach* of Raaen et al. (2001), who observed that when the pressure inside a hydraulically opened fracture is lowered, in a controlled manner, the resulting pressure decline curve will show distinct breaks caused by changes in the stiffness of the hydraulic system. They further explained how these breaks could be linked to the normal stress acting across the fracture, by using the

fracture closure model of Hayashi and Haimson (1991). In this model fracture closure is described as a three-stage process:

- Stage 1: The fracture closes in a hinge-like manner, i.e. closure by width reduction but with constant fracture length
- Stage 2: Fracture closure by length reduction, meaning that the asperities of the fracture surfaces progressively will make contact, starting from the tip continuing towards the borehole
- Stage 3: The fracture is fully closed

Raaen et al. (2001) showed how these stages could readily be detected in pressure vs. volume (*PV*) or pressure vs. time (*Pt*) plots from flowback tests. Referring to the schematic pressure decline curve shown in Fig. 9, they argued that the initial linear pressure decay represents the constant stiffness associated with hinge-like fracture closure (Stage 1), and that the gradual pressure decline starting at Point A represent the onset of *mechanical closure,* where the asperities of the fracture start to make contact, causing a corresponding increase of stiffness (Stage 2), which ends at Point B, where a new linear decay can be seen, representing the system stiffness with a closed fracture, termed *hydraulic closure* (Stage 3). It should be noted that even though the term *hydraulic closure* originally indicated a fracture closed for flow, it will be expanded in this paper to include fractures closing back to their residual aperture, and thus not necessarily full closure in the sense that fluid cannot permeate the fracture.

Raaen et al. (2001) further suggested that the best estimate of fracture normal stress was found by picking the pressure at the end of Stage 1, Point A in Fig. 9, when the fracture starts to close by length reduction, indicating the onset of mechanical closure. Other authors have suggested to pick the point where the lines drawn through the two linear segments intersect, as seen in Fig. 9 (Plahn et al. (1997); Jung et al. (2016)), or picking the point where the fracture is hydraulically closed, i.e. Point B in Fig. 9, (Shlyapobersky (1989); Savitski and Dudley (2011)).

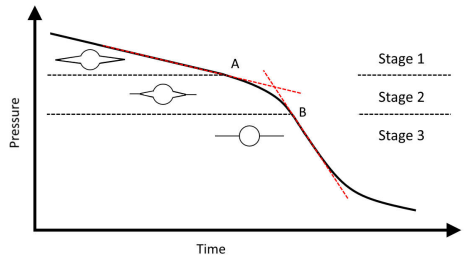

Fig. 9 Typical pressure decline curve during controlled fracture closure. The borehole with a fully open fracture (top) indicates the schematic situation during the first linear pressure decline, the partially closed fracture (middle) indicates the closing fracture resulting in a gradually increasing pressure decline, and the closed fracture (bottom) indicates the last linear stage. Figure modified after Savitski and Dudley (2011) and Raaen et al. (2001)

Instead of flowing back fluid at the surface, as is done during a flowback test, a slightly different method to achieve the same controlled fracture closure is used in the RSRT protocol, by reducing the injected flowrate q_{inj} in a controlled and stepwise manner, effectively reducing the system volume since the ratio of q_{inj} to q_{leak} (leakage into the rock mass) diminishes as the test progresses.

Since the interpretative model described by Raaen et al. (2001) is considered directly relevant also for the interpretation of the RSRT, some details of their original arguments will be iterated in the following. Their interpretation is linked to the concept of system stiffness, i.e. the how changes in pressure, dP, relates to changes in system volume, dV, described by

$$S = \frac{dP}{d\mathrm{V}} \tag{1}$$

where S is the stiffness of the test system, including the combined stiffnesses of hoses, borehole, water, and the stimulated fracture. As the system volume change originating from the deformation of hydraulic lines, borehole and the water itself can be considered negligible compared to the volume change caused by fracture closure, the latter will dominate the system stiffness during fracture closure. It is therefore useful to look only at the fracture stiffness, S_f, during closure.

$$S_f = \frac{dp}{dV_f} \tag{2}$$

where dV_f is the fracture volume change. Sneddon and Mott (1946) showed that the maximum fracture width of an idealised disk-shaped fracture, an ellipsoid, as a function of the net pressure acting on the fracture, would be:

$$w_f = \frac{8}{\pi}(1-\nu^2) r_f \frac{P_{\mathrm{inj}} - \sigma_n}{E} \tag{3}$$

where w_f is the fracture width, ν the Poisson's ratio, r_f the fracture radius, P_{inj} the test interval pressure, E Young's modulus of the rock and σ_n the normal stress acting across the stimulated fracture. The fracture volume, V_f, can then be expressed as the volume of an ellipsoid with w_f as the minor axis, such that:

$$V_f = \frac{2}{3}\pi {r_f}^2 w_f \tag{4}$$

Which, when inserting for w_f gives:

$$V_f = \frac{16}{3}(1-\nu^2){r_f}^3 \frac{P_{inj} - \sigma_n}{E}$$

Using Equation 2 it can then be shown that the system stiffness is constant during Stage 1 when the fracture length is constant:

$$S_f = \frac{dp}{dV_f} = \frac{3E}{16{r_f}^3(1-\nu^2)} \quad (5)$$

This also shows that the fracture stiffness is not affected by fracture width, and consequently that fracture opening or closing at constant fracture length, i.e. hinge-like closure, will have constant stiffness (Raaen et al. 2006). A linear pressure decline is thus expected when the fracture closes in a hinge-like manner, and any reduction of fracture length must cause an increase in system stiffness.

In Chapter 2.2.2 it was described how the forward-step stage of the test was maintained for some time when the pressure was increasing after fracture opening. The main reason why this is done is to ensure that P_{inj} sufficiently exceeds the normal stress acting across the stimulated fracture, so that a longer stage of linear pressure decline can be achieved during the backward-step stage, making it easier to pick the breakpoint at the end of Stage 1.

2.2.4 Test location

The tests were all performed at the junction between the access tunnel and the downstream end of the pressure tunnel of Løkjelsvatn HPP, see Fig. 10. As mentioned in Chapter 1, stress measurements had already been performed at this location for the plant owner's final liner design considerations. The boreholes used for this purpose are given the prefix "H", and they are all located along the southern tunnel wall, as can be seen in Fig. 10. The boreholes on the opposite tunnel wall, marked with the prefix "L", are the boreholes drilled exclusively for the field experiments described herein.

A company specializing in hydraulic testing and grouting works, Injeksjonsteknikk AS, was engaged to aid in the practical execution of the RSRT field tests. The company provided all equipment required for the tests and had made several modifications and adaptions to the pump setup and monitoring system to accommodate the specifications required for the planned RSRT protocol. Arguably the most important adaption was the software programming, enabling semi-automated control of the test procedure, in pre-determined flow-increments. The company also contributed with experienced personnel as support during the test execution.

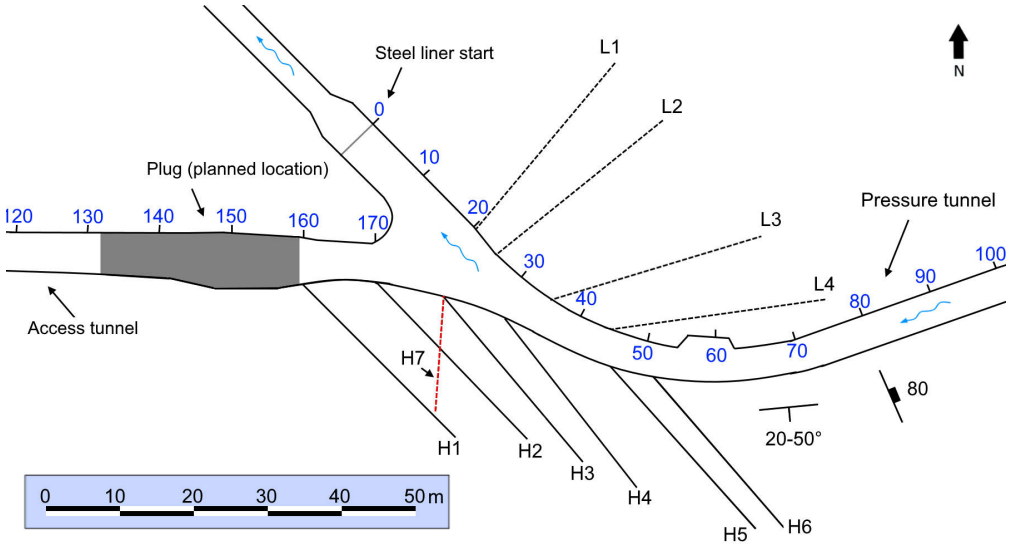

Fig. 10: Detailed view of the test location in the downstream end of the pressure tunnel. The blue coloured numbers represent the chainage of each of the two tunnel branches. The access tunnel ends at Ch. 170, where it meets the unlined pressure tunnel. Chainage 0 marks the downstream end of the unlined pressure tunnel

The normal width of the pressure tunnel is 4.5 m but is somewhat larger at the junction with the access tunnel. At the time of testing the pressure tunnel had been excavated from Ch. 0 to 80.

When rigging up for the RSRT experiments, it was discovered that the directions of the "L" boreholes deviated somewhat from what was originally planned. Therefore, it was deemed necessary to perform a rough field control of azimuth and inclination for all boreholes. This was done by using a geological compass and clinometer. The depth of observation was typically limited to a couple of metres, thus any borehole deviation deeper than this could not be detected. The easy downhole deployment of rigid steel tubes of 8 to 10 m length into the boreholes suggested, however, that the boreholes were fairly straight. The measured azimuths and inclinations of all boreholes are shown in Table 3. Unfortunately, it was discovered that borehole L4 had been moved from the planned location and given a direction that made the borehole alignment very close to the tunnel periphery, as can be seen in Fig. 10.

Table 3: Borehole geometry for all exploratory boreholes at the test location

ID	Ø (mm)	L (m)	Azimuth ± 4°	Inclination[1] ± 2°
L1	64	30	040	-6
L2	64	30	051	0
L3	64	30	074	-7
L4	64	30	083	3
H1	64	30	135	3
H2	64	30	136	2
H3	64	30	140	4
H4	64	30	142	5
H5	64	30	138	5
H6	64	30	139	4

H7	76	18.5	185	5

[1]Relative to the horizontal, with negative values indicating inclination below the horizontal

Due to a rather tight construction schedule, access to the test site could only be granted during a brief holiday standstill of the tunnelling activities. Despite the somewhat limited available time for testing, only two days, the halt in tunnelling activities ensured good testing conditions and effective testing.

3 Results from the field testing at Løkjelsvatn HPP

3.1 Rapid Step-Rate Tests

During the course of the field testing campaign, a total of 29 individual test cycles, from 7 boreholes, were performed, all using the RSRT protocol. In the following sub-chapters, test results will be presented as graphs showing injection pressure (P_{inj}), flowrate (q_{inj}) and the time derivative of pressure (dP/dt) plotted versus time. The derivative plot is included to reduce the subjectivity associated with picking the point best representing the onset of mechanical fracture closure, i.e. the transition from linear to gradual pressure decline. Derivative plots are useful since the time derivative of pressure versus time is linear when the system stiffness is constant, and thus stiffness changes may be detected from distinct breaks in such plots (Raaen et al. 2001).

An individual graph for each test cycle is presented, but graphs from consecutive cycles in the same borehole are collected in one figure, for ease of comparison, see Fig. 11 through Fig. 16. The number of test cycles performed in each borehole varied but was typically 3–4. In borehole L1, however, were 9 cycles performed, primarily as an initial check of the rate-dependency of fracture closure determination.

The start point of each test, $t = 0$ s, is defined by the start of the pumping, and the test ends at the time when the backward-step flow cycle reaches zero flow, $q_{inj} = 0$. Data are, however, plotted for some time after zero flow, for the sake of clarity. It can be commented that the somewhat jagged appearance of the pressure graphs is caused mainly by the 0.1 MPa resolution of the pressure monitoring system. An overview of all boreholes at the test location, including and the number of RSRT cycles executed for each borehole, is provided in Table 4.

Tests in boreholes L2 and H2 turned out inconclusive and therefore will not be presented here. Instead, an extract of the results from these boreholes will be presented in Chapter 4.3 together with a discussion on the characteristic pressure development.

Table 4: Overview of the boreholes at the test location

Borehole	Test section interval (m)	Performed tests, this campaign	Comment
L1	8.5[1] – 30	9×RSRT	Successful tests
L2	8.5 – 30	3×RSRT	Inconclusive tests
L3	10.5 – 30	3×RSRT	Successful tests
L4	8.5 – 30	3×RSRT	Successful tests
H1	10.5 – 30	4×RSRT	Successful tests
H2	10.5 – 30	4×RSRT	Inconclusive tests
H3	No tests	-	Borehole blocked by metal rods
H4	8.5 – 30	3×RSRT	Successful tests
H5	No tests	-	No pressure build-up
H6	No tests	-	No pressure build-up
H7	No tests	-	Borehole used for OC tests

[1] For the last three test cycles the test section interval was 10.5 – 30 m

The following sub-chapters include a description of the characteristic pressure development observed during the tests, including an assessment of the fracture closure pressures based on the principles outlined in Chapter 2.2.3. The pressure observed at the breakpoint from the initial linear pressure decay, i.e. Point A in Fig. 9, will hereafter be termed P_{CL1}, and the pressure observed at the onset of hydraulic closure, i.e. Point B in Fig. 9, will be referred to as P_{CL2}. A dashed straight line is drawn to highlight the interpreted linear stages of the graphs, and vertical arrows are used to indicate P_{CL1}—believed to best represent the fracture normal stress across the stimulated fracture. The fracture re-opening pressures, (P_{RO}), are also presented for reference, but is generally not considered a reliable measure for the magnitude of normal stress, due to its rate-dependency, and gradual nature (Cornet (1981); Rutqvist and Stephansson (1996); Zoback (2007); Ødegaard and Nilsen (2021)).

To avoid tedious repetition of pressure data, we refrain from providing detailed text descriptions of all test cycles in the same borehole, but instead prioritize to comment the main observations, considered of interest for the understanding of the tests and the pressure behaviour.

3.1.1 Borehole L1

A total of 9 RSRT cycles were carried out in borehole L1, with test results as presented in Fig. 11 and Fig. 12. The first test cycle, test L1-1, is characterised by an initial linear pressure increase until approximately t = 62 s, where a sudden pressure drop from the peak P_{inj} = 12.8 MPa indicates a breakdown event, i.e. the creation of a new fracture. After this event, the pressure is stabilizing at a 10.5 MPa plateau, suggesting further fracture propagation until the backward-step stage is initiated at t = 320 s, followed by a linear pressure decline until about t = 480 s, where a deviation from the initial linear trend can be observed in both the P-t graph and in the dP/dt plot, suggesting the onset of mechanical

fracture closure and that P_{CL1} = 7.8 MPa. Then, a rather long period of gradual pressure decay can be seen, lasting until t = 595 s where the onset of a second linear pressure decay indicates hydraulic closure and that P_{CL2} = 5.2 MPa.

During the next test cycle, L1-2, an initial linear pressure increase can be seen until P_{inj} = 6.7, where a distinct deviation from the initial linear trend indicates re-opening of the fracture created during the first cycle. After fracture re-opening a gradual pressure increase can be seen until t = 310 s, when the backward-step stage starts. Thereafter, a stage of linear pressure decline can be observed until t = 445 s, when deviation from the initial linear pressure decline suggesting that P_{CL1} = 7.6 MPa. Following a period of gradual pressure decline a new linear decline can be observed from t = 580 s, and that P_{CL2} = 5.0 MPa. As the remaining test cycles executed in borehole L1 for the most part show very similar behaviour as L1-2, the following examination of the test data for this borehole will be limited to highlighting some key observations.

To investigate the effect of a slower flowrate change was the step duration, Δt, increased from 2 s to 3 s for tests L1-4, L1-5 and L1-6. The resulting graphs show that, even though P_{RO} are seen to gradually decrease for consecutive tests, P_{CL1} remain essentially the same, see also Table 5.

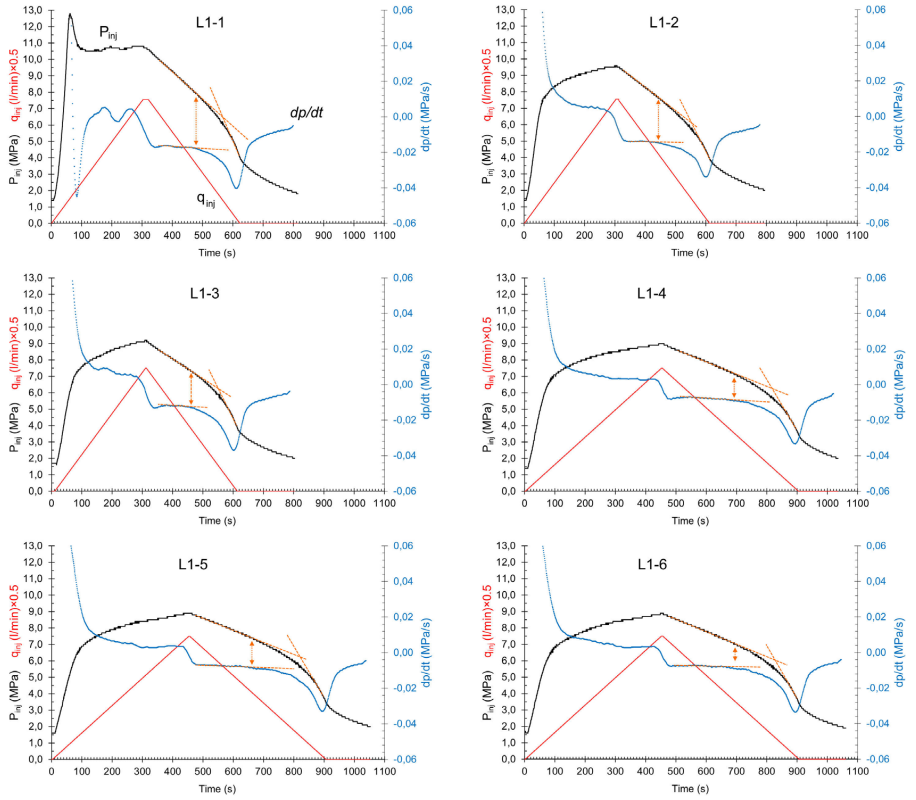

Fig. 11: Test results from borehole L1, including the first 6 test cycles L1-1 through L1-6. A dashed line is drawn to show the deviation from linearity, and a double arrow to indicate the interpreted onset of mechanical fracture closure

After the conclusion of the initial six tests cycles in borehole L1 it was decided to add an additional 2 m rod extension to enable packer placement at 10.5 m depth, two meters deeper than the first six cycles in this borehole. This was done to investigate if the test results would be affected by this deeper packer placement. Three additional test cycles, L1-7, L1-8 and L1-9 were therefore conducted the following day. Test cycles L1-8 and L1-9 showed essentially the same results as the first six test cycles, but the premature flow reversal during test L1-7, caused by an operator mistake, provided some interesting new insights: Referring to Fig. 12, a very different pressure response can be observed during test cycle L1-7, including the striking absence of any initial linear pressure decay. This behaviour is believed to be caused by the fact that the interval pressure, due to the operator mistake, never sufficiently exceeded the normal stress of the stimulated fracture. Hence, no initial linear pressure decay associated with hinge-like closure could be observed, since the fracture more or less directly entered the stage of closure by length reduction.

In the succeeding tests, L1-8 and L1-9, where the pressure was sufficiently increased, curves with a distinct break following an initial linear pressure decay could be observed, suggesting P_{CL1} values of 6.6 MPa and 7 MPa, respectively. The interpreted opening- and closure pressures for all test cycles in L1 are summarised in Table 5.

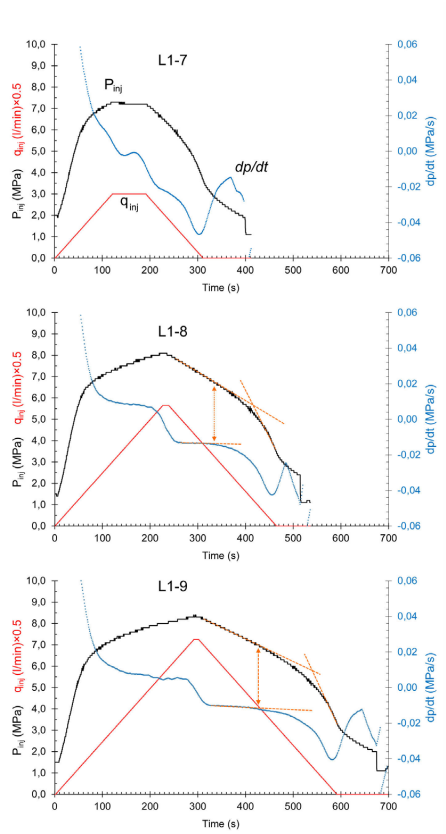

Fig. 12 Test results from borehole L1, including tests L1-7 through L1-9

Table 5: Test results from RSRT performed in Borehole L1

Test ID	Pressure–time plots			Test steps	
	P_{RO} (MPa)	P_{CL1} (MPa)	P_{CL2} (MPa)	Δq (l/min)	Δt (s)
L1-1	12.8[1]	7.8	5.2	0.1	2
L1-2	6.7	7.6	5.0	0.1	2
L1-3	6.1	7.3	4.8	0.1	2
L1-4	6.0	7.2	4.9	0.1	3
L1-5	6.0	7.4	4.9	0.1	3
L1-6	5.8	7.0	4.6	0.1	3
L1-7	5.4	N/A[2]	4.8	0.1	2
L1-8	5.2	6.6	4.7	0.1	2
L1-9	5.2	7.0	4.4	0.1	2

[1] Breakdown event
[2] Failed test cycle

3.1.2 Borehole L3

Three RSRT cycles were performed in borehole L3, the resulting graphs from which are presented in Fig. 13. The first test cycle, L3-1, is characterised by initial steep pressure increase to a peak at P_{inj} = 16.8 MPa, followed by a sudden drop in pressure, first to an intermittent 11 MPa level, then further down to 7.5 MPa, suggesting two breakdown events. The fairly stable pressure plateau of $P_{inj} \approx 7.5$ MPa suggests fracture propagation. The backward-step stage starts at $t = 315$ s and is followed by a fairly linear pressure decline until t = 460 s, where a distinct deviation from the initial linear pressure decline suggests the onset of mechanical fracture closure and that $P_{CL1} = 7.1$ MPa. After a brief period of pressure decline can a new stage of linear pressure decay be seen at $t = 500$ s, suggesting that $P_{CL2} = 7.0$ MPa.

The succeeding two test cycles did not show equally distinct breaks in the backward-step stage, making fracture closure uncertain. Starting with the second test cycle, L3-2, a linear pressure increase can be observed until re-opening is indicated with $P_{RO} = 4.3$ MPa. Thereafter, the pressure can be seen to increase steadily until the maximum capacity of the pump is reached, forcing the end of the forward-step stage at t = 400 s. The backward-step stage is initiated at t = 420 s and is followed by an initial period of almost constant pressure, before starting to decline gradually from t = 550. Even though a slight change of curvature can be observed both in Pt- and dP/dt plots at t = 670 s, possibly suggesting that $P_{CL1} = 7.6$ MPa, the response is considered too uncertain to firmly conclude that it is the onset of fracture closure. Similar behaviour is observed for the last test cycle L3-3, but here the forward-step stage was again stopped prematurely, so that the backward-step stage started when the pressure was almost the same as the anticipated normal stress found from test cycle L3-1. The somewhat erratic pressure fluctuations seen at the end of test cycle L3-3 were caused by the operator performing some manual manoeuvring of the outlet valve. A summary of the interpreted opening- and closure pressures is given in Table 6.

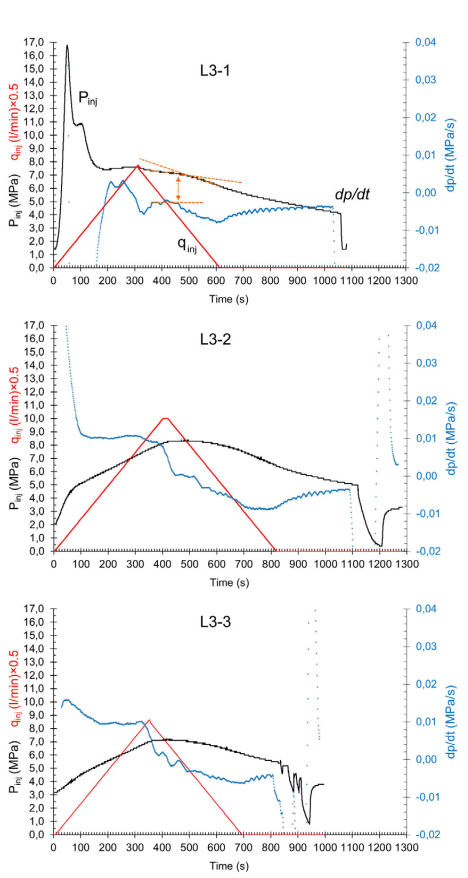

Fig. 13 Test results from borehole L3, including tests L3-1 through L3-3

Table 6: Interpreted pressure values from the tests performed in Borehole L3

Test ID	Pressure–time plots			Test steps	
	P_{RO} (MPa)	P_{CL1} (MPa)	P_{CL2} (MPa)	Δq (l/min)	Δt (s)
L3-1	16.8[1]	7.1	7.0	0.1	2
L3-2	4.3	(7.6)[2]	N/A	0.1	2
L3-3	4.2	N/A	N/A	0.1	2

[1]Breakdown event
[2]Uncertain

3.1.3 Borehole L4

Testing in borehole L4 comprised 3 RSRT cycles, which are all presented in Fig. 14. A summary of the interpreted pressure values is provided in Table 7. Starting with test cycle L4-1 a steep pressure increase can be observed until t = 220 s, where a deviation from the linear trend indicates that some fluid starts to leak from the test section, often termed leak-off. Following the leak-off a further pressure

rise can be seen to until $t = 275$ s, where a small pressure drop indicates fracture opening. Two additional pressure drop events can also be observed, at $t = 400$ s and $t = 525$ s, suggesting fracture propagation events. After the backward-step stage is initiated at $t = 545$ s, a linear pressure decline can be seen until a breakpoint is observed at $t = 765$ s, suggesting that $P_{CL1} = 4.4$ MPa. After a short period of gradual pressure decline can a second linear pressure decline be seen, suggesting that $P_{CL2} = 3.9$ MPa. The backward-step stage of the last two tests L4-2 and L4-3 are very similar to that of the first, with P_{CL1} of 4.5 MPa and 4.4 MPa, respectively, in close agreement with that of the first test cycle.

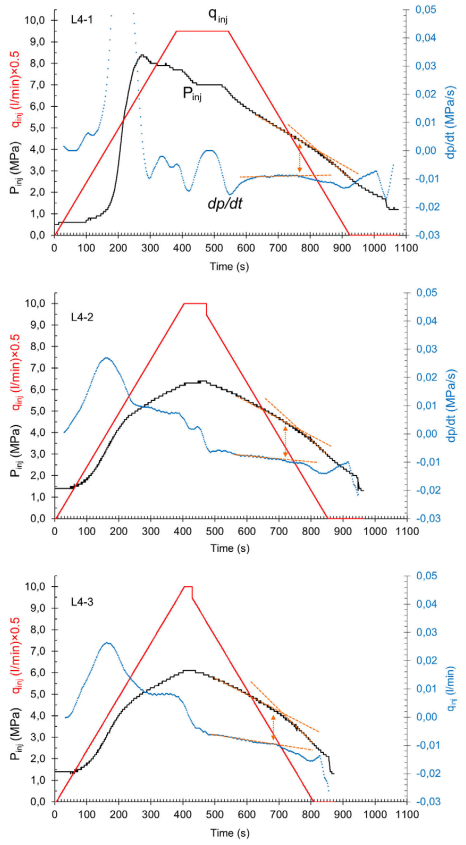

Fig. 14 Test results from borehole L4. The double arrow indicates the interpreted point of mechanical closure

It must be noted that due to the unfavourable borehole orientation of L4, running fairly close to the tunnel periphery, it is considered likely that the tests are affected by the stress perturbations of the tunnel, i.e. the near-field stress. The too short distance between borehole and tunnel was also evident from the observation of a slight water leakage showing on the tunnel wall both upstream and downstream of the borehole during testing, suggesting a hydraulic communication between the test section and the tunnel.

Table 7: Test results from RSRT performed in Borehole L4

Test ID	Pressure–time plots			Test steps	
	P_{RO} (MPa)	P_{CL1} (MPa)	P_{CL2} (MPa)	Δq (l/min)	Δt (s)
L4-1	5.6	4.4	3.9	0.1	2
L4-2	4.2	4.5	3.8	0.1	2
L4.3	4.2	4.4	3.6	0.1	2

3.1.4 Borehole H1

Starting with test H1-1, the first RSRT cycle in this borehole, see Fig. 15, shows a linear pressure increase developing from t = 190 s, following an initial stage of fairly slow pressure increase. After this linear pressure increase, a pressure drop can be observed when the pressure reaches 11.8 MPa. Even though this pressure drop resembles a breakdown event, the rather blunt pressure peak and relatively low pressure drop after the peak indicate that the event is fracture re-opening. The succeeding 11 MPa pressure plateau could, however, indicate that a new fracture is created, alternatively that a pre-existing fracture is further propagated (several pre-existing fractures should be present in the borehole due to the HF tests). After the backward-step stage is initiated at t = 340 s, a linear pressure decline can be seen until t = 570 s where a downward break in the Pt-curve suggests onset of mechanical fracture closure with P_{CL1} = 8.2 MPa. A brief period of gradual pressure decay is then followed by a new linear decay, suggesting hydraulic closure and that P_{CL2} = 8.0 MPa. Quite similar pressure development can be observed during the three consecutive RSRT cycles, indicating P_{CL1} values within an 8.6 – 9.0 MPa range. It is interesting to observe that the value of P_{CL1} remained rather unchanged when Δt was increased from 2 s to 4 s during the backward step stage of test cycle H1-4. A summary of the interpreted pressure values is provided in Table 8.

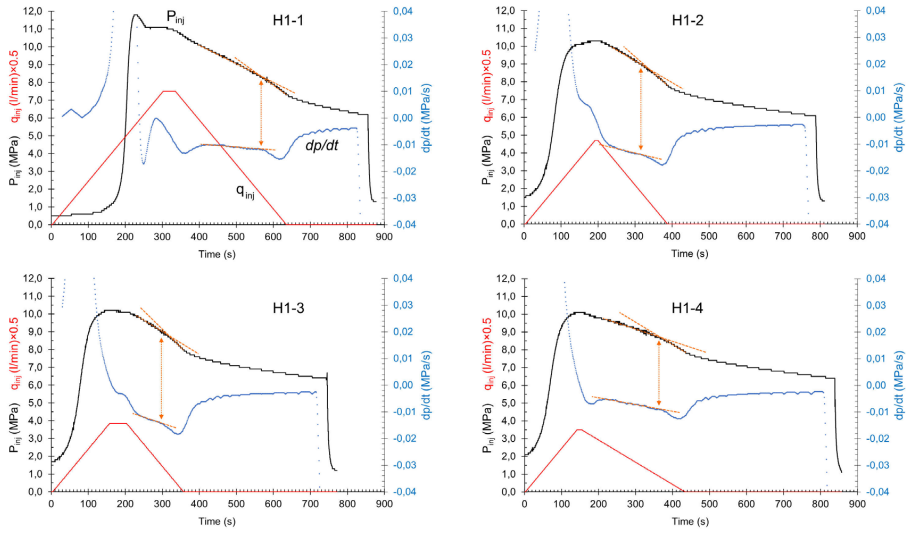

Fig. 15 Test results from borehole H1

Table 8: Test results from RSRT performed in Borehole H1

Test ID	Pressure–time plots			Test steps	
	P_{RO} (MPa)	P_{CL1} (MPa)	P_{CL2} (MPa)	Δq (l/min)	Δt (s)
H1-1	11.8	8.2	8.0	0.1	2
H1-2	7.8	9.0	8.6	0.1	2
H1-3	7.8	9.0	8.7	0.1	2
H1-4	7.6	8.6	8.5	0.1	2/4[1]

[1]Δt changed from 2 s to 4 s during backward step

3.1.5 Borehole H4

Testing in borehole H4 comprises 3 RSRT cycles, the results from which are presented in Fig. 16, and with a summary of the interpreted opening- and closure pressures provided in Table 9. The first test cycle, H4-1, displays a linear pressure increase before a distinct deviation from this trend, occurring at t = 275 s, suggesting re-opening of a pre-existing fracture when P_{inj} reaches 6.1 MPa. The backward-step cycle starts at t = 470 s and is followed by a fairly linear pressure decline until t = 670 s where the deviation from the initial linear pressure suggests that P_{CL1} = 6.2 MPa. After a period of gradual pressure decay a second linear pressure decline can be seen developing from t = 830 s, suggesting that P_{CL2} = 4.2 MPa. Similar behaviour could be observed during the backward-step cycle of the next two test cycles H4-2 and H4-3, with P_{CL1} = 6.0 and P_{CL1} = 5.9 MPa, respectively.

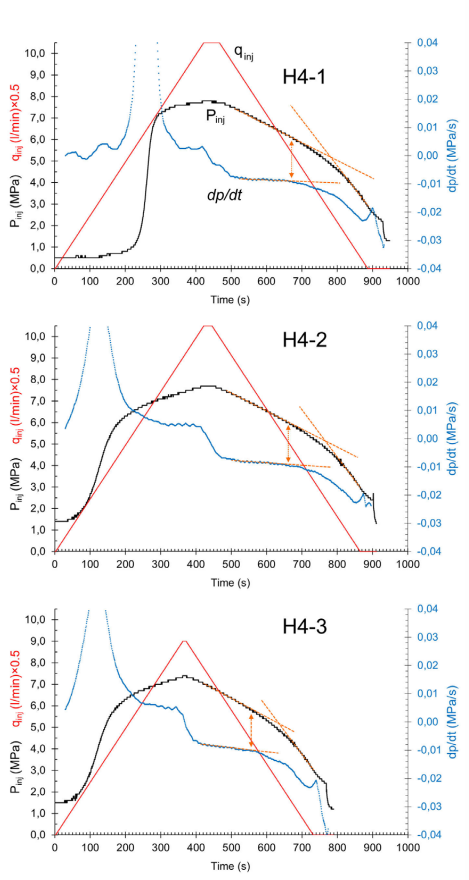

Fig. 16 Test results from borehole H4

Though not as extreme as borehole L4, it can be commented that H4 also runs quite close to the tunnel periphery, which might cause the test section to be affected by the stress re-distribution of the tunnel, and consequently that the stress estimates also could be affected by the near-field stresses.

Table 9: Test results from RSRT performed in Borehole H4

Test ID	Pressure–time plots			Test steps	
	P_{RO} (MPa)	P_{CL1} (MPa)	P_{CL2} (MPa)	Δq (l/min)	Δt (s)
H4-1	6.1	6.2	4.2	0.1	2
H4-2	4.9	6.0	4.4	0.1	2
H4-3	5.0	5.9	4.4	0.1	2

3.1.6 Summary of results

A summary of the interpreted closure pressures, averaged for each borehole, is provided in Table 10. As can be seen, the P_{CL1} values range from 4.4 to 8.7 MPa, with an average value across the boreholes of 6.7 MPa. Disregarding the tests performed in boreholes L4 and H4, considered less representative for the in-situ stress due to the proximity of the tunnel, narrows this range to 7.2–8.7 MPa, which is quite comparable to the σ_3 estimate of 7–9.5 MPa, found from the preceding HF and OC stress measurements. The corresponding values for P_{CL2}, range between 4.8 and 8.5 MPa, the low range of which is clearly lower than the σ_3 estimate from the HF and OC stress measurements.

Table 10: Summary of test results from interpretation of the backward-step stage, average value for each borehole

Borehole	Mechanical fracture closure P_{CL1}, average (MPa)	Hydraulic fracture closure P_{CL2}, average (MPa)	Test cycles (no.)
L1	7.2	4.8	8
L3	7.3	7	2
L4	4.4	3.8	3
H1	8.7	8.5	4
H4	6.0	4.3	3

4 Discussion

4.1 Fracture behaviour during testing

A series of hydraulic jacking experiments were conducted to assess the ability of a new hydraulic jacking test protocol, the RSRT, to assess fracture normal stresses under field-scale conditions. Through analysis of the test results several encouraging observations could be made, strengthening the theory that reliable normal stress estimates can be made by assessing pressure decline curves during the backward-step stage of the RSRT, in the same manner as done for flowback tests.

During the backward-step stage of the tests two characteristic downward slope breaks could usually be observed, displaying pressure decline curves that are similar to those seen during the preceding laboratory campaign, also corresponding with the pressure decline observed during successful flowback tests. The pressure at which the breakpoints occur are repeatable for consecutive test cycles in the same borehole, even when the step-rate change is varied between consecutive cycles. Since the breaks occur without any other concurrent changes to the hydraulic system (the flowrate is reduced at a constant rate), it is believed that the distinct changes in the rate of pressure decline are caused by the fracture closing process, and that the RSRT successfully captures the fracture behaviour predicted by the fracture closure model of Hayashi and Haimson (1991).

In the traditional interpretation of flowback tests, the accelerated pressure decline observed at fracture closure was attributed to a flow restriction introduced when the asperities of the fracture surfaces started to close (Nolte 1982). However, since the exact same behaviour is seen during the RSRT, where water always is injected and not flowed back, we tend to favour the explanation that this

effect is caused by the asperities touching, causing an increase in the fracture stiffness (Shlyapobersky (1989); Raaen et al. (2001); Jung et al. (2016)). Another way to explain the same effect is that when the fracture is open, the full normal stress will act across it as "push-back" on the fluid, but once the asperities start to touch, some of the normal stress will be carried by the asperities, thus in a sense shielding the fluid and causing a more rapid pressure drop as the fluid leaks into the rock mass.

A simplified sketch, intended to explain our conceptual understanding of the system behaviour during the RSRT is shown in Fig. 17. Whilst entirely conceptual, the sketch might provide some overall understanding of the pressure development during a RSRT cycle: In (A) an isolated borehole is injected with water according to the stepwise flow increase of the RSRT protocol, causing a corresponding increase in pressure until; (B), a fracture is created, causing a pressure drop since volume is added to the system by the fracture opening, and then; (C) the fracture propagates further, ideally in a plane normal to σ_3, until the operator reverses the flow steps, whereupon in; (D) the stepwise reduction of flow, and corresponding linear pressure decay, cause the fracture to close in a hinge-like manner, before; (E) the pressure inside the fracture drops below the normal stress acting across it, causing the fracture to start to close by length reduction (mechanical closure), seen as a distinct downward break from the linear pressure decay in the pressure decline curve at P_{CL1}, before the gradual pressure decline continues until (F) hydraulic fracture closure is indicated by the start of a second stage of linear pressure decay, P_{CL2}.

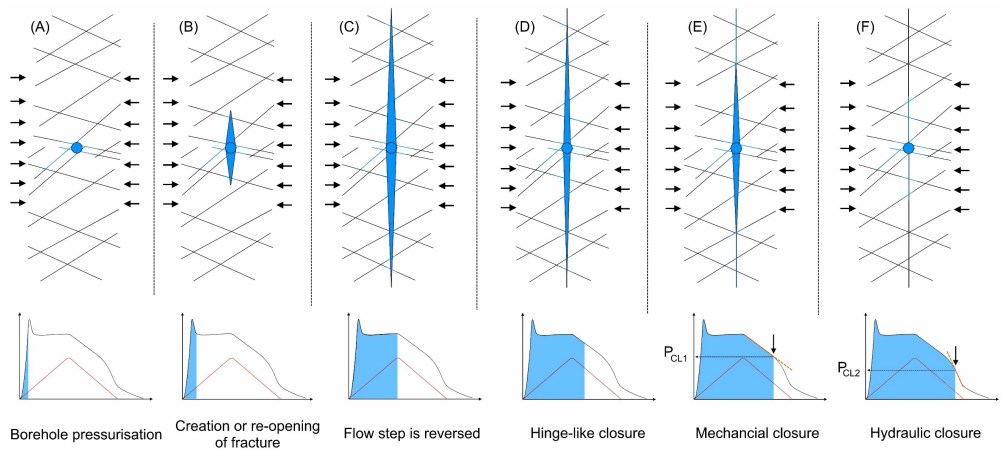

Fig. 17: Principal sketch ("cartoon representation") of the idealised fracture behaviour and corresponding pressure development during the RSRT. The array of small arrows signifies the direction of the minimum principal stress

In cases where there is significant re-orientation of the fracture away from the borehole, a tortuous flow path can be created, potentially causing a bottleneck for flow (Zoback (2007); Jung et al. (2016)). Such near-borehole flow restriction will cause a pressure drop between the borehole and the fracture, thus potentially causing the interpretation of the RSRT to over-estimate the magnitude of minimum principal stress since the measured pressure exceeds that inside the fracture. This effect will, however, be largest when the fracture is narrowest since it is known from the cubic law that the pressure drop is

inversely proportional to the cube of the fracture width (Witherspoon et al. (1980); Economides and Nolte (2000)). This suggests that the effect of near-borehole flow restrictions generally is less prominent when picking the P_{CL1} values from the RSRT, since the fracture at this stage of the test is fully open.

4.2 Estimating minimum principal stress from the RSRT

The test results from the RSRT cycles yielded P_{CL1} values varying between 7.2–8.7 MPa for tests in boreholes L1, L3 and H1, where effects of the tunnel near-field stress were considered minimal. This estimate is surprisingly close to the σ_3 estimate of 7–9.5 MPa found from the HF and OC measurements, suggesting that the stimulated fractures must have aligned rather normal to the direction of σ_3, instead of following some pre-existing weakness plane. This assumption is also supported by the fact that the σ_3 magnitude is substantially (about 6-9 MPa) lower than the two other principal stresses, making fracture propagation in a plane that is not normal to σ_3 unlikely, and in any case requiring higher pressures than were observed during the tests. Consequently, the P_{CL1} value found from the RSRT should provide reasonable estimates of the minimum principal stress, σ_3.

The results from the preceding laboratory trials did, however, suggest that the upper breakpoint, P_{CL1}, could over-estimate the normal stress, thus seemingly in contradiction with the interpretation from the field experiments. It is, however, believed that the reason for the deviating interpretations is linked to limitations in the laboratory conditions. Specifically, the difficulty of maintaining an open fracture due to the leaky periphery, thus masking the stage of hinge-like fracture closure (Stage 1), could make the detection of mechanical fracture closure difficult.

Even though the above conjecture of fractures propagating normal to σ_3 cannot be confirmed due to the lack of information on fracture geometry away from the borehole, it finds support in the literature: From field-, laboratory-, and numerical studies it is now reasonably well-established that hydraulically induced fractures will align in a plane that is normal to the minimum principal stress when propagating away from the borehole, simply because this is what requires least energy (Warren and Smith (1985); Abass et al. (1994); Zoback (2007); Dusseault (2013); Lavrov et al. (2016); Mao et al. (2017)). In a recent study conducted at the Sanford Underground Research Facility (SURF), re-orientation of hydraulically induced fractures was demonstrated in a particularly compelling manner (Guglielmi et al. 2021): Based on microseismic monitoring and continuous borehole displacement monitoring the authors were able to show how a hydraulic fracture re-oriented away from the borehole and propagated in a plane normal to σ_3, even when the fracture first initiated along a foliation plane with a different orientation. During the fracture closure stages of these tests, the fracture closed in a direction normal to the main fracture, and only during the final stages of closure displacement aligned to the foliation plane normal where the fracture first initiated. This is relevant for the interpretation of the RSRT data since it demonstrates how the normal stress estimates made from identifying the pressure at onset of mechanical

closure (which is early in the fracture closure process) is representative for σ_3 even when the fracture initiated in a plane that is not normal to the σ_3 direction.

While P_{CL1} was considered quite representative for the magnitude of σ_3, the pressure found at the second breakpoint, P_{CL2}, was usually less representative, in accordance with the findings of Raaen et al. (2001). Assuming a pervious rock mass, and that the pre-excavation groundwater table at the test location corresponded with the level of the numerous lakes situated directly above, the undisturbed groundwater pressure at the test location would be about 5.8 MPa. This is significantly higher than the average P_{CL2} value found in borehole L1, suggesting that P_{CL2} in this case must be less than σ_3, since groundwater pressures in excess of the minimum principal stress would be inadmissible due to the occurrence of natural hydrofracturing (Dahlø et al. (2003); Zoback (2007)).

4.3 Failed tests in boreholes L2 and H2

Tests in boreholes L2 and H2 all turned out inconclusive, preventing assessments of fracture closure stress due to anomalous pressure development. The reason for the irregular test behaviour is believed to be linked to unfavourable test conditions, as will be described in the following. Looking at the start of the backward-step stage of test cycle L2-1 in Fig. 18, one can see an almost linear, or gently decreasing slope all the way down to zero flow—contrary to the expected downward break in the P_{inj}–t curve associated with fracture closure. The same type of irregular pressure decline was observed during all three test cycles in this borehole and it is believed to be caused by air trapped in the borehole. The presence of air inside the hydraulic system could effectively dominate the system stiffness, thus masking any stiffness contrast during the backward-step cycle. That air can have detrimental effect on fracture closure assessments was also pointed out by Raaen and Brudy (2001). It can be questioned, however, why tests in boreholes L4, H1 and H4 all yielded interpretable results, despite also being air-filled at the start of the test (they are all upwards slanting and hence drained). This can be explained by the air being expelled sufficiently far during testing to avoid the negative effect of the less stiff air in hydraulic contact with the test system. The proximity of borehole L4 to the tunnel surface, and the presence of several pre-existing fractures in boreholes H1 and H4, would make it easier for air to leak out of the test section than in borehole L2.

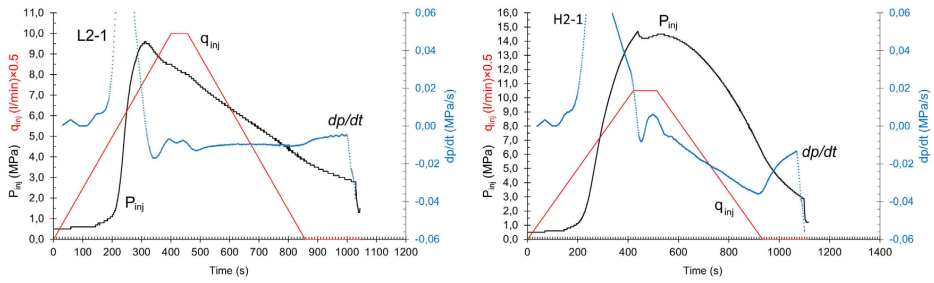

Fig. 18 Two examples of failed tests. Test results from the first test cycles of boreholes L2 (left) and H2 (right)

Testing in borehole H2 was seriously hampered by a cross-hole hydraulic communication where water leaked from the H2 test section into the neighbouring borehole H7. This leakage is believed to have entirely dominated the pressure response, effectively preventing the controlled fracture opening and -closure, resulting in a gradual pressure decline during the backward-step stage of the test, devoid of discernible breaks in all test cycles. That a hydraulic communication could be created between the two boreholes, with borehole H2 crossing above borehole H7 with only 1-2 meter spacing, was expected—but it was still considered worthwhile to try testing in this borehole. The reason why this borehole arrangement was originally chosen for the preceding HF and OC stress measurements is not known to the authors.

4.4 Suggestions for proper test execution

Based on the field experiments conducted at the Løkjelsvatn HPP we believe that the following three conditions should first be addressed when planning stress estimates using the RSRT protocol:

1. Ensure that the test section is established outside the stress perturbations of the tunnel. Though site specific, keeping the test section away from the tunnel periphery with a distance equivalent to two times the tunnel will in most cases be sufficient.
2. Minimize risk of cross-hole leakage by ensuring sufficient distance between neighbouring boreholes. A minimum distance of about 10 m is recommended.
3. Avoid air in the test system by flushing hydraulic lines prior to testing and by ensuring that all boreholes are given a sub-horizontal inclination so that they can be water-filled prior to placing the packer.

Adherence to these three basic requirements will significantly reduce the risk of test failure, but there are also other considerations of importance. One aspect is to ensure that the fracture is fully opened against the *in-situ* normal stress, so that the initial linear pressure decay can be detected during the backward-step stage of the test. Failure to fully open the fracture is believed to have made normal stress

estimates for test cycles L1-7, L3-2 and L3-3 uncertain. The stimulated fracture should thus extend sufficiently far away from the borehole to not be affected by the near-field stress concentration of the borehole, but also to ensure that the fracture volume is sufficiently large to create a stiffness contrast when opening and closing. As a rough guide, based on the field data from testing at Løkjelsvatn HPP, it is believed that the fracture will have extended sufficiently far once the forward-step stage has been continued to about 30 % above the fracture re-opening pressure. This must, however, be adjusted by trial and error in the field, simply by adjusting the test variables (Δq, Δt and test duration) until test cycles show an initial linear pressure decline from the start of the backward-step stage. This requires the pump to be able to provide sufficient flow, which it in some cases during the field campaign did not. To increase the robustness of the testing system it is therefore recommended to have a pump with a somewhat higher pumping capacity than the 20 l/min limitation of the pump used during our tests.

Even though a straddle-packer arrangement could be used with the RSRT, single packers were preferred due to their simplicity and low cost. A drawback of using single packers is that this introduces the risk of sudden packer ejection, caused by slippage of the packer during testing, as experience by the authors during testing. Similar events are also known from rock mass grouting, even with fatal consequences. It is therefore of utmost importance that the packer assembly is physically restrained from being ejected from the borehole, e.g. by mechanical anchorage. If this cannot be done, an alternative can be to establish a zone of no entry in front of the packer during testing.

5 Conclusions

A series of experimental hydraulic jacking tests were conducted underground at the Løkjelsvatn HPP, in an effort to assess the field applicability of the RSRT, a novel hydraulic jacking test protocol first presented in the laboratory study of Ødegaard and Nilsen (2021). The experimental results confirm the preceding laboratory findings, suggesting that rapid and reliable estimates of fracture normal stress can be made by using the RSRT, thus providing a successful first field verification of the test.

It has also been found that the normal stress estimates correspond fairly well to the magnitude of minimum principal stress σ_3, provided that measurements were done sufficiently far from the tunnel contour to actually measure the far-field stress. This suggests that the stimulated fractures in these cases have propagated in a plane that is normal to σ_3, thus enabling direct estimates of σ_3 from the RSRT.

The RSRT protocol allows for fairly rapid test execution, with average test duration of approximately 10 minutes and test cycles rarely exceeding 15 min. Even with three test cycles, which is usually recommended, testing in one borehole will last less than one hour. Test interpretation can be made on-site, and quite rapidly, not requiring specialized software—only standard spreadsheets. When it comes to the equipment required for the test, all components are readily available (off the shelf), though the computer control of the pump requires some programming. Boreholes for the tests can be

drilled using drilling jumbos, which for D&B excavated tunnels are readily available. Combined, this makes the RSRT highly cost- and time-efficient.

Overall, the experience from the field campaign suggests that, provided proper execution, the RSRT represents an efficient and reliable method to assess the magnitude of σ_3, particularly useful for the final design of unlined pressure tunnels. Still, since the performed experiments are relatively few, and limited to a single test location, more field tests are required to further verify the aptness of the test, ideally by performing the RSRT at locations where the underground state of stress has been assessed already by other stress estimation techniques.

Though we cannot offer any concrete advice on the optimal spacing between tests performed as part of the stress estimation campaign for unlined pressure tunnels, it will be a major step in the right direction if measurements are done at regular intervals, rather than only at a few select locations. Ideally, one could envisage that the RSRT was incorporated in the normal excavation cycle so that one or two boreholes for RSRT was drilled every 20-50 m of tunnel, or even closer—depending on risk acceptance, economy, and rock mass complexity of the project.

As a potential extension to the original intended scope of the RSRT, it could be interesting to try out this test during grouting operations, as a potential way to delineate the "safe" grouting pressures during pre-excavation grouting in tunnels. This is particularly relevant for infrastructure projects where high-pressure pre-excavation grouting is performed, known to quite frequently produce undesirable hydraulic fracturing events (Strømsvik et al. 2018).

6 Acknowledgements

The Research Council of Norway (NFR) is acknowledged for financing this ongoing research through the Norwegian Research Centre for Hydropower Technology (HydroCen). Access to the two test sites Leikanger Kraftverk and Løkjelsvatn kraftverk was kindly granted by the respective plant owners, Leikanger Kraft AS and Sunnhordaland Kraftlag AS. Injeksjonsteknikk AS, and their skilled operators are warmly thanked for showing keen interest before, during and after our field experiments, and for providing both equipment and personnel to facilitate the field tests. Erlend Andreassen, master student at our department, is also thanked for a fruitful collaboration during the planning and execution of the tests at the Løkjelsvatn Kraftverk. Finally, we thank Arne Marius Raaen for encouraging discussions on fracture closure and for his kind interest in our work.

7 Conflict of interest

The authors confirm that there are no known conflicts of interest associated with the publication of this article, and that are no financial or non-financial interests that has affected the outcome of this work.

8 References

Abass HH, Brumley JL, Venditto JJ (1994) Oriented Perforations - A Rock Mechanics View. Paper presented at the SPE Annual Technical Conference and Exhibition, New Orleans, Louisiana, 1994/1/1/

Amadei B, Stephansson O (1997) Rock Stress and Its Measurement. doi:https://doi.org/10.1007/978-94-011-5346-1

Benson RP (1989) Design of unlined and lined pressure tunnels Tunnelling and Underground Space Technology incorporating Trenchless Technology Research 4:155-170 doi:https://doi.org/10.1016/0886-7798(89)90049-7

Brekke TL, Ripley BD (1993) Design of Pressure Tunnels and Shafts. In: Hudson JA (ed) Comprehensive Rock Engineering; Analysis and Design Methods, vol 2. Pergamon Press, Oxford,

Christiansson R, Janson T (2003) A test of different stress measurement methods in two orthogonal bore holes in Äspö Hard Rock Laboratory (HRL), Sweden International Journal of Rock Mechanics and Mining Sciences 40:1161-1172 doi:https://doi.org/10.1016/j.ijrmms.2003.07.006

Cornet FH Analysis of injection tests for in-situ stress determination. In: Zoback MD, Haimson B (eds) Workshop on Hydraulic Fracturing Stress Measurements, California, U.S., 1981. vol Open File Rep. 82-1075. U.S. Geol. Surv., pp 414-443

Cornet FH, Valette B (1984) In situ stress determination from hydraulic injection test data Journal of Geophysical Research 89:11527-11537 doi:https://doi.org/10.1029/JB089iB13p11527

Dahlø T, Evans KF, Halvorsen A, Myrvang A (2003) Adverse effects of pore-pressure drainage on stress measurements performed in deep tunnels: an example from the Lower Kihansi hydroelectric power project, Tanzania International Journal of Rock Mechanics and Mining Sciences 40:65-93 doi:https://doi.org/10.1016/S1365-1609(02)00114-4

Doe TW, Korbin GE (1987) A Comparison Of Hydraulic Fracturing And Hydraulic Jacking Stress Measurements. Paper presented at the The 28th U.S. Symposium on Rock Mechanics (USRMS), Tucson, Arizona, 1987.1.1

Dusseault MB (2013) Geomechanical Aspects of Shale Gas Development. Paper presented at the ISRM International Symposium - EUROCK 2013, Wroclaw, Poland, 2013/1/1/

Economides MJ, Nolte KG (2000) Reservoir stimulation. Wiley, Chichester

Evans K, Dahlø T, Roti JA (2003) Mechanisms of Pore Pressure-stress Coupling which Can Adversely Affect Stress Measurements Conducted in Deep Tunnels Pure and Applied Geophysics 160:1087-1102 doi:https://.doi.org/10.1007/PL00012562

Guglielmi Y, Cook P, Soom F, Schoenball M, Dobson P, Kneafsey T (2021) In Situ Continuous Monitoring of Borehole Displacements Induced by Stimulated Hydrofracture Growth Geophysical research letters 48:n/a doi:https://.doi.org/10.1029/2020GL090782

Haimson B (1992) Designing pre-excavation stress measurements for meaningful rock characterization. Paper presented at the ISRM Eurock '92 Symposium on Rock Characterization, London, 4–17 September

Hayashi K, Haimson BC (1991) Characteristics of shut-in curves in hydraulic fracturing stress measurements and determination of in situ minimum compressive stress Journal of Geophysical Research: Solid Earth 96:18311-18321 doi:https://.doi.org/10.1029/91JB01867

Hubbert MK, Willis DG (1957) Mechanics of hydraulic fracturing Journal of Petroleum Technology:153-168

Jung H, Sharma MM, Cramer DD, Oakes S, McClure MW (2016) Re-examining interpretations of non-ideal behavior during diagnostic fracture injection tests Journal of Petroleum Science and Engineering 145:114-136 doi:https://doi.org/10.1016/j.petrol.2016.03.016

Lavrov A, Larsen I, Bauer A (2016) Numerical Modelling of Extended Leak-Off Test with a Pre-Existing Fracture Rock Mechanics and Rock Engineering 49:1359-1368 doi:https://.doi.org/10.1007/s00603-015-0807-x

Mao R, Feng Z, Liu Z, Zhao Y (2017) Laboratory hydraulic fracturing test on large-scale pre-cracked granite specimens J Nat Gas Sci Eng 44:278-286 doi:https://.doi.org/10.1016/j.jngse.2017.03.037

Martin CD, Chandler NA (1993) Stress heterogeneity and geological structures International Journal of Rock Mechanics and Mining Sciences & Geomechanics Abstracts 30:993-999 doi:https://doi.org/10.1016/0148-9062(93)90059-M

Marulanda A, Ortiz C, Gutierrez R Definition of the use fo steel liners based on hydraulic fracturing tests. A case history. In: Stephansson O (ed) Rock stress and rock stress measurements : proceedings of the International Symposium on Rock Stress and Rock Stress Measurements, Stockholm, 1-3 September 1986, Luleå, 1986. Centek Publishers, pp 599-604

Merritt AH (1999) Geologic and geotechnical considerations for pressure tunnel design. Paper presented at the Geo-Engineering for Underground Facilities, University of Illinois, 13-17 June

Nolte KG Fracture Design Considerations Based on Pressure Analysis. In: SPE Cotton Valley Symposium, 1982. SPE-10911-MS. doi:https://doi.org/10.2118/10911-ms

NVE (2020) Vannkraft utbygd og ikke utbygd. The Norwegian Water Resources and Energy Directorate. https://temakart.nve.no/tema/vannkraft. Accessed November 9th 2020

Plahn SV, Nolte KG, Miska S (1997) A Quantitative Investigation of the Fracture Pump-In/FIowback Test SPE-24823-PA 12:20-27 doi:https://.doi.org/10.2118/30504-pa

Quirion M, Tournier J-P Hydraulic Jacking Tests In Crystalline Rocks For Hydroelectric Projects In Quebec, Canada. In: ISRM International Symposium on In-Situ Rock Stress, 2010. ISRM-ISRS-2010-083,

Rutqvist J, Stephansson O (1996) A cyclic hydraulic jacking test to determine the in situ stress normal to a fracture International Journal of Rock Mechanics and Mining Sciences and Geomechanics Abstracts 33:695-711 doi:https://doi.org/10.1016/0148-9062(96)00013-7

Raaen AM, Brudy M (2001) Pump-in/Flowback Tests Reduce the Estimate of Horizontal in-Situ Stress Significantly. Paper presented at the SPE Annual Technical Conference and Exhibition, New Orleans, Louisiana, September

Raaen AM, Horsrud P, Kjørholt H, Økland D (2006) Improved routine estimation of the minimum horizontal stress component from extended leak-off tests International Journal of Rock Mechanics and Mining Sciences 43:37-48 doi:https://.doi.org/10.1016/j.ijrmms.2005.04.005

Raaen AM, Skomedal E, Kjørholt H, Markestad P, Økland D (2001) Stress determination from hydraulic fracturing tests: the system stiffness approach International Journal of Rock Mechanics and Mining Sciences 38:529-541 doi:https://doi.org/10.1016/S1365-1609(01)00020-X

Savitski AA, Dudley JW Revisiting Microfrac In-situ Stress Measurement via Flow Back - A New Protocol. In: SPE Annual Technical Conference and Exhibition, 2011. SPE-147248-MS. doi:https://doi.org/10.2118/147248-ms

Shlyapobersky J (1989) On-site interactive hydraulic fracturing procedures for determining the minimum in situ stress from fracture closure and reopening pressures International journal of rock mechanics and mining sciences & geomechanics abstracts 26:541-548 doi:https://doi.org/10.1016/0148-9062(89)91432-0

Sintef Community (2021) Bergspenningsmåling ved Løkjelsvatn Kraftverk (In Norwegian). Report 2021:00008 (Unpublished),

Sneddon IN, Mott NF (1946) The distribution of stress in the neighbourhood of a crack in an elastic solid Proceedings of the Royal Society of London Series A Mathematical and Physical Sciences 187:229-260 doi:https://doi.org/10.1098/rspa.1946.0077

Strømsvik H, Morud JC, Grøv E (2018) Development of an algorithm to detect hydraulic jacking in high pressure rock mass grouting and introduction of the PF index Tunnelling and Underground Space Technology incorporating Trenchless Technology Research 81:16-25 doi:https://doi.org/10.1016/j.tust.2018.06.027

Warren WE, Smith CW (1985) In situ stress estimates from hydraulic fracturing and direct observation of crack orientation Journal of Geophysical Research 90:6829-6839 doi:https://doi.org/10.1029/JB090iB08p06829

Witherspoon PA, Wang JSY, Iwai K, Gale JE (1980) Validity of Cubic Law for fluid flow in a deformable rock fracture Water Resources Research 16:1016-1024 doi:10.1029/WR016i006p01016

Zoback MD (2007) Reservoir geomechanics. Cambridge University Press, Cambridge

Ødegaard H, Nilsen B (2018) Engineering Geological Investigation and Design of Transition Zones in Unlined Pressure Tunnels. Paper presented at the ISRM International Symposium - 10th Asian Rock Mechanics Symposium, Singapore, 29.10-2.11 2018

Ødegaard H, Nilsen B (2021) Rock Stress Measurements for Unlined Pressure Tunnels: A True Triaxial Laboratory Experiment to Investigate the Ability of a Simplified Hydraulic Jacking Test to Assess Fracture Normal Stress Rock Mechanics and Rock Engineering doi:https://doi.org/10.1007/s00603-021-02452-9

Ødegaard H, Nilsen B, Barkved H (2020) Design of Unlined Pressure Tunnels in Norway – Limitations of Empirical Overburden Criteria and Significance of In-Situ Rock Stress Measurements. Paper presented at the ISRM International Symposium - EUROCK 2020, physical event not held, 2020/11/4/

Paper V

Improved design of unlined air cushion surge chambers

H. Ødegaard, NTNU, Norway
K. Vereide, NTNU and Sira-Kvina, Norway
B.Nilsen, NTNU, Norway

An overview of important design considerations for unlined air cushion surge chambers is given and three innovative solutions that can enable a safer and more economic design are presented. The paper is based on information from ten Norwegian air cushion surge chambers and includes important lessons learned from more than 30 years of operational experience with these facilities.

Common for all pressure tunnels over a certain length is that they must be equipped with surging facilities to reduce the starting time according to the grid requirements, and reduce the water-hammer effect, the potentially large and harmful pressure build-up occurring whenever the turbine discharge changes. This water-hammer can cause damage to pipes, gates, plugs and other installations in the waterway if not reduced by a surging facility. Compared to an open type surging facility, an air cushion surge chamber (ACSC) has many benefits, such as:

- higher degree of freedom in placing the tunnel system as no connection of the surging facility to the surface is needed;
- the entire waterway can be excavated from a single point of attack since the entire tunnel is accessible by vehicles;
- no requirement of an access road in remote areas to reach to the top of the surging facility; and,
- reduced water-hammer and faster ramping of the turbine load.

Surging facilities are either built as surge shafts or surge tunnels, which are open to the atmosphere, or as a pressurised air cushion surge chamber. The two alternatives are shown in Fig. 1.

A total of ten ACSCs have been built in Norway, and nine of these are still in operation, working satisfactorily since commissioning in the 1970s and 1980s. A notable aspect of the Norwegian ACSCs is that they are unlined, meaning that there is no impermeable liner ensuring containment of the pressurised air. The air is contained by low rock mass permeability or hydrodynamic containment such as groundwater flow towards the cavern, or by a combination of the two.

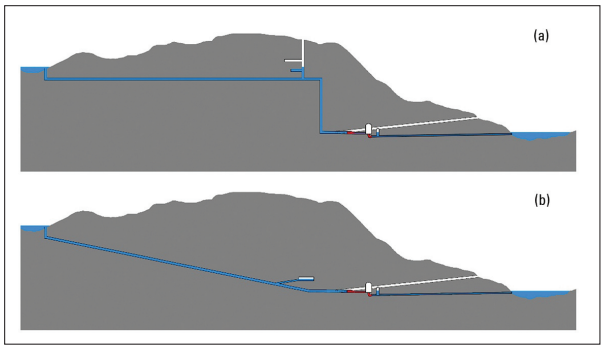

Fig. 1. Schematic sections from hydro plants using (a) an open type surging facility; and (b) an ACSC. The blue tunnel stretches indicate unlined water tunnels and red sections indicate steel lined sections. The water flow is in both cases from left to right.

Despite their many benefits, unlined ACSCs have not yet achieved widespread use, and to the authors' knowledge, only two unlined ACSCs are known outside Norway, at the Ziyli and Xiaotiandu hydroelectric plants in China [China Renewable Energy Engineering Institute, 2016[1] and Luo *et al* 2012[2]]. Since unlined ACSCs can represent a cost-effective and very flexible design for hydroelectric projects, it could be argued that their adoption should have been more widespread than the current number indicates. From the authors' experience, the main reason why project developers tend to favour the traditional open-type surging facilities is related to the risk of excessive air leakage and the economic and operational challenges associated with such leakages.

We believe that these challenges can be significantly reduced by incorporating new design solutions for unlined ACSCs. The objectives of this paper are therefore to revitalize the unlined ACSC technology, by summarizing Norwegian experience, to discuss the basics of ACSC design with regard to engineering geology and hydraulics, and finally, to present three ideas on how the traditional Norwegian design of unlined ACSC could be improved.

The idea of using an air cushion to reduce water-hammer in pipes was first introduced by Michaud [1878[3]], who was working on water mains. Johnson [1908[4]] was the first to describe the use of ACSCs for hydropower plants. The first ACSCs were constructed as steel tanks connected to the pipes of the hydropower plants. Several early hydro plants were constructed with this design, but challenges related to governor stability became a limiting factor [Thoma 1910[5]]. In addition, as the size of hydropower plants became larger, the size and pressure of steel tanks became unfeasible.

During the early 1950s, underground construction of hydropower plants became more and more common. In Norway, this development enabled a reinvention of the ACSC. The concept of an ACSC constructed as an unlined rock cavern for hydroelectric purposes was first introduced in 1969 for the Driva hydroelectric plant in Norway [Svee, 1972[6] and Rathe 1975[7]]. Svee reviewed the stability criterion suggested by Thoma [1910[5]] and expanded the theory to air cushion surge tanks. The first two unlined ACSC where commissioned for the Driva hydro scheme in 1973 and for the Jukla scheme in 1974.

Broch [1982[8]] described how the same engineering geological design criteria as used for unlined pressure tunnels would be valid also for ACSCs, addressing

leakage issues, rock stress requirements and necessary investigations for ACSCs. The Electric Power Research Institute published its Design Guidelines for Pressure Tunnels and Shafts [Brekke *et al* 1987[9]] summarizing the experience from the nine completed ACSCs at the time, including issues on time-consuming watering up of the pressurized waterways as a result of air-filling. The 'Design Code for Air Cushion Surge Chambers for Hydropower Stations', with an extensive review of most aspects related to the design of ACSCs, was published by the China Renewable Energy Engineering Institute [2016[1]].

In recent years, research on the hydraulic and thermodynamic behaviour of ACSCs has been conducted [Vereide *et al* 2015[10], and Vereide 2016[11]]. New techniques for hydraulic scale modelling of ASCSs for laboratory-scale model tests, and new theoretical models for calculation and 1D numerical simulations of the dynamic behaviour are now available. Currently, a new hydropower plant with an ACSC is under construction at the 220 MW Upper Kon Tum project in Vietnam [Røse 2018[12]]. This one is, however, constructed as a concrete- and steel-lined rock cavern. No application of an unlined ACSC since the construction of the 240 MW Xiaotiandu project in 2006 is known to the authors.

1. Basic design criteria

1.1 Hydraulic design

The purpose of the surge facility is to reduce the acceleration time of the water column and reduce the water-hammer in the hydropower plant. This is because hydro plants must be able to change power production rapidly, and the control of the power output must satisfy the demands of the grid as stated by the transmission system operator (TSO).

The closer a surge facility is placed to the turbine, the lower the water acceleration time becomes. In simple terms, the surge facility is an intermittent reservoir closer to the turbine, reducing the length of water to be accelerated. The placement of the surge facility must be close enough to the turbine to enable a fast enough acceleration time.

The necessary size of the ACSC is decided based on the Thoma criterion. Thoma [1910[5]] proved that the surge facility needs to be larger than a certain size to avoid unstable and self-amplifying water level oscillations in the surge facility, when operating with an automatic turbine governor. Such unstable oscillations were experienced at several early powerplants. To avoid such instability, the necessary water surface area in open surge facilities must be larger than the Thoma area (A_{th}) as calculated with Eq. (1), which is the authors revised version of the original equation from Thoma. For an ACSC the Thoma area is calculated to an equivalent minimum air volume (V_{min}) with Eq. (2).

$$A_{th} = \frac{k}{2gH_0}\sum_{i=1}^{i=x}\frac{L_i A_i v_i^2}{h_{f_i}} \quad \ldots 1$$

$$V_{min} = \kappa H_{air} A_{th} \quad \ldots 2$$

Where k (-) is the safety factor, L_i (m), A_i (m^2), v_i (m/s) and h_{fi} (m) are respectively the tunnel or pipe segment lengths, cross sectional area, velocity and head loss between the surge facility and the intake reservoir (headrace systems) or outlet reservoir (tailrace systems), κ (-) is the adiabatic constant and $H_{air} = p_{air}/\rho g(m)$ is the hydrostatic air pressure inside the ACSC.

Eqs. (1) and (2) usually provide a rough estimation of the dimensions of the ACSC for prefeasibility design. For detailed design, numerical simulations are necessary to decide the resulting water-hammer, mass oscillations, governor stability and to control that the resulting conditions for the powerplant are acceptable. The size of the ACSC may in some cases need to be further increased compared with the minimum volume (V_{min}) to provide sufficient safety against drawdown of the water level, or to further reduce the pressure rise in the system during turbine shutdown.

1.2 Rock engineering design

Most Norwegian ACSCs are located in hard and durable rock types, such as Precambrian gneisses. Adopting a design with an unlined ACSC requires both sufficient rock stress and a rock mass of suitable quality. In the context of designing an unlined ACSC, suitable rock mass quality would comprise a rock mass that is;

- sufficiently strong, and able to withstand the loads acting upon it during both the construction and later operational phases, without significant deformations.
- durable for the long term and not prone to slaking nor having any significant amount of soluble constituents; and,
- of low permeability, which disqualifies some volcanic rocks, sandstones and heavily jointed rock masses.

Sufficient rock stress is essential to the design of unlined pressure tunnels and unlined ACSCs since too low stresses can cause pneumatic or hydraulic failure of unfavourably oriented fractures, potentially causing very large leakage. One example is the ACSC at the Tafjord 5 project, the only Norwegian ACSC that is not in operation. This ACSC had to be decommissioned as a result of excessive air leakage caused by pneumatic jacking of the rock mass [Brekke 1987[9]].

The final location of the ACSC must be based on a detailed investigation of the local rock mass conditions, which in Norway is done from within the pressure tunnel during the constructional phase. Typically, such investigations are aimed at identifying a rock mass with sufficient stress, that is sparsely jointed and without weakness zones, faults, or other major conductive structures.

2. Norwegian ACSCs: layout and air-loss mitigation

Some 30 years since their construction, nine out of the ten unlined ACSCs in Norway are still in operation, demonstrating that unlined ACSCs can be both reliable and durable. However, challenges of various natures have been faced, and for the most part solved, during planning, construction and operation of these ACSCs. Consequently, learning from this experience can be useful for designers and clients investigating the pos-

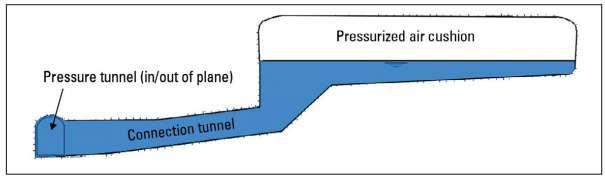

Fig. 2: Example of the ACSC design for the Kvilldal hydro project.

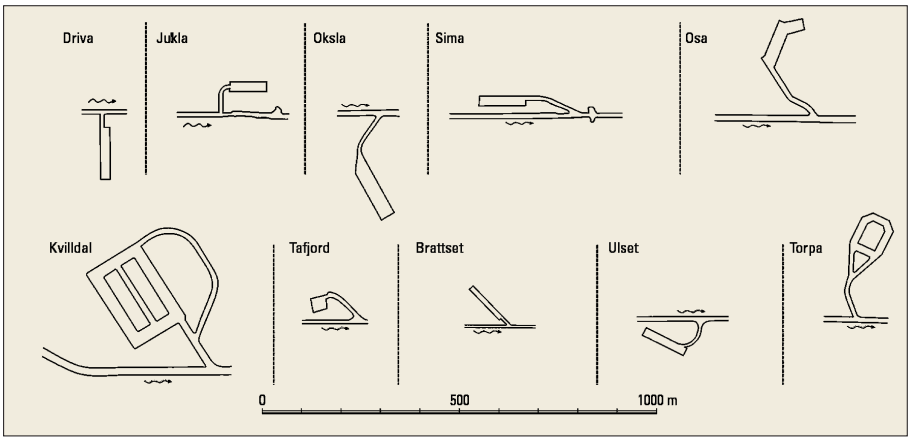

Fig. 3. Plan view of all the Norwegian air cushion surge chambers.

sibility of using unlined ACSCs. In the following, some aspects related to the Norwegian ACSCs are discussed.

Norwegian unlined ACSCs consist of a rock cavern connected to the headrace, with an inclined and relatively short connection tunnel, leaving quite a short barrier of rock between the ACSC and the pressure tunnel. The water surface in the ACSCs is maintained at a higher elevation than the pressure tunnel crown to avoid blowout to the pressure tunnel. During waterfilling of the tunnel system, compressors supply pressurised air to the cavern through preinstalled pipes such that an air cushion resting on top of the water is established, as shown in principle by Fig. 2. The air typically occupies 60 to 80 per cent of the total chamber volume. When the power station is operating and the ACSC is air-filled, any air leaking out of the system will be replaced by the compressors. Since running the compressors is energy demanding it is desirable to reduce this leakage.

From a hydraulic perspective, the shape and layout of the chamber itself is more or less irrelevant, as long as the minimum requirements for free water surface area and air volume, as elaborated in Svee [1972[6]] are satisfied. The shape, size, and orientation of the ten Norwegian ACSCs is highly variable, as shown by the plan views of all Norwegian ACSCs in Fig. 3. While the size of the ACSC naturally varies depending on the specific plant requirement, the various cavern shapes and orientations are mainly associated with local geological conditions and the desire to avoid crossing unfavourable structures.

The Norwegian ACSCs are for the most part given a fairly conventional cavern shape, with vertical walls and an arched crown, as shown in Fig. 4. This shape, though enabling rapid and cost-effective excavation, is not always optimal to promote the best confinement around the cavern periphery, which is relevant for the local permeability of the rock mass surrounding the cavern, as will be discussed later.

Air loss is arguably one of the main project uncertainties related to the use of unlined ACSCs. Air loss represents not only a direct cost for compressor operation, but in the case of excessive leakage also costly mitigating measures such as installation of infiltration facilities (water curtains) or extensive post-grouting might be needed.

Loss of air into the rock mass has been found to be the primary source of air-loss from unlined ACSCs [Goodall, 1988[14]]. To evaluate the economic and tech-

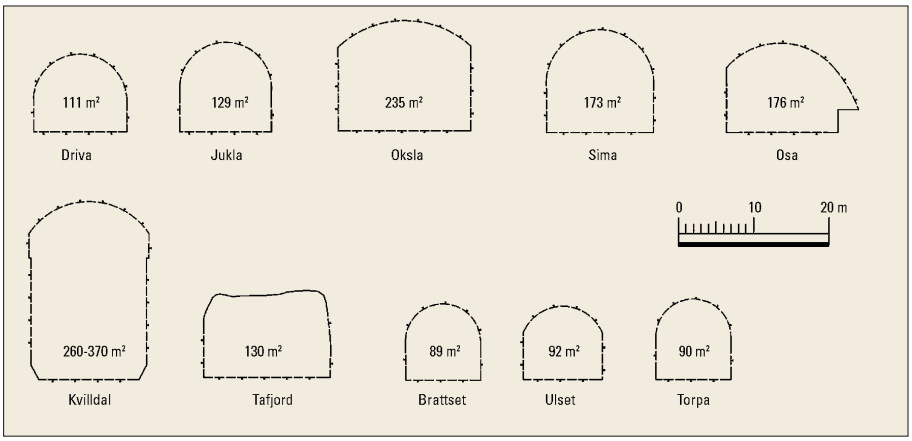

Fig. 4. Cross sectional shapes of the Norwegian ACSCs, according to Kjørholt [1991[13]].

nical feasibility of an unlined ACSC for a given hydroelectric project, it is important to understand which main factors affect this air leakage and how it can be minimized. In hard rock conditions, control of air leakage can be achieved based on the following two main principles [1991[13]]:

- By making sure that the rock mass surrounding the cavern has sufficiently low permeability, either due to intrinsic properties, or from rock mass grouting.
- By hydrodynamic confinement, i.e. making sure that there exists a net water pressure gradient towards the chamber. This can be fulfilled by either having a natural ground water level that is equal to or higher than the pressure line, or by the introduction of an artificial water pressure; a water curtain.

Water curtains, originally introduced for petroleum storage by Professor Ingvar Janelid at the University of Technology in Stockholm, have proven extremely effective in limiting air escape from otherwise leaking ACSCs, and it has been shown that they can practically eliminate air losses [Goodall, 1988[15]]. Whether or not a water curtain is needed depends the air loss from the cavern, the magnitude of which is hard to properly assess without full-scale pressurisation of the cavern. Such testing has traditionally only been possible after water filling of the tunnel system, causing serious delay of the construction schedule. Incorporation of a plug in the connection tunnel, as elaborated below, will make air loss measurements during the construction phase possible, thus facilitating the timely execution of any mitigating measure deemed necessary from leakage measurement.

3. Three innovative design recommendations

To reduce the challenges associated with air leakage and time-consuming filling and emptying of ACSCs, three recommendations for new design are suggested in the following. These measures can be adopted individually or in combination when designing new projects. The proposed closing device can also be installed in existing plants.

3.1 Closing device with a gated plug

A gated plug is proposed to be installed in the connection tunnel between the ACSC and the pressure tunnel. This can reduce the outage associated with dewatering of the pressure tunnel dramatically, enabling faster dewatering and filling during planned and unplanned shutdowns. The concept is sketched in Fig. 5.

A gated plug is conventional from a rock engineering perspective considering that the situation with one-sided pressurisation is not different than for the numerous high-pressure plugs that have been built at existing hydropower plants [Bergh-Christensen, 2013[16]]. In the case with drained pressure tunnel and pressurised ACSC, the plug would normally not be in contact with the pressurised air since the water level is maintained as indicated in Fig. 5.

The plug is to be equipped with a side hinged circular steel gate that can be remotely operated. A hydraulic piston ensures robust manoeuvring of the gate during submerged conditions. Due to environmental reasons a water-servo hydraulic piston should be used. Since the piston only will be operated when the pressure is compensated, the working pressure of the piston needs to overcome only the inertia of the gate plus any resistance from rusty hinges. The gate also must be equipped with a man-hole and the plug with a drainage pipe and dewatering valve for manual draining when the gate is closed.

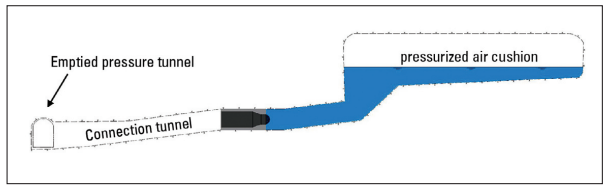

Fig. 5. Tentative location of a gated plug in the connection tunnel between the pressure tunnel and the air cushion.

It is crucial for the design that the gate in the open position can handle the high flow of water through the plug during operation. Assuming a gate diameter of 5 m, as calculations show is required for the Kvilldal project, the speed of the flowing water could reach 14 m/s during shutdown of the turbines. Therefore, the gate must be flush fitted to the side wall of the concrete plug, as is indicated in the conceptual drawing in Fig. 6.

The design of the gate and plug must be robust to survive in submerged conditions for decades. From a security point of view, there are two critical situations which must be avoided. First, failure of the gate when the ACSC is pressurized and the pressure tunnel drained; and, second, accidental closure of the gate during plant operation. The former can cause uncontrolled discharge of air and water into the emptied pressure tunnel, while the latter will decouple the ACSC from the hydraulic system. Both situations may potentially have very damaging and harmful consequences, such as flooding of the power station or bursting of steel pipes and gates. Accidental opening of the gate during full one-sided pressurization is unlikely, considering the very large pressure acting to close the gate. In any case, gate manoeuvring should be activated by two independent mechanisms, such as an electrical lock in addition to a hydraulic system. The gate cannot be interlocked in the open position but can be fixed with bolts in closed position.

3.2 Rock mass grouting

One would expect pre-grouting of the rock mass surrounding unlined ACSC to be an obvious design choice since systematic pre-grouting in general has proven very effective in reducing rock mass permeability. A review of the Norwegian ACSCs indicates this does is not the case. According to Kjørholt [1991[13]] extensive grouting efforts has been performed only at the Osa and Torpa ACSCs, in both cases with

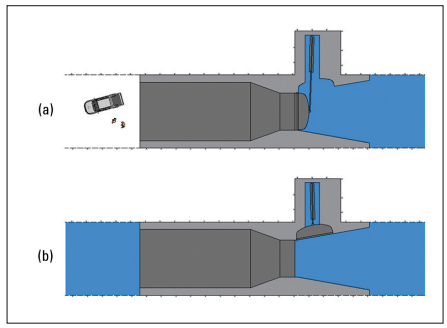

Fig. 6. Plan view showing (a) the plug with closed gate representing the situation with a pressurized ACSC and drained pressure tunnel, and (b) the plug with open gate, representing the situation during running of the plant. In (a) a vehicle and workers are shown for scale.

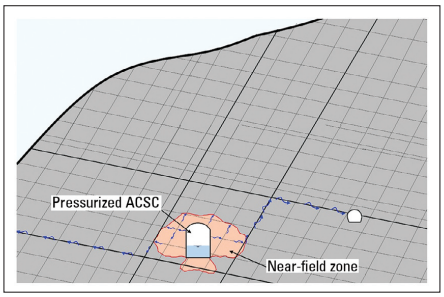

Fig. 7. Principle drawing showing the near-field zone surrounding the opening where rock mass permeability is altered due to opening or closing of joints.

good results. None or only limited grouting efforts has been made for the other eight chambers.

Major improvements in both grouting equipment, materials, and in the understanding of the grouting process have been made since commissioning of the last Norwegian ACSCs. This development, which is connected to road and railway tunnels in urban areas, oil and gas storage caverns and many other types of projects, should be taken advantage of when designing new ACSCs.

Whether or not the costs associated with pre-grouting can be justified must be based on an evaluation for each individual project, comparing grouting costs with cost associated with excessive leakage, such as installation and maintenance of a water curtain, post-grouting and increased running time of compressors.

3.3 Optimization of cavern shape

Any excavation in rock will redistribute rock stresses, generating a zone around the opening where the original stress situation is altered. In this so-called near-field zone the stresses will differ from the initial stress situation (the far-field) both in magnitude and direction, see Fig. 7. The permeability in the near-field zone will also be affected by the altered normal stress across joints, changing the area available for water- or air flow in the rock mass [Lamas, 2014[17]]. The degree of confinement can thus be used as an indicator for permeability, since the latter is generally reduced with increasing confinement and vice versa.

For a given site little can be done with the in-situ stress conditions, but the cavern geometry and layout can be optimised. It would therefore be desirable to choose an excavation geometry that ensures the best confinement, and thus the least permeability, in the rock mass surrounding the opening. Provided adequate knowledge of the in-situ state of stress, simple finite element analysis can be used to assess the near-field stress distribution for various excavation geometries, as input to decide the optimum cavern shape. In general, it is known that high vertical walls can give unfavourable (lower) confinement in the surrounding rock mass than do curved walls. In addition, a single cavern layout would be preferable, since twin caverns, ring-shaped caverns or other complex layouts increase the risk of creating zones of poor confinement.

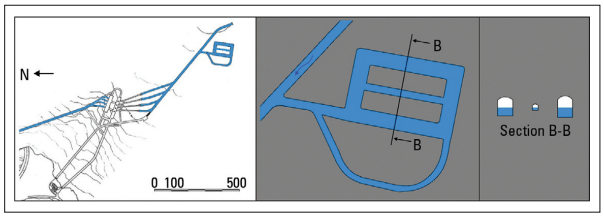

Fig. 8. Overview of the downstream part of the Kvilldal hydro scheme tunnel system with details of the ACSC. The figure is modified from Goodall and Kjørholt [1988[15]].

4. Case-study: Installation of a closing device at the Kvilldal ACSC

The Kvilldal hydro plant is located in the south-western part of Norway and is equipped with the world's largest unlined ACSC, with a chamber volume of more than 120 000 m^3. During operation the chamber is pressurized to 4.2 MPa with an air volume of 90 000 m^3, equivalent to 3.1 × 10^6 Nm^3. The ACSC is located about 600 m upstream from the Kvilldal power station and is shaped as a rectangular ring tunnel surrounding a central pillar, as shown in Fig. 8. The vertical rock cover at the ACSC location is 520 m.

Despite the favourable rock mass conditions, initially considered to be well suited to host the ACSC, major air leakage was detected after the first pressurization of the chamber in 1981 [Goodall, 1988[15]]. Initial measurements showed leakage of 240 Nm^3/h, significantly higher than the anticipated 60 Nm^3/h, and exceeding what could be accepted as regards operating costs and the capacity of the compressors. It was therefore decided to dewater the tunnel system and to install a water infiltration system; a water curtain. The water curtain proved highly effective, reducing air leakage to 10 Nm^3/h [Goodall, 1988[15]].

A challenge which is particularly problematic for large ACSCs, such as Kvilldal, is the very long time it can take to fill and empty the cavern. As an example, it takes five to seven weeks to fill the Kvilldal ACSC fully, holding 3.1 × 10^6 Nm^3 of air [Pleym, 2013[18]]. This outage represents a large potential for production losses, especially if sudden events should call for unplanned dewatering of the system.

4.1 Economic analysis

A cost estimate for the post-construction installation of a closing device at the Kvilldal hydro project is summarised in Table 1. The profitability of the installation is primarily due to the reduced outage of the plant during dewatering. In addition, the direct cost for air-filling is reduced. It is assumed that the installation works can be performed during a period of planned dewatering and that the installation itself does not result in outage of the plant.

It usually takes about one week to empty the Kvilldal ACSC and around five to seven weeks for the subse-

Table 1: Cost estimate for installing a closing mechanics at the Kvilldal ACSC

Component	Cost (€ × 10^6)
Concrete plug and steel works	0.33
Hydraulics and control system	0.2
Rock excavation	0.02
Concrete works	0.2
Project management	0.1
Total	0.85

quent air filling. The equivalent time duration with a conventional surge shaft would be approximately three days for emptying and five days for filling, indicating an extra five to seven weeks for the ACSC, depending on the compressor capacity. It is, however, possible to start two of the machines (620 MW) after a couple of weeks and three machines (930 MW) a few weeks after that. As an estimate, it is assumed in the following that the ACSC causes 20 days additional full outage compared with an open surging facility.

The costs of these 20 days of extra outage can be estimated. As a rough approximation, one can divide the annual energy production from Kvilldal (3 TWh) on the number of days in a year (365 days), to get the daily average production (8 GWh/day). The average production during a 20-day period is then equal to 160 GWh. Because of the large upstream reservoir, one would not expect this energy to be lost as flood spill, but one can expect that the power price obtained is reduced because of the outage. If one assumes a €50 /MWh reduced power price for these 160 GWh, the economic loss becomes €0.8 million. If one includes additional economic losses because of system services (frequency and voltage control) not sold, the total economic loss is assumed to be about €1 million for 20 days of outage.

Filling of the air for the Kvilldal ACSC is done with a combination of electric and diesel compressors. As a simplification, it is assumed that all the compressors are electric, and that the power consumption is 200 Wh/Nm^3 at 4.2 MPa. This gives an energy consumption of 650 MWh to fill the 3.2×10^6 Nm^3. With a power price of €300 /MWh, the cost of electric energy to the compressors is about €0.2 million. If the compressors must be rented for the filling, the rental cost is estimated to €0.3 million. Based on the assumptions describe the total cost of dewatering, refilling and 20 days outage in Kvilldal is about €1.05 million.

In the period from 1981 to 2012, the waterway at Kvilldal was emptied four times. On two occasions this was caused by rehabilitation needs in the ACSC. In normal conditions one could expect that the Kvilldal waterway would be dewatered once every 15 years, maximum.

A net present value (NPV) calculation can be done to assess the profitability of the closing mechanism for the Kvilldal ACSC. An economic lifetime of 60 years, discount rate 5 per cent, and investment costs of € 0.85 million are assumed. It is assumed that the installation is conducted at the same time as a planned dewatering, and that it does not require any additional outage of the plant. The NPV becomes €10 000. Based on this simple calculation, it is concluded that there is a marginal profitability of installing a closing mechanism. The profitability is, however, very sensitive to the outage costs of future dewatering, which is very challenging to predict. Also, the calculation does not include the potential for unplanned and unexpected needs for dewatering. If such uncertainties are considered, the potential profitability will increase.

5. Conclusions

Based on investigation and a compilation of information regarding the design and operational experience from the ten unlined air cushion surge chambers in Norway, the following highlights can be extracted:

- Hydropower plants with air cushion surge chambers have obvious advantages as regards flexibility of tunnel system design, reduction of environmental impact, reduction of water-hammer and improved operation of the plant.
- Sufficient rock stress is an absolute prerequisite for the successful operation of an unlined ACSC.
- A functioning water curtain can practically eliminate air loss from the ACSC into the rock mass.
- Rock mass grouting can significantly reduce air leakage.

Whenever unlined pressure tunnels are considered feasible, unlined ACSC should also be a feasible option. Sufficient rock stress, a combination of systematic pre-grouting and an ACSC shape and layout that promotes confinement will in most cases satisfy the requirements for a functioning unlined ACSC. For cases where this is not sufficient, operational experience from Norwegian ACSCs has shown that the installation of a water curtain can practically eliminate air leakage, although at an additional cost.

Installing a gated plug in the connection tunnel to the ACSC can enable closing off the ACSC during dewatering of the main tunnel system. This represents a major improvement, as it will reduce outage of the power plant for inspection and maintenance in addition to significantly reducing costs associated with refilling of air with compressors. ◊

Acknowledgements

We would like to thank Statkraft for allowing us to use Kvilldal as a case for evaluating the new design recommendations. We also extend warm thanks to the engineers at Rainpower for their patience during our discussion on the feasibility of introducing the suggested ACSC closing device, and to Atlas Copco for providing updated cost estimates for compressor operation. Finally, we would like to thank HydroCen who have made this work possible as part of the research centre activity.

References

1. **China Renewable Energy Engineering Institute.** "Design Code for Air Cushion Surge Chamber of Hydropower Stations". Beijing: China Electric Power Press; 2016.
2. **Luo G, Hu Y, and Huang K.** "Research on the Effect of Gas Leaking and Gas-Supplementing Measurements of Air Cushion Surge Chamber". *Applied Mechanics and Materials*. 238:414; 2012.
3. **Michaud J.** "Coups de bélier dans les conduites: étude des moyens employés pour en atténuer les effets" (in French). *Bulletin de la Société vaudois des ingénieurs et des architectes*. 4(3):56; 1878.
4. **Johnson RD.** "The Surge Tank in Water Power Plants". *Transactions of the American Society of Mechanical Engineers*. 30. Paper 1204, 1908.
5. **Thoma D.** "Zur Theorie des Wasserschlosses: bei selbsttätig geregelten Turbinenanlagen" (in German). München: R. Oldenbourg; 1910.
6. **Svee R.** "Surge chamber with an enclosed, compressed air-cushion". *Proceedings:* International Conference of Pressure Surges; England: BHRA Fluid Engineering; 1972.
7. **Rathe L.** "An innovation in surge-chamber design". *Water Power & Dam Construction*; 1975.
8. **Broch E.** "The Development of Unlined Pressure Shafts And Tunnels In Norway". *Proceedings*. International Society for Rock Mechanics Symposium; 1982.
9. **Brekke T. L, and Ripley B.D**. "Design Guidelines for Pressure Tunnels and Shafts". University of California, Berkeley, DoCE, Institute EPR. Report No.: EPRI AP-5273. 1987.
10. **Vereide K, Lia L, and Nielsen TK.** "Hydraulic scale modelling and thermodynamics of mass oscillations in closed surge tanks". *Journal of Hydraulic Research*. 53(4):519-24; 2015.

11. **Vereide K.** "Hydraulics and thermodynamics of closed surge tanks for hydropower plants". Trondheim: Norwegian University of Science and Technology; 2016.
12. **Røse T.E, Koksæter A, Dalsviken K, Skuncke O, Børresen B, and Vereide K.** "Design of an ACSC for Upper Kon Tum HPP". *Proceedings:* Asia 2018; 13-15 March; Vietnam; 2018.
13. **Kjørholt H.** "Gas tightness of unlined hard rock caverns". Trondheim: Norwegian University of Science and Technology; 1991.
14. **Goodall D, Kjørholt H, Tekle T, and Broch E.** "Air cushion surge chambers for undeground power plants". *Water Power & Dam Construction*. 29-34; 1988.
15. **Goodall D, and Kjørholt H.** "Documentation of the Kvilldal Air Cushion Surge Chamber". Trondheim, Norway: SINTEF; 1988-05-26. Report No. STF36 A87085; 1988.
16. **Bergh-Christensen J, Broch E, and Ravlo A.** "Norwegian High Pressure Concrete Plugs". In: Broch E, Grasbakken E, Stefanussen W, editors. Norwegian Hydropower Tunnelling II. Oslo: Norwegian tunnelling society NFF; 2013.
17. **Lamas L, Leitão N, Esteves C, and Plasencia N. "**First Infilling of the Venda Nova II Unlined High-Pressure Tunnel: Observed Behaviour and Numerical Modelling". *Rock Mechanics and Rock Engineering*. 47(3):885-904; 2014.
18. **Pleym A. "**Luftputekammer i vankraftverk - driftserfaringer" (in Norwegian); Unpublished, internal report prepared by Pleym for the Owner (Kvilldal Hydro Project). 2013.

H. Ødegaard

K. Vereide

B. Nilsen

H. Ødegaard is currently doing his doctorate at the Department of Geoscience and Petroleum, Norwegian University of Science and Technology (NTNU). Here, he is working on topics related to rock mechanics and the design of unlined pressure tunnels. He is currently on leave from the consultancy company Multiconsult, where, for more than 10 years, he has worked as consulting engineer for several hydroelectric projects and other rock engineering projects.

Norwegian University of Science and Technology, Department of Geoscience and Petroleum, 7491 Trondheim, Norway.

K. Vereide is an Adjunct Associate Professor at the Norwegian University of Science and Technology (NTNU) and a Project Developer at Sira-Kvina power company. At NTNU, Vereide works as with areas of hydraulic design and hydraulic transients at hydropower plants. At Sira-Kvina power company he works with the upgrading of existing hydropower plants and the design of new hydropower plants.

Norwegian University of Science and Technology, Department of Civil and Environmental Engineering, 7491 Trondheim, Norway.

B. Nilsen is Professor of Geological Engineering at NTNU. Nilsen has more than 40 years of experience on various aspects of rock engineering, including site investigation, planning and design, stability analyses and construction control. He has been expert advisor for several large projects in Norway and abroad. His main current projects relate to subsea tunnelling, engineering geological aspects of mechanical excavation, hydropower tunnelling and rock slope stability.

Norwegian University of Science and Technology, Department of Geoscience and Petroleum, 7491 Trondheim, Norway.

ISBN 978-82-326-6292-0 (printed ver.)
ISBN 978-82-326-6139-8 (electronic ver.)
ISSN 1503-8181 (printed ver.)
ISSN 2703-8084 (online ver.)

NTNU

Norwegian University of
Science and Technology